



**FACULTY
OF MATHEMATICS
AND PHYSICS**
Charles University

MASTER THESIS

Daniel Jahn

Generalized random tessellations, their properties, simulation and applications

Department of Probability and Mathematical Statistics

Supervisor of the master thesis: prof. RNDr. Viktor Beneš, DrSc.

Study programme: Mathematics

Study branch: Probability, mathematical statistics
and econometrics

Prague 2019

I declare that I carried out this master thesis independently, and only with the cited sources, literature and other professional sources.

I understand that my work relates to the rights and obligations under the Act No. 121/2000 Sb., the Copyright Act, as amended, in particular the fact that the Charles University has the right to conclude a license agreement on the use of this work as a school work pursuant to Section 60 subsection 1 of the Copyright Act.

In date

signature of the author

I would like to thank my supervisor prof. RNDr. Viktor Beneš, DrSc. for all the time and effort he put into helping me on the often thorny path of writing this thesis. I am also grateful for all the opportunities he provided me with to present and discuss my work on seminars and conferences.

If there is one other person without whom this thesis would have been much more difficult to write, it is my partner, Adela Nguyễn. I am grateful for having her by my side throughout the whole process of writing this thesis. She has far surpassed the official requirements for the partner of a mathematician, that is to be emotionally supportive and understanding, especially when waking up in the middle of the night to find the said mathematician working, again. She has spent countless hours listening to me talk about circles and tetrahedrons and, on several occasions, picked up a pen and paper and actively helped me solve the problems. Thank you for everything.

For helping me with a difficult programming language I knew nothing about, as well as for general advice on programming, I thank my friend and an excellent programmer Jan Noha.

I thank Colin Beet for helping me improve the linguistic aspects of this thesis. He would like the reader to know that, contrary to what Remark 9 claims, abuse of any kind can never be justified.

I thank my family for supporting my academic endeavours even though they still have no idea what it is I am actually doing.

Finally, I'd like to thank the following people who have provided valuable insights and comments: Prof. David Dereudre, Jeremy Tan, Matěj Kovář, Prof. Volker Schmidt, Prof. David Eppstein.

Title: Generalized random tessellations, their properties, simulation and applications

Author: Daniel Jahn

Department: Department of Probability and Mathematical Statistics

Supervisor: prof. RNDr. Viktor Beneš, DrSc., Department of Probability and Mathematical Statistics

Abstract: The past few years have seen advances in modelling of polycrystalline materials using parametric tessellation models from stochastic geometry. A promising class of tessellations, the Gibbs-type tessellation, allows the user to specify a great variety of properties through the energy function. This text focuses solely on Gibbs-type tetrahedrizations, a three-dimensional tessellation composed of tetrahedra. The existing results for two-dimensional Delaunay triangulations are extended to the case of three-dimensional Laguerre tetrahedrization. We provide a proof of existence, a **C++** implementation of the MCMC simulation and estimation of the models parameters through maximum pseudolikelihood.

Keywords: Gibbs point process tetrahedrization Laguerre existence simulation maximum pseudolikelihood estimation

Contents

Glossary of terms and abbreviations	3
Introduction	4
1 Geometric preliminaries	5
1.1 Tetrahedrizations	5
1.1.1 Delaunay tetrahedrization	6
1.1.2 Laguerre tetrahedrization	7
1.2 Hypergraph structures	14
1.2.1 Tetrahedrizations as hypergraphs	14
1.2.2 Hyperedge potentials and locality	17
2 Stochastic geometry	20
2.1 Point processes	20
2.1.1 Basic terms	20
2.1.2 Finite point processes with density	23
2.2 Gibbs Point Processes	24
2.2.1 The energy function	24
2.2.2 Finite volume Gibbs point processes	25
2.2.3 Infinite volume Gibbs point processes	26
2.2.4 Hereditary GPP	27
2.2.5 Non-hereditary GPP	28
3 Existence of Gibbs-type models	29
3.1 Existence theorem	29
3.1.1 Stability	29
3.1.2 Range condition	29
3.1.3 Upper regularity	30
3.2 Verifying the assumptions	31
3.2.1 The choice of Γ and M for Laguerre-Delaunay models . . .	32
3.2.2 Geometric properties of the tetrahedrizations defined by Γ^A and M	33
3.2.3 Existence theorems	37
4 Simulation	42
4.1 Monte Chain Markov Carlo	42
4.1.1 Basic notions	42
4.1.2 Birth-Death-Move Metropolis-Hastings algorithm	44
4.2 Simulating Gibbs-Laguerre-Delaunay tetrahedrizations	46
4.2.1 Definition of the model	46
4.2.2 Simulation algorithm	46
4.2.3 Simplified form of proposal densities	48
4.2.4 Practical implementation	49
4.2.5 Convergence of the algorithm	49

5	Estimation	51
5.1	Estimation of the hardcore parameter	51
5.2	Estimation of the smooth interaction parameters	51
5.2.1	Practical implementation	52
5.2.2	Consistency	53
6	Numerical Results	54
6.1	Simulation	54
6.1.1	Convergence	54
6.1.2	Role of the parameter θ	54
6.1.3	Difference between Laguerre and Delaunay	56
6.2	Estimation	59
	Conclusion	61
	Bibliography	62
	List of Figures	65
	List of Tables	66
A	Appendix: Geometry	67
A.1	Calculating the circumdiameter	67
A.2	Bounding the circumdiameter	68
A.2.1	Statement of the problem	68
A.2.2	Solution to the problem	69
A.2.3	Apollonius problem in \mathbb{R}^3	71
B	Appendix: Implementation details	74

Glossary of terms and abbreviations

Mathematical operators and notation

The following list only serves as a reference. Most of the following terms are defined more precisely when they are first used in the text.

\mathbb{N}_0	$\mathbb{N} \cup \{0\}$
$B(x, r)$	Open ball with center x and radius r
$\text{diam}(A)$	Diameter of the set A ; $\sup_{x, y \in A} \ x - y\ $
$\text{card}(A)$	Cardinality of the set A
$\text{conv}(A)$	Convex hull of the set A
$\lambda(A), A $	Lebesgue measure of the set A
∂	Topological boundary of a set
$A + B$	Minkowski sum of the sets A and B ; the set $\{a + b : a \in A, b \in B\}$.
$\text{pr}_{\mathbb{R}^3}(\cdot)$	Projection from \mathbb{R}^4 to \mathbb{R}^3
$\angle pqr$	Angle formed by pqr
\propto	Proportional to
$\delta_x(A)$	Dirac delta function at x . Equals to 1 if $x \in A$, 0 otherwise.
$\det M$	Determinant of the matrix M
$\ \cdot\ $	Euclidean norm
$d(p, x)$	Power distance of the point x and weighted point p
$\rho(p, q)$	Power product of two weighted points p and q
$\chi(\eta)$	For $\text{card}(\eta) = 4$, circumdiameter of the tetrahedron $\text{conv}(\eta)$.

Abbreviations

DLR	Dobrushin-Lanford-Ruelle (equations)
GNZ	Georgii-Nguyen-Zessin (equation)
MCMC	Markov chain Monte carlo
MPLE	Maximum pseudolikelihood estimation

Introduction

An important area in materials science is the study of polycrystalline materials. Advances in understanding now allow us to accurately characterize the macro-scale properties of such materials using only their microscopic structure. It is therefore essential to develop adequate three-dimensional (3D) mathematical models to accurately capture and describe the microscopic geometrical properties of these materials. Stochastic models have provided an extremely useful way of capturing the irregularities of the real world, and the study of polycrystalline materials is no different. In particular, the random tessellation models from stochastic geometry have proven to be especially appropriate for the mosaic-like grain structure of polycrystalline materials.

This work, as a part of the project solution of GACR 17-00393J (investigator V. Beneš), studies a type of tessellations closely related to the grain structure of polycrystalline materials — tetrahedrizations, in particular Gibbs-type tetrahedrizations. These tessellations, based on the Gibbs point process, allow a great flexibility in modelling the different properties of the resulting structure. In the study of polycrystalline materials, tetrahedrizations are also used as a mesh for the finite element method (Quey et al. [2011]). The main contribution of this text is twofold — theoretical and practical.

Chapters 1 and 2 contain the necessary theoretical background. We would in particular like to draw attention to Section 1.1.2 which provides a stand-alone presentation of the theory Laguerre tetrahedrization without relying on its duality to Laguerre tessellation, as the existing literature does, and thus provides a direct understanding of the structure.

The theoretical contribution of this text is the proofs of existence of the Gibbs-Laguerre-Delaunay models used in the practical part. The two-dimensional Gibbs-Delaunay model presented in Dereudre et al. [2012] is extended here to three dimensions and further generalized to Gibbs-Laguerre-Delaunay, a tessellation model which allows to attach a weight to each point. Using the approach of Dereudre et al. [2012] the intricate interactions present in our models are analyzed through the hypergraph structures they generate. The proofs themselves can be found in Theorems 3-6 in Chapter 3. However, all of Section 3.2 as well as Section A.2 are composed of original work.

The practical contribution is an extension of the work done in Dereudre and Lavancier [2011]. In Chapters 4 and 5, we present the approach used in simulation of parametric tessellation models and estimation of their parameters. Chapter 6 then presents the numerical results. However, these three chapters are merely a report of the most important part of the work not present in this text — the C++ implementation, see Appendix B for more details.

1. Geometric preliminaries

Before diving into the mathematics of Gibbs-Laguerre-Delaunay tetrahedrization models, we must first lay out the fundamentals of their geometric and combinatorial structure. The key geometric components are the circumball for Delaunay tetrahedrizations and the characteristic point for Laguerre tetrahedrizations. In Section 1.1 we study the geometric properties of the Delaunay and Laguerre tetrahedrization and in Section 1.2 we analyze their structure in terms of hypergraphs.

Notation and basic terms

This text will predominantly focus on *marked* points in \mathbb{R}^3 , that is elements of $\mathbb{R}^3 \times S$, where $S = [0, W]$, $W > 0$ is the *mark set*. A great deal of care must be dedicated to clearly distinguish between *positions* of points (their projection to \mathbb{R}^3) and their *marks*¹ (projection to S). To this end, we adopt the following notation. A point $p \in \mathbb{R}^3 \times S$ has the position $p' \in \mathbb{R}^3$ and mark $p'' \in S$. Borel σ -algebra on \mathbb{R}^3 will be denoted \mathcal{B} . The subset of \mathcal{B} containing only bounded sets is \mathcal{B}_0 .

A *configuration* is a set $\mathbf{x} \in \mathbf{N}_{lf}$, where

$$\mathbf{N}_{lf} = \{\mathbf{x} \subset \mathbb{R}^3 \times S : \text{card}(\mathbf{x} \cap B) < \infty, B \in \mathcal{B}_0\}$$

is the set of locally finite sets on $\mathbb{R}^3 \times S$. Let $\mathbf{N}_f \subset \mathbf{N}_{lf}$ be the set of all finite sets on $\mathbb{R}^3 \times S$. Any observation window Λ will always be assumed to have a positive Lebesgue measure. We denote the Lebesgue measure on \mathbb{R}^3 by λ and often use the notation $|\cdot| = \lambda(\cdot)$. Let $\eta \subset \mathbf{x}$, $\mathbf{x} \in \mathbf{N}_{lf}$. A subset of \mathbf{x} will be denoted η . If $\text{card}(\eta) = 4$, then η is called *tetrahedral*. The symbols $\mathbf{x}' = \text{pr}_{\mathbb{R}^3}(\mathbf{x})$, $\eta' = \text{pr}_{\mathbb{R}^3}(\eta)$ again refer only to the positional part, where $\text{pr}_{\mathbb{R}^3}$ denotes the projection to \mathbb{R}^3 .

Lastly, for $\Lambda \in \mathcal{B}_0$, playing the role of the observation window, we denote

$$\mathbf{N}_\Lambda = \{\mathbf{x} \in \mathbf{N}_f : \mathbf{x}' \subset \Lambda\}.$$

1.1 Tetrahedrizations

The aim of this section is to introduce the geometric concepts necessary for the understanding of two types of tetrahedrizations: Delaunay and Laguerre. The main focus of this text lies on the Laguerre tetrahedrization and thus Delaunay tetrahedrization will receive significantly less attention and often will be treated only as a special case. Note that although this text focuses solely on the three dimensional case, most ideas remain valid for a triangulation in any dimension.

While this section does not aim to be a comprehensive overview of Delaunay and Laguerre tetrahedrizations, it also functions as a standalone text with proofs derived specifically for the setting of this text. The literature on this topic tends to focus on the duals of the tetrahedrizations, that is the Voronoi and Laguerre diagrams. Furthermore most literature treats the two-dimensional equivalent,

¹Marks will also be sometimes called weights.

the Delaunay and Laguerre triangulations. One must thus piece together the understanding of the tetrahedrizations through various sources not directly pertaining to this topic. For general mathematical introductions, we recommend Okabe et al. [1992], Gavrilova [1998]. For a survey on Laguerre (power) diagrams, see Aurenhammer [1987] and Hummel [2015]. Lastly we recommend two books that contain mostly information on (Delaunay) triangulations and related objects: De Loera et al. [2010] and Aurenhammer et al. [2013].

We now introduce the notion of (reinforced) general position, a traditional assumption on configurations. Recall that the points $\{x'_0, x'_1, \dots, x'_k\} \subset \mathbb{R}^3, k \in \mathbb{N}$ are *affinely independent* if the vectors $x'_1 - x'_0, \dots, x'_k - x'_0$ are linearly independent.

Definition 1. Let $\mathbf{x} \in \mathbf{N}_{lf}$. We say \mathbf{x} is in **general position** if

$$\eta \subset \mathbf{x}, 2 \leq \text{card}(\eta) \leq 4 \Rightarrow \eta' \text{ is affinely independent in } \mathbb{R}^3.$$

Denote $\mathbf{N}_{gp} \subset \mathbf{N}_{lf}$ the set of all locally finite configurations in general position.

We call points $\{x'_0, x'_1, \dots, x'_k\} \subset \mathbb{R}^3, k \in \mathbb{N}$ *cospherical* if there exists a sphere $S \subset \mathbb{R}^3$ such that $\{x'_0, \dots, x'_k\} \subset S$. In this text, a sphere will always refer to the boundary of a ball, never to the interior.

Definition 2. Let $\mathbf{x} \in \mathbf{N}_{gp}$. We say \mathbf{x} is in **reinforced general position** if

$$\eta \subset \mathbf{x}, \text{card}(\eta) = 4 \Rightarrow \eta' \text{ is not cospherical.}$$

Denote \mathbf{N}_{rgp} the set of all locally finite configurations in reinforced general position.

1.1.1 Delaunay tetrahedrization

This section will shortly introduce the three dimensional equivalent of the well known Delaunay triangulation. While the configurations in this section are technically marked sets, none of the terms take marks into consideration, as the Delaunay tetrahedrization relies on positions only.

Definition 3. Let $\eta \in \mathbf{N}_{gp}$. An open ball $B(\eta)$ such that $\eta' \subset \partial B(\eta)$ is called a *circumball* of η . The boundary $\partial B(\eta)$ is called a *circumsphere*.

Definition 4. Let $\mathbf{x} \in \mathbf{N}_{gp}$ and $\eta \subset \mathbf{x}$. We say that (η, \mathbf{x}) satisfies the *empty ball property* if there exists a circumball $B(\eta)$ such that $B(\eta) \cap \mathbf{x}' = \emptyset$ and call $B(\eta)$ an *empty ball* (of η). For convenience, for $\mathbf{x} \in \mathbf{N}_{lf} \setminus \mathbf{N}_{gp}$, we define any $\eta \subset \mathbf{x}$ that does not satisfy the assumptions of general position as not satisfying the empty ball property.

Definition 5. Let $\mathbf{x} \in \mathbf{N}_{lf}$. Define the set

$$\mathcal{D}(\mathbf{x}) := \{\eta \subset \mathbf{x} : \eta \text{ satisfies the empty ball property}\}.$$

and its subsets

$$\mathcal{D}_k(\mathbf{x}) := \{\eta \in \mathcal{D}(\mathbf{x}) : \text{card}(\eta) = k\}, \quad k = 1, \dots, 4.$$

We then define the *Delaunay tetrahedrization* of \mathbf{x} as the set $\mathcal{D}_4(\mathbf{x})$.

The set \mathcal{D}_4 contains the structure we would expect from the name tetrahedrization, namely it contains sets of 4-tuples of points whose convex hull are the tetrahedra forming the Delaunay tetrahedrization. The difference here is that we have allowed even cospherical points to form tetrahedra. The fact that we have defined the set $\mathcal{D}_k(\mathbf{x})$ for any $k = 1, \dots, 4$ reflects the hypergraph approach to these structures presented in Section 1.2.

Note that for $\mathbf{x} \in \mathbf{N}_{rpg}$ the following relationship between sets $\mathcal{D}_2(\mathbf{x})$ and $\mathcal{D}_4(\mathbf{x})$ holds:

$$\eta \in \mathcal{D}_2(\mathbf{x}) \iff \text{there exists } \tilde{\eta} \in \mathcal{D}_4(\mathbf{x}) \text{ such that } \eta \subset \tilde{\eta}. \quad (1.1)$$

The following proposition shows one important property of the set $\mathcal{D}_2(\mathbf{x})$ for any $\mathbf{x} \in \mathbf{N}_{lf}$ — it contains the edges of the (undirected) nearest neighbor graph.

Proposition 1. *Let $\mathbf{x} \in \mathbf{N}_{lf}$. Define the set*

$$\text{NNG}(\mathbf{x}) = \left\{ \{p, q\} \subset \mathbf{x} \times \mathbf{x} : p \neq q, \|p - q\| \leq \|p - s\|, s \in \mathbf{x} \setminus \{p\} \right\}.$$

Then

$$\text{NNG}(\mathbf{x}) \subset \mathcal{D}_2(\mathbf{x}).$$

Proof. Let $\mathbf{x} \in \mathbf{N}_{lf}$ and $\eta = \{p, q\} \in \text{NNG}(\mathbf{x})$. Without loss of generality assume that q is the nearest neighbor of p . Then $B(p, \|p - q\|) \cap \mathbf{x}' = \{p\}$. Then η satisfies the empty ball property with the circumball $B(\eta) := B((p + q)/2, \|p - q\|/2) \subset B(p, \|p - q\|)$. \square

1.1.2 Laguerre tetrahedrization

The main object of our study is the Laguerre tetrahedrization. This tetrahedrization utilizes the marks of the configuration and allows them to change the structure of the tetrahedrization.

The key information to understanding the geometry of Laguerre tetrahedrizations is that a point $p = (p', p'') \in \mathbb{R}^3 \times S$ can be interpreted as an open ball $B(p', \sqrt{p''})$. For a point $p \in \mathbb{R}^3 \times S$, we will call $B_p = B(p', \sqrt{p''})$ the *ball defined by p* . We further define the sphere $S_p = \partial B_p$.

Definition 6. Define the *power distance* of the unmarked point $q' \in \mathbb{R}^3$ from the point $p = (p', p'') \in \mathbb{R}^3 \times S$ as

$$d(q', p) = \|q' - p'\|^2 - p''.$$

Much intuition can be gained from properly understanding the geometric interpretation of the power distance.

Remark 1 (Geometric interpretation of the power distance). We split the interpretation into two cases.

- $d(q', p) \geq 0$. The point q' lies outside of B_p . The quantity $\sqrt{d(q', p)}$ can be understood as the length of the line segment from q' to the point of tangency with B_p , see Figure 1.1. The power distance is equal to zero precisely when q' lies on the boundary B_p .

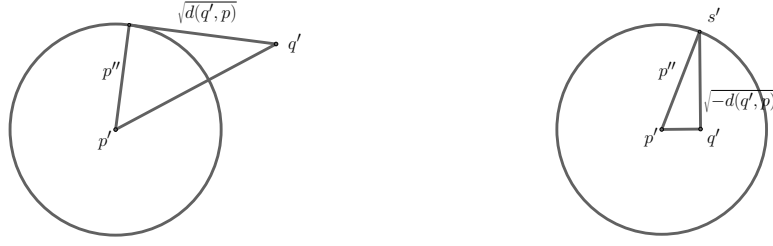


Figure 1.1: Geometrical interpretation of the power distance.

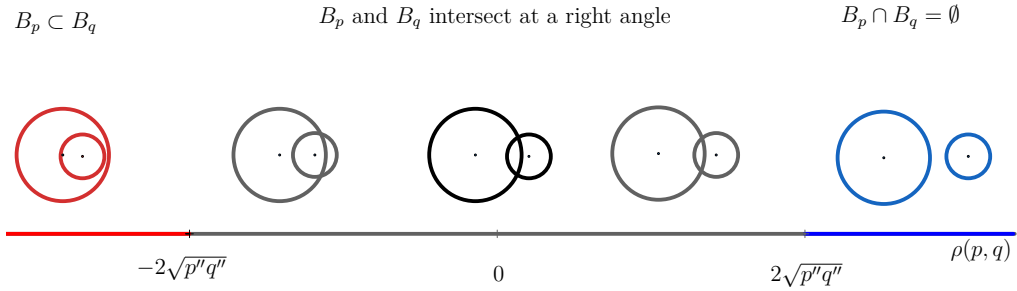


Figure 1.2: Geometrical interpretation of the power product. Horizontal scale depicts values of $\rho(p, q)$, diagrams show an illustration of the arrangement of the balls B_p and B_q .

- $d(q', p) < 0$. The point q' lies inside of B_p . The quantity $\sqrt{-d(q', p)}$ now describes the length of the segment $q's'$, where $s' \in S_p$ such that the triangle $\Delta p'q's'$ has a right angle $\angle p'q's'$, see Figure 1.1.

Definition 7. For two (marked) points $p = (p', p'')$ and $q = (q', q'')$, define their *power product*² by

$$\rho(p, q) = \|p' - q'\|^2 - p'' - q''.$$

Notice that $\rho(p, q) = d(q', p) - q'' = d(p', q) - p''$ and that $\rho(p, (q', 0)) = d(q', p)$.

Similarly to the power distance, the power product has a geometric interpretation that is vital to the understanding of the geometry of Laguerre tessellations.

Remark 2 (Geometric interpretation of the power product). Let $p, q \in \mathbb{R}^3 \times S$ be two points. The following observations follow immediately from the definition.

² The motivation for calling the quantity $\rho(p, q)$ a product is most fascinating. It was first introduced by G. Darboux in 1866 as a generalization of the power distance. However, it was later discovered that the spheres can be represented as vectors in a pseudo-Euclidean space where the power product plays the role of the quadratic form that defines the space, often called the inner product. The resulting space is then the Minkowski space — the setting in which the special theory of relativity is formulated. The positions of the sphere centres are then the positions in space, whereas the radius denotes a position in time. More can be found in e.g. Kocik [2007].

- $B_p \cap B_q = \emptyset$. We obtain $\|p' - q'\|^2 \geq (\sqrt{p''} + \sqrt{q''})^2 = p'' + q'' + 2\sqrt{p''}\sqrt{q''}$ and thus $\rho(p, q) \geq 2\sqrt{p''q''}$.
- $B_p \subset B_q$. We obtain $\|p' - q'\| + \sqrt{p''} \leq \sqrt{q''}$. Squaring the inequality yields $\rho(p, q) \leq -2\sqrt{p''q''}$.
- $B_p \cap B_q \neq \emptyset$ and neither of the balls is a proper subset of the other. This case is the most important for us. In this case, the spheres S_p and S_q intersect and $S_p \cap S_q$ is a circle. Denote $a' \in S_p \cap S_q$ the point of their intersection (it does not matter which one) and θ the angle $\angle p'a'q'$. We then obtain from the law of cosines that

$$-2\sqrt{p''q''} \cos \theta = \|p' - q'\|^2 - p'' - q'' = \rho(p, q).$$

Note that $\theta = \pi \Rightarrow \rho(p, q) = 0$.

The contents of this remark are illustrated in Figure 1.2

The above observations allow us to interpret the power product as a kind of distance of two marked points. The case $\rho(p, q) = 0$ is crucial for the Laguerre geometry. If p and q satisfy this equality then they are said to be *orthogonal*.

We are now well-equipped to define the central terms necessary for the definition of the Laguerre tetrahedrization.

Definition 8. Let $\eta \in \mathbf{N}_{gp}$. Define the *characteristic point* of η as the point $p_\eta = (p'_\eta, p''_\eta) \in \mathbb{R}^3 \times \mathbb{R}$ which is orthogonal to every $p \in \eta$. If such point exists, we call η *Laguerre-cospherical*.

An illustration of Laguerre-cospherical points can be found in Figure 1.3. For a comparison with the circumsphere, see Figure 1.4.

An alternative way to describe the characteristic point is by the equality

$$d(p'_\eta, p) = p''_\eta \text{ for each } p \in \eta. \quad (1.2)$$

Note that the mark of the characteristic point can be any real number and thus is not limited to $S = [0, W]$, unlike the points of \mathbf{x} . If its weight is positive, the characteristic point can be interpreted as a sphere that intersects each sphere $S_p, p \in \eta$ at a right angle. If negative, Edelsbrunner and Shah [1996] has suggested p_η to be thought of as a sphere with an imaginary radius.

The following proposition looks at the existence and uniqueness of the characteristic point.

Proposition 2 (Existence and uniqueness of the characteristic point). *Let $\eta \in \mathbf{N}_{gp}$. Then the following holds for the characteristic point p_η .*

1. *If $\text{card}(\eta) < 4$, then the p_η exists and is not unique.*
2. *If $\text{card}(\eta) = 4$, then the p_η exists and is unique.*
3. *If $\text{card}(\eta) > 4$, then the p_η exists if and only if η is Laguerre-cospherical.*

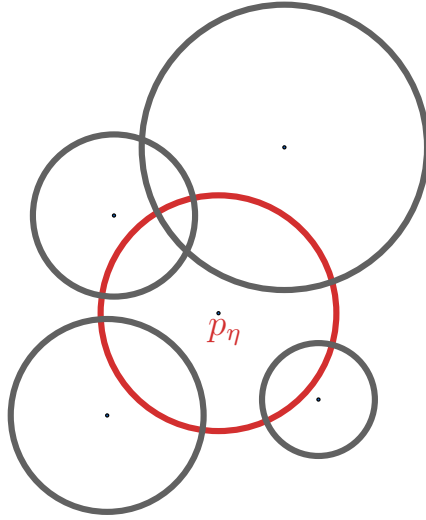


Figure 1.3: Laguerre-cospherical points in \mathbb{R}^2 . The characteristic point is in red.

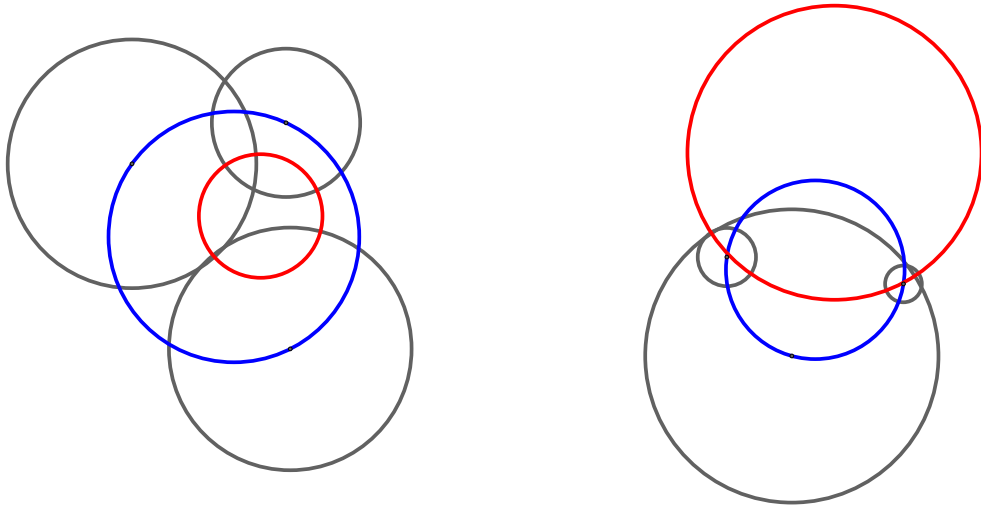


Figure 1.4: Illustration of the circumisphere (blue) and characteristic point (red). Note also that there is no simple relationship between the two objects.

Proof. . We will consider the case $\text{card}(\eta) = 4$, from which the proof of the other statements will be directly observable. Let $\eta = \{p_1, \dots, p_4\}$ and denote the coordinates of p'_i as $x_i, y_i, z_i, i = 1, \dots, 4$. The characteristic point p_η must satisfy the set of equations

$$\|p'_\eta - p'_i\|^2 - p''_\eta - p''_i = 0 \quad i = 1, \dots, 4.$$

If we denote $\alpha = x_\eta^2 + y_\eta^2 + z_\eta^2 - p''_\eta$, where (x_η, y_η, z_η) are the coordinates of p'_η , we obtain the equations

$$\alpha - 2x_i x_\eta - 2y_i y_\eta - 2z_i z_\eta = p''_i - x_i^2 - y_i^2 - z_i^2, i = 1, \dots, 4,$$

a system of equations which is linear with respect to $(\alpha, x_\eta, y_\eta, z_\eta)$. In an augmented matrix form, the system is written as

$$\left(\begin{array}{cccc|c} 1 & -2x_1 & -2y_1 & -2z_1 & p''_1 - x_1^2 - y_1^2 - z_1^2 \\ 1 & -2x_2 & -2y_2 & -2z_2 & p''_2 - x_2^2 - y_2^2 - z_2^2 \\ 1 & -2x_3 & -2y_3 & -2z_3 & p''_3 - x_3^2 - y_3^2 - z_3^2 \\ 1 & -2x_4 & -2y_4 & -2z_4 & p''_4 - x_4^2 - y_4^2 - z_4^2 \end{array} \right). \quad (1.3)$$

The fact that $\eta \in \mathbf{N}_{gp}$ implies that p'_1, \dots, p'_4 are affinely independent, i.e. not coplanar. This means that the homogeneous system of linear equations defined by the matrix

$$\left(\begin{array}{cccc} 1 & x_1 & y_1 & z_1 \\ 1 & x_2 & y_2 & z_2 \\ 1 & x_3 & y_3 & z_3 \\ 1 & x_4 & y_4 & z_4 \end{array} \right) \quad (1.4)$$

does not have a solution, that is, the matrix has full rank. The matrix (1.4) has the same column space as the left hand side of (1.3) and therefore the system has a unique solution.

If $\text{card}(\eta) < 4$, we would obtain an underdetermined system, having either infinitely many or no solutions. Here, again, the general position property gives us full row rank of the left side of the corresponding augmented matrix, implying that there are infinitely many solutions. For $\text{card}(\eta) = 2$, general position implies that the points are unequal. For $\text{card}(\eta) = 3$, general position implies that the points are not collinear.

If $\text{card}(\eta) > 4$, the system is overdetermined and has no solution, unless the whole augmented matrix has rank 4. For e.g. $|\eta| = 5$, this means that the homogeneous system given by the matrix

$$\left(\begin{array}{ccccc} 1 & x_1 & y_1 & z_1 & x_1^2 + y_1^2 + z_1^2 - p''_1 \\ 1 & x_2 & y_2 & z_2 & x_2^2 + y_2^2 + z_2^2 - p''_2 \\ 1 & x_3 & y_3 & z_3 & x_3^2 + y_3^2 + z_3^2 - p''_3 \\ 1 & x_4 & y_4 & z_4 & x_4^2 + y_4^2 + z_4^2 - p''_4 \\ 1 & x_5 & y_5 & z_5 & x_5^2 + y_5^2 + z_5^2 - p''_5 \end{array} \right) \quad (1.5)$$

has a solution. However, this is equivalent to saying that there exists p_η such that $\rho(p_\eta, p_i) = 0$ for all $i = 1, \dots, 5$, i.e. that η is Laguerre-cospherical. \square

Definition 9. Let $p, q \in \mathbb{R}^3 \times S$. We call the set

$$H(p, q) = \{x \in \mathbb{R}^3 : d(x, p) = d(x, q)\}$$

the *radical hyperplane* of p and q .

For the next proposition, recall that a hyperplane in \mathbb{R}^3 is a set of the form $\{x \in \mathbb{R}^3 : \langle y, x \rangle = a\}, y \in \mathbb{R}^3, a \in \mathbb{R}$.

Proposition 3. $H(p, q)$ is a hyperplane in \mathbb{R}^3 for any $p, q \in \mathbb{R}^3 \times S$. Let $\mathbf{x} \in \mathbf{N}_{gp}$ and $\eta = \{p_1, \dots, p_k\} \subset \mathbf{x}$, and $k = 2, 3, 4$. If

$$p' \in \bigcap_{i,j=1,\dots,k} H(p_i, p_j), \quad (1.6)$$

then p' is the position of a characteristic point of η . Lastly, if $|\eta| = 4$, then the uniquely defined characteristic point p_η is characterized by

$$p'_\eta = H(p_1, p_2) \cap H(p_1, p_3) \cap H(p_1, p_4). \quad (1.7)$$

Proof. By simple calculation we have

$$H(p, q) = \{x \in \mathbb{R}^3 : 2\langle q' - p', x \rangle = \|q'\|^2 - \|p'\|^2 - q'' + p''\}.$$

From (1.2) we obtain the characterization (1.6). For a tetrahedral η , we know from Proposition 2 that p_η is uniquely defined. To obtain (1.7), we only need to realize that three hyperplanes are sufficient to specify the set of points $x \in \mathbb{R}^3$ for which $d(x, p_i) = d(x, p_j), i, j = 1, \dots, 4$. \square

Notice that changing the weight of either of the points amounts to translation of the hyperplane.

We now introduce the equivalent of the empty ball property for the Laguerre case.

Definition 10. Let $x \in \mathbf{N}_{gp}$ be a configuration, $\eta \subset \mathbf{x}$ and p_η its characteristic point. We say that the pair (η, \mathbf{x}) is *regular*, or that η is *regular in \mathbf{x}* , if $\rho(p_\eta, p) \geq 0$ for all $p \in \mathbf{x}$. For convenience, for $\mathbf{x} \in \mathbf{N}_{lf} \setminus \mathbf{N}_{gp}$, we define any $\eta \subset \mathbf{x}$ that does not satisfy the assumptions of general position as not regular.

The condition in the definition can also be equivalently stated as

$$\text{There is no point } q \in \mathbf{x} \text{ such that } d(p'_\eta, q) < p''_\eta. \quad (1.8)$$

The regularity property ensures that no point of \mathbf{x} is closer to the characteristic point p_η in the power distance than the points of η . This is analogous to the empty ball property in Delaunay tetrahedrization, where the circumball plays the role of the characteristic point (see also Remark 5).

Definition 11. Let $\mathbf{x} \in \mathbf{N}_{lf}$. Define the set

$$\mathcal{LD}(\mathbf{x}) := \{\eta \subset \mathbf{x} : \eta \text{ is regular}\},$$

and its subsets

$$\mathcal{LD}_k(\mathbf{x}) := \{\eta \in \mathcal{LD}(\mathbf{x}) : \text{card}(\eta) = k\}, \quad k = 1, \dots, 4.$$

We then define the *Laguerre tetrahedrization of \mathbf{x}* as the set \mathcal{LD}_4 .

Remark 3 (Constructing Laguerre and Delaunay tetrahedrization). The proof of Proposition 2 also gives a hint on how to check whether η is regular. We have seen that the determinant of the matrix (1.5) is zero if and only if the five points are Laguerre-cospherical. However, the said determinant provides us with more information than that.

More specifically, we can use it to perform the so-called INCIRCLE test on five points p_1, \dots, p_5 to tell whether the point p_5 violates the regularity of the tetrahedron defined by p_1, \dots, p_4 . This amounts to checking the positivity of the determinant of (1.5), assuming the points p_1, \dots, p_4 are correctly oriented, which can be checked through the determinant of the matrix (1.4).

For details and a derivation, see Chapter 4 in Gavrilova [1998], which also contains a short description of the *incremental insertion* algorithm using *local transformations*, called *swaps* or *flips*. The algorithm was first presented in Lawson [1972] in two dimensions. For more information on the algorithm in three dimensions, see Joe [1989] and Joe [1991] for the Delaunay tetrahedrization, and Edelsbrunner and Shah [1996] for Laguerre tetrahedrization.

Remark 4 (Invariance in weights). Let $w \in \mathbb{R}$. Let

$$\mathbf{x}_w = \{(p', p'' + w) : (p', p'') \in \mathbf{x}\}$$

be the set of points of \mathbf{x} with added weight w . Take $\eta \in \mathcal{LD}(\mathbf{x})$ and the corresponding $\eta_w \in \mathcal{LD}(\mathbf{x}_w)$ such that $\eta' = \eta'_w$. Then η is regular in $\mathcal{LD}(\mathbf{x})$ if and only if η_w is regular in $\mathcal{LD}(\mathbf{x}_w)$. This follows from the fact that the point $p_{\eta_w} = (p'_\eta, p''_\eta - w)$ is a characteristic point of η_w and satisfies the definition of regularity for η_w . This implies that the Laguerre tetrahedrization is invariant under the map $\mathbf{x} \mapsto \mathbf{x}_w$ for any w such that the marks of \mathbf{x}_w still lie in $[0, W]$.

Remark 5 (Delaunay as a special case of Laguerre). Let $\mathbf{x} \in \mathbf{N}_{gp}$ be a configuration where all points have mark 0. Then for any $\eta \subset \mathbf{x}$, $\text{card}(\eta) = 4$ the ball B_{p_η} defined by the characteristic point of η becomes precisely $B(\eta)$, the circumball of η . Similarly η is regular if and only if η satisfies the empty ball property. Notice that by the previous remark, the same property must hold if we replace the mark 0 by any $w \in [0, W]$. Thus for a configuration \mathbf{x} with equal marks we have

$$\mathcal{D}_4(\mathbf{x}) = \mathcal{LD}_4(\mathbf{x})$$

and the Delaunay tetrahedrization can be seen as merely a special case of Laguerre tetrahedrization, albeit very important.

Redundant points

A major difference in the Laguerre case from the Delaunay case is the fact that some points may not play any role in the resulting structure.

Definition 12. We call a point $p \in \mathbf{x}$ *redundant in \mathbf{x}* if $\mathcal{LD}(\mathbf{x}) = \mathcal{LD}(\mathbf{x} \setminus \{p\})$.

To find more about redundant points, it is useful to introduce the notion of a Laguerre cell.

Definition 13. Let $p \in \mathbf{x}$. We then define the *Laguerre cell of p in \mathbf{x}* , denoted C_p , as the set

$$C_p := \{x' \in \mathbb{R}^3 : d(x', p) \leq d(x', q) \text{ for all } q \in \mathbf{x}\}.$$

Proposition 4. *A point p is redundant if and only if $C_p = \emptyset$.*

Proof. (\Leftarrow) Assume p is not redundant. That means there exists a regular $\eta \subset \mathbf{x}$ with a characteristic point p_η such that $\rho(q, p_\eta) = 0$ for all $q \in \eta$ and $\rho(q, p_\eta) \geq 0$ for all $q \in \mathbf{x}$. This however means that $d(p'_\eta, p) = p''_\eta \leq d(p'_\eta, q)$ for all $q \in \mathbf{x}$, implying $p'_\eta \in C_p$.

(\Rightarrow) Assume $C_p \neq \emptyset$. Then there exist $x' \in C_p$ and $q \in \mathbf{x}, q \neq p$, such that $d(x', q) = d(x', p)$, due to continuity of the power distance. But this implies that the point $p_\eta = (x', d(x', p))$ is the characteristic point of $\eta = \{p, q\}$ and that η is regular. \square

Apart from the empty Laguerre cell, there is, to our knowledge, no simple geometric characterization of a redundant point. There is however a necessary condition.

Proposition 5. *Let $\mathbf{x} \in \mathbf{N}_{lf}$. If p is redundant in \mathbf{x} , then the ball B_p is completely contained in the balls of other points in \mathbf{x} , that is*

$$B_p \subset \bigcup_{q \in \mathbf{x} \setminus \{p\}} B_q.$$

Proof. Assume there exists $x' \in B_p$ such that $x' \notin B_q$ for any $q \neq p$. Then $x' \in C_p$, since $d(x', p) \leq 0$, while $d(x', q) \geq 0$ for all $q \in \mathbf{x}, q \neq p$. \square

From the above proposition we can also see why there cannot be any redundant points in $\mathcal{D}(\mathbf{x})$, since in the Delaunay case all balls can be taken to have radius 0.

1.2 Hypergraph structures

Both Delaunay and Laguerre tetrahedrizations can be seen as graphs where two vertices $p, q \in \mathbf{x}$ are joined as an edge if they are part of the same tetrahedron with the empty ball property, or the regularity property. However, for the purposes of this text, a more natural structure will be the hypergraph, introduced into the analysis of Gibbs point processes in Dereudre et al. [2012].

1.2.1 Tetrahedrizations as hypergraphs

Before defining a hypergraph structure, we first define a σ -algebra on \mathbf{N}_{lf} and \mathbf{N}_f .

$$\mathcal{N}_{lf} = \sigma(\{\mathbf{x} \in \mathbf{N}_{lf} : \text{card}(\mathbf{x}' \cap B) = n\} : B \in \mathcal{B}_0, n \in \mathbb{N}_0).$$

We define \mathcal{N}_f as the trace of \mathcal{N}_{lf} on $(\mathbf{N}_{lf}, \mathcal{N}_{lf})$.

Definition 14. A *hypergraph structure* is a measurable subset \mathcal{E} of $(\mathbf{N}_f \times \mathbf{N}_{lf}, \mathcal{N}_f \otimes \mathcal{N}_{lf})$ such that $\eta \subset \mathbf{x}$ for all $(\eta, \mathbf{x}) \in \mathcal{E}$. We call η a *hyperedge* of \mathbf{x} and write $\eta \in \mathcal{E}(\mathbf{x})$, where $\mathcal{E}(\mathbf{x}) = \{\eta : (\eta, \mathbf{x}) \in \mathcal{E}\}$. For a given $\mathbf{x} \in \mathbf{N}_{lf}$, the pair $(\mathbf{x}, \mathcal{E}(\mathbf{x}))$ is called a *hypergraph*.

A hypergraph is thus a generalization of a graph in the sense that edges are now allowed to "join" any number of points and not just two. A hypergraph structure can be thought of as a rule that turns a configuration \mathbf{x} into the

hypergraph $(\mathbf{x}, \mathcal{E}(\mathbf{x}))$. The subsets $\eta \subset \mathbf{x}$ from Section 1.1 now play the role of hyperedges. e.g. tetrahedra.

The benefit of this approach is that we do not need to impose any additional structure on $\mathcal{D}(\mathbf{x})$ or $\mathcal{LD}(\mathbf{x})$ as they already define a hypergraph structure. Using the notation from Definitions 5 and 11, we can now introduce the Delaunay and Laguerre-Delaunay hypergraph structures.

Definition 15 (Delaunay and Laguerre-Delaunay hypergraph structures). Define the hypergraph structures

- $\mathcal{D} = \{(\eta, \mathbf{x}) : \eta \in \mathcal{D}(\mathbf{x})\},$
- $\mathcal{D}_k = \{(\eta, \mathbf{x}) : \eta \in \mathcal{D}_k(\mathbf{x})\}, k = 1, \dots, 4,$
- $\mathcal{LD} = \{(\eta, \mathbf{x}) : \eta \in \mathcal{LD}(\mathbf{x})\},$
- $\mathcal{LD}_k = \{(\eta, \mathbf{x}) : \eta \in \mathcal{LD}_k(\mathbf{x})\}, k = 1, \dots, 4.$

This text will focus on the tetrahedrizations \mathcal{D}_4 and \mathcal{LD}_4 .

Hyperedge potentials

The set \mathcal{E} defines the structure of the hypergraph. What we are ultimately interested in is assigning a numerical value to each hyperedge and thus to (a region of) the hypergraph. To this end, we define the *hyperedge potential*.

Definition 16. A *hyperedge potential* is a measurable function $\varphi : \mathcal{E} \rightarrow \mathbb{R} \cup \{+\infty\}$.

Hyperedge potential is *shift-invariant* if

$$(\vartheta_x \eta, \vartheta_x \mathbf{x}) \in \mathcal{E} \text{ and } \varphi(\vartheta_x \eta, \vartheta_x \mathbf{x}) = \varphi(\eta, \mathbf{x}) \text{ for all } (\eta, \mathbf{x}) \in \mathcal{E} \text{ and } x \in \mathbb{R},$$

where $\vartheta_x(\mathbf{x}) = \{(x', x'') \in \mathbb{R}^3 \times S : (x' + x, x'') \in \mathbf{x}\}$ is the translation of the positional part of the configurations by the vector $-x \in \mathbb{R}^3$.

For notational convenience, we set $\varphi = 0$ on \mathcal{E}^c .

The fact that the hyperedge potential contains \mathbf{x} as a second argument suggests that it is allowed to depend on points of \mathbf{x} other than those in η .

For the remainder of this text, we will always assume any hyperedge potential to be shift-invariant.

Example 1. (Hyperedge potentials) The hyperedge potential can take various forms. As we will see later, its specification radically alters the distribution of the resulting Gibbs point process and thus it allows a great freedom in the types of hypergraphs we can obtain.

Volume of tetrahedron: For $\eta \in \mathcal{E}(\mathbf{x})$ on \mathcal{D}_4 or \mathcal{LD}_4 define

$$\varphi(\eta, \mathbf{x}) = |\text{conv}(\eta)|,$$

where $\text{conv}(\eta)$ is the convex hull of the tetrahedral η .

Hard-core exclusion: For $\eta \in \mathcal{E}(\mathbf{x})$ on \mathcal{D}_4 or \mathcal{LD}_4 , $\alpha > 0$ define

$$\varphi(\eta, \mathbf{x}) = \chi(\eta) \quad \text{if } \chi(\eta) \leq \alpha,$$

$$\varphi(\eta, \mathbf{x}) = \infty \quad \text{if } \chi(\eta) > \alpha,$$

where $\chi(\eta) = \text{diam}B(\eta)$ is the diameter of the circumscribed ball. Notice that this potential becomes infinite on tetrahedra with circumdiameter larger than α . As we will see later, this allows us to restrict the resulting tetrahedrization to only tetrahedra η for which $\varphi(\eta, \mathbf{x}) \leq \alpha$.

Laguerre cell interaction: For $\eta \in \mathcal{E}(x)$ on \mathcal{LD}_2 such that $\eta = \{p, q\}$ and $|C_p| < \infty, |C_q| < \infty, \theta \neq 0$, define

$$\varphi(\eta, \mathbf{x}) = \theta \left(\frac{\max(|C_p|, |C_q|)}{\min(|C_p|, |C_q|)} - 1 \right)$$

where the potential now depends on the volume of neighboring Laguerre cells. Notice that θ can be negative, yielding a negative potential.

Tetrahedral interaction: In the present setting, we cannot specify interaction between tetrahedra in \mathcal{D}_4 or \mathcal{LD}_4 as easily as between Laguerre cells. This can be solved by for example defining a new hypergraph structure

$$\mathcal{LD}_4^2 = \{(\eta, \mathbf{x}) : \exists \eta_1, \eta_2 \in \mathcal{LD}_4(\mathbf{x}), \text{card}(\eta_1 \cap \eta_2) = 3, \eta = \eta_1 \cup \eta_2\},$$

which contains the quintuples of points which form adjacent tetrahedra in $\mathcal{LD}_4(\mathbf{x})$. Any hyperedge potential defined on this hypergraph structure would however need to take into account that the hyperedges can define two, three, or even four tetrahedra (see Joe [1991]).

Definition 17. A hyperedge potential ϕ is *unary* for the hypergraph structure \mathcal{E} if there exists a measurable function $\hat{\varphi} : \mathbf{N}_{lf} \rightarrow \mathbb{R} \cup \{+\infty\}$ such that

$$\varphi(\eta, \mathbf{x}) = \hat{\varphi}(\eta) \text{ for } \eta \in \mathcal{E}(\mathbf{x}).$$

The value of a unary hyperedge potential depends only on the points from η , as long as $\eta \in \mathcal{E}(x)$. Recall however the convention $\varphi = 0$ on \mathcal{E}^c , thus the equality above cannot be extended to all $\eta \subset \mathbf{x}$. In Example 1, only the first two potentials are unary. However, for the remainder of this text, we will assume all potentials to be unary.

For a given hypergraph structure \mathcal{E} , the *energy function* of a finite configuration $\mathbf{x} \in \mathbf{N}_f$ is defined as the function³

$$H(\mathbf{x}) = \sum_{\eta \in \mathcal{E}(\mathbf{x})} \varphi(\eta, \mathbf{x}).$$

However, in our case, we will typically deal with $\mathbf{x} \in \mathbf{N}_{lf}$, for this such potentials would typically be equal to $\pm\infty$ or even be undefined. We will therefore be interested in the energy for only a bounded window $\Lambda \in \mathcal{B}_0$. Currently, we do not have the necessary terms to describe such energy function precisely, thus we will postpone its definition to the next section.

The words *potential* and *energy* point to a connection with statistical mechanics, which gave rise to many of the concepts used in this text. Indeed, Gibbs measure and concepts related to them continue to be an area with a rich interplay between statistical mechanics and probability theory⁴.

³The energy H is often also called *Hamiltonian* in statistical mechanics.

⁴In fact, Gibbs measures, named after Josiah Willard Gibbs, stood at the forefront of emergence of statistical mechanics — Gibbs, who coined the term “statistical mechanics” was one of the founders of the field.

1.2.2 Hyperedge potentials and locality

A natural question to ask is “How do the hyperedges of $\mathcal{E}(\mathbf{x})$ influence each other?”. We have seen that there is a type of locality at play, for example the empty ball property of a tetrahedral $\eta \in \mathcal{D}_4(\mathbf{x})$ does not depend on the behaviour of \mathbf{x} outside $B(\eta)$. This section will refine our understanding of the question by examining different locality properties.

As we will see in Chapters 2 and 3, this locality is essential for the existence of our models and Gibbs measures in general.

Definition 18. A set $\Delta \in \mathcal{B}_0$ is a *finite horizon* for the pair $(\eta, \mathbf{x}) \in \mathcal{E}$ and the hyperedge potential φ if for all $\tilde{\mathbf{x}} \in \mathbf{N}_{lf}, \tilde{\mathbf{x}} = \mathbf{x}$ on $\Delta \times S$

$$(\eta, \tilde{\mathbf{x}}) \in \mathcal{E} \text{ and } \varphi(\eta, \tilde{\mathbf{x}}) = \varphi(\eta, \mathbf{x}).$$

The pair (\mathcal{E}, φ) satisfies the *finite-horizon property* if each $(\eta, \mathbf{x}) \in \mathcal{E}$ has a finite horizon.

The finite horizon of (η, \mathbf{x}) delineates the region outside which points can no longer violate the regularity (or the empty ball property) of η . Note also that for a unary potential, the finite horizon of $(\eta, \mathbf{x}) \in \mathcal{E}$ depends only on η .

Remark 6 (Finite horizons for \mathcal{D} and \mathcal{LD}). Let the hyperedge potential be given and assume it is unary.

For \mathcal{D} , the closed circumball $\bar{B}(\eta)$ itself is a finite horizon for (η, \mathbf{x}) .

For \mathcal{LD} , the situation is slightly more difficult. For one, $B(p'_\eta, \sqrt{p''_\eta})$ does not contain the points of η . To see this, take two points p, q with $p'', q'' > 0$ such that $\rho(p, q) = 0$. Then $q'' = d(q', p) < \|q' - p'\|^2$ and thus $\sqrt{q''} < \|q' - p'\|$. More importantly, however, any point s outside of $B(p'_\eta, \sqrt{p''_\eta})$ with a sufficiently large weight can violate the inequality $\rho(p_\eta, s) = \|p'_\eta - s'\|^2 - p''_\eta - s'' \geq 0$.

To obtain a finite horizon for \mathcal{LD} , we need to use the fact that the mark space is bounded, $S = [0, W]$. If $s'' \leq W$, then $\Delta = B(p'_\eta, \sqrt{p''_\eta + W})$ is sufficient as a horizon, since any point s outside Δ satisfies

$$\rho(p_\eta, s) = \|p'_\eta - s'\|^2 - p''_\eta - s'' \geq \left(\sqrt{p''_\eta + W}\right)^2 - p''_\eta - W = 0.$$

Let us now return again to the task of defining an energy function H that depends on the configuration in some bounded window $\Lambda \in \mathcal{B}_0$. To that end, we must define the set of hyperedges for which the hyperedge potential depends on the configuration inside Λ .

Definition 19. Let $\Lambda \in \mathcal{B}_0$. Define the set

$$\mathcal{E}_\Lambda(\mathbf{x}) := \{\eta \in \mathcal{E}(\mathbf{x}) : \varphi(\eta, \zeta \cup \mathbf{x}_{\Lambda^c}) \neq \varphi(\eta, \mathbf{x}) \text{ for some } \zeta \in \mathbf{N}_\Lambda\}.$$

Recall that we have defined $\varphi = 0$ on \mathcal{E}^c . This means that for $\eta \in \mathcal{E}(\mathbf{x})$ such that $\varphi(\eta, \mathbf{x}) \neq 0$ we have

$$\eta \notin \mathcal{E}(\zeta \cup \mathbf{x}_{\Lambda^c}) \text{ for some } \zeta \in \mathbf{N}_\Lambda \Rightarrow \eta \in \mathcal{E}_\Lambda(\mathbf{x}).$$

Notice that \mathbf{x}_Λ does not play any role in the definition in the sense that $\mathcal{E}_\Lambda(\mathbf{x}) = \mathcal{E}_\Lambda(\zeta \cup \mathbf{x})$ for any $\zeta \in \mathbf{N}_\Lambda$. The configuration \mathbf{x} thus only plays the role of a boundary condition.

We will use the symbols $\mathcal{D}_\Lambda(\mathbf{x})$ and $\mathcal{LD}_\Lambda(\mathbf{x})$ to denote the set $\mathcal{E}_\Lambda(\mathbf{x})$ when \mathcal{E} is Delaunay and Laguerre-Delaunay, respectively.

To further characterize $\mathcal{E}_\Lambda(\mathbf{x})$, we present the following lemma.

Lemma 1. *Let $\eta \in \mathcal{E}(\mathbf{x})$ have the finite horizon Δ . Then*

$$\eta \in \mathcal{E}_\Lambda(\mathbf{x}) \Rightarrow \Delta \cap \Lambda \neq \emptyset.$$

Proof.

$$\begin{aligned} \eta \in \mathcal{E}_\Lambda(\mathbf{x}) &\iff \exists \zeta \in \mathbf{N}_\Lambda : \varphi(\eta, \mathbf{x}) \neq \varphi(\eta, \zeta \cup \mathbf{x}_{\Lambda^c}) \\ &\Rightarrow \exists \zeta \in \mathbf{N}_\Lambda : \zeta' \cap \Delta \neq \emptyset \\ &\Rightarrow \Lambda \cap \Delta \neq \emptyset. \end{aligned}$$

□

With the definition of $\mathcal{E}_\Lambda(\mathbf{x})$, we are now ready for the desired definition of the energy function.

Definition 20. Let $\Lambda \in \mathcal{B}_0$, $\zeta \in \mathbf{N}_\Lambda$. The *energy of ζ in Λ with boundary condition \mathbf{x}* is given by the formula

$$H_{\Lambda, \mathbf{x}}(\zeta) = \sum_{\eta \in \mathcal{E}_\Lambda(\zeta \cup \mathbf{x}_{\Lambda^c})} \varphi(\eta, \zeta \cup \mathbf{x}_{\Lambda^c})$$

for $\zeta \in \mathbf{N}_\Lambda$, provided the sum is well-defined.

For the case $\zeta = \mathbf{x}_\Lambda$ we use the shortened notation $H_\Lambda(\mathbf{x}) := H_{\Lambda, \mathbf{x}}(\mathbf{x}_\Lambda)$.

Remark 7 ($\mathcal{E}_\Lambda(\mathbf{x})$ for \mathcal{D} and \mathcal{LD}). For \mathcal{D} , we have that

$$\eta \in \mathcal{D}_\Lambda(\mathbf{x}) \iff B(\eta) \cap \Lambda \neq \emptyset.$$

For \mathcal{LD} , using the characterization (1.8), we obtain

$$\eta \in \mathcal{LD}_\Lambda(\mathbf{x}) \iff d(p'_\eta; \Lambda) < \sqrt{p''_\eta + W},$$

where $d(p'_\eta; \Lambda) = \inf\{\|p'_\eta - x\| : x \in \Lambda\}$ is the distance of p'_η from Λ .

The final basic term again characterizes a type of finite-range property, this time as a property of the configuration \mathbf{x} .

Definition 21. Let $\Lambda \in \mathcal{B}_0$ be given. We say a configuration $\mathbf{x} \in N$ *confines the range of φ from Λ* if there exists a set $\partial\Lambda(\mathbf{x}) \in \mathcal{B}_0$ such that $\varphi(\eta, \zeta \cup \tilde{\mathbf{x}}_{\Lambda^c}) = \varphi(\eta, \zeta \cup \mathbf{x}_{\Lambda^c})$ whenever $\tilde{\mathbf{x}} = \mathbf{x}$ on $\partial\Lambda(\mathbf{x}) \times S$, $\zeta \in \mathbf{N}_\Lambda$ and $\eta \in \mathcal{E}_\Lambda(\zeta \cup \mathbf{x}_{\Lambda^c})$. In this case we write $\mathbf{x} \in \mathbf{N}_{\text{cr}}^\Lambda$. We denote $r_{\Lambda, \mathbf{x}}$ the smallest possible r such that $(\Lambda + B(0, r)) \setminus \Lambda$ satisfies the definition of $\partial\Lambda(\mathbf{x})$. We will use the abbreviation $\partial_\Lambda \mathbf{x} = \mathbf{x}_{\partial\Lambda(\mathbf{x})}$.

While the set $\mathcal{E}_\Lambda(\mathbf{x})$ contains hyperedges η which can be influenced by points in Λ , the set $\partial_\Lambda \mathbf{x}$ contains those points of \mathbf{x} that influence the potential of those η . This allows us to express $H_{\Lambda, \mathbf{x}}$ truly locally.

Proposition 6. *Let $\mathbf{x} \in \mathbf{N}_{\text{cr}}^\Lambda$. Then*

$$H_{\Lambda, \mathbf{x}}(\zeta) = \sum_{\eta \in \mathcal{E}_\Lambda(\zeta \cup \partial_\Lambda \mathbf{x})} \varphi(\eta, \zeta \cup \partial_\Lambda \mathbf{x}).$$

Proof. The definition of $\mathbf{N}_{\text{cr}}^\Lambda$ implies the hyperedge potential does not depend on the points $\mathbf{x} \setminus \partial_\Lambda \mathbf{x}$ and $\mathcal{E}_\Lambda(\mathbf{x})$ inherits this property by its definition through the hyperedge potential. \square

Remark 8 (Adding and removing points in \mathcal{D}_4 and \mathcal{LD}_4). Let $\mathbf{x} \in \mathbf{N}_{lf}$ be a configuration and $x \in (\mathbb{R}^3 \times S) \setminus \mathbf{x}$ a point outside the configuration. The question is: how does $\mathcal{LD}_4(\mathbf{x} \cup \{x\})$ differ from $\mathcal{LD}_4(\mathbf{x})$? First imagine we want to add the point x to \mathbf{x} . Denote the set

$$\mathcal{LD}_4^\otimes(x, \mathbf{x}) := \{\eta \in \mathcal{LD}_4(\mathbf{x}) : \rho(p_\eta, x) < 0\}.$$

Then this set contains precisely those tetrahedra, which cannot be present in $\mathcal{LD}_4(\mathbf{x} \cup \{x\})$, that is

$$\mathcal{LD}_4(\mathbf{x}) \setminus \mathcal{LD}_4(\mathbf{x} \cup \{x\}) = \mathcal{LD}_4^\otimes(x, \mathbf{x}).$$

Now take $\eta \in \mathcal{LD}_4(\mathbf{x} \cup \{x\})$ such that $x \notin \eta$. Then $\eta \notin \mathcal{LD}_4^\otimes(x, \mathbf{x})$ and thus $\eta \in \mathcal{LD}_4(\mathbf{x})$, yielding

$$\mathcal{LD}_4(\mathbf{x} \cup \{x\}) \setminus \mathcal{LD}_4(\mathbf{x}) = \{\eta \in \mathcal{LD}_4(\mathbf{x} \cup \{x\}) : x \in \eta\} =: \mathcal{LD}_4^\ell(x, \mathbf{x} \cup \{x\}).$$

Using the same logic we can now remove the point x from $\mathbf{x} \cup \{x\}$. This means we remove $\eta \in \mathcal{LD}_4^\ell(x, \mathbf{x} \cup \{x\})$ and add $\eta \in \mathcal{LD}_4^\otimes(x, \mathbf{x})$.

In \mathcal{D}_4 , we obtain similar sets

$$\mathcal{D}_4^\otimes(x, \mathbf{x}) := \{\eta \in \mathcal{D}_4(\mathbf{x}) : x \in B(\eta)\} \text{ and}$$

$$\mathcal{D}_4^\ell(x, \mathbf{x}) := \{\eta \in \mathcal{D}_4(\mathbf{x}) : x \in \eta\}.$$

We note that the sets denoted by \otimes stand for *conflicting* tetrahedra and the ℓ stands for tetrahedra *linked* to x .

2. Stochastic geometry

In the first chapter we introduced tetrahedrizations as hypergraph structures and defined their energy in terms of the hyperedge potential. Ultimately we want to study their behaviour under some probabilistic assumptions on the distribution of the configurations. In this chapter, the view is shifted from a configuration as a fixed deterministic set to a configuration being a particular realization of a random process.

We introduce the theory of point processes which will allow us to add stochasticity to the hypergraph structures. The main goal of this chapter is to introduce the Gibbs-type tessellation, where the locations of the points in the configurations are allowed to interact with the geometric properties of the tetrahedrization.

Section 2.1.1 introduces the basics of point processes, including the Poisson point process. The Poisson point process is a basis for Section 2.1.2, where we define finite point processes with density with respect to the Poisson point process. Finally in Section 2.2 we define the Gibbs point process as a point process with a density and show some of its properties.

2.1 Point processes

Here we develop only the bare minimum of the theory of point processes necessary to define and use Gibbs point processes. For a comprehensive introductory text, we recommend Møller and Waagepetersen [2003], as it is most relevant to our case.

In general, we assume E to be a locally compact separable space. This is the setting in many texts, such as Schneider and Weil [2008].

The main aim of this text is to build Gibbs point processes with interactions based on the Laguerre tetrahedrization. As such, the focus is on marked points and the Delaunay case is treated as secondary. To avoid having a dual marked and unmarked theory, we will treat unmarked point as a special case of marked points in the following way.

- Marked case: We take $E = \mathbb{R}^3 \times S$ where $S = [0, W]$, $W > 0$ is the space of marks. The measure on E is $z\lambda \otimes \mu$, where μ is a finite non-atomic measure governing the distribution of marks, $z > 0$.
- Unmarked case: We use the same space, but the distribution of marks $\mu = \delta_0$, where δ_0 is the Dirac delta function, is now concentrated on 0.

Denote $\tau = \lambda \otimes \mu$.

2.1.1 Basic terms

Definition 22. Define a *counting measure* on E as a measure ν on E for which

$$\nu(B) \in \mathbb{N} \cup \{0, \infty\}, B \in \mathcal{B}_0(E) \quad \text{and} \quad \nu(\{x\}) \leq 1, x \in E.$$

We say a measure ν is *locally finite* if $\nu(B) < \infty$ for any $B \in \mathcal{B}_0(E)$. Denote $\mathbf{N}_{lf}(E)$ the space of all locally finite counting measures on E . We equip the space $\mathbf{N}_{lf}(E)$ with the σ -algebra

$$\mathcal{N}_{lf}(E) = \sigma(\{\nu \in \mathbf{N}_{lf}(E) : \nu(B) = n : B \in \mathcal{B}_0(E), n \in \mathbb{N}_0\}).$$

We further define the set $\mathbf{N}_f(E) \subset \mathbf{N}_{lf}(E)$ of finite measures on E by

$$\mathbf{N}_f(E) = \{\nu \in \mathbf{N}_{lf}(E) : \nu(E) < \infty\}$$

with the σ -algebra \mathcal{N}_f defined as the trace σ -algebra of $\mathbf{N}_f(E)$ on $(\mathbf{N}_{lf}(E), \mathcal{N}_{lf}(E))$.

For the case $E = \mathbb{R}^3 \times S$, we use the shortened notation $\mathbf{N}_{lf}(\mathbb{R}^3 \times S) := \mathbf{N}_{lf}$. Similarly for the terms $\mathbf{N}_f, \mathcal{N}_f, \mathcal{N}_{lf}$. However, \mathcal{B} and \mathcal{B}_0 refers to the (bounded) Borel sets in \mathbb{R}^3 . To be able to limit the configurations to a specific set $\Lambda \in \mathcal{B}_0$, we define

$$\mathbf{N}_\Lambda = \{\nu \in \mathbf{N}_{lf} : \nu((\mathbb{R}^3 \setminus \Lambda) \times S) = 0\}$$

and the σ -algebra \mathcal{N}_Λ as its trace σ -algebra on \mathbf{N}_{lf} . Lastly we will need the σ -algebra $\tilde{\mathcal{N}}_\Lambda = \text{pr}_\Lambda^{-1}\mathcal{N}_\Lambda \subset \mathcal{N}_{lf}$, where $\text{pr}_\Lambda(\nu) = \nu|_{\Lambda \times S}$.

Remark 9 (Duality of locally finite counting measures and configurations). In Chapter 1, we introduced the sets \mathbf{N}_{lf} and \mathbf{N}_f as spaces of (finite) configurations — locally finite sets. This abuse of notation is justified by the fact that there is a measurable bijection between the space of locally finite counting measures (as defined here) and locally finite sets with the Borel σ -algebra on the Fell topology. For details, see Lemma 3.1.4. in Schneider and Weil [2008].

Whether a configuration is treated as a set or a counting measure will be clear from the context. With this in mind, we introduce the notation

$$x \in \nu \text{ if } \nu(\{x\}) = 1, \quad \nu \in \mathbf{N}_{lf}.$$

Definition 23. A *point process* on E is a measurable mapping $\Phi : (\Omega, \mathcal{A}, P) \rightarrow (\mathbf{N}_{lf}(E), \mathcal{N}_{lf}(E))$.

A *marked point process* Φ_m is a point process on $\mathbb{R}^3 \times S$ for which the projection $\Phi_m(\cdot \times S)$ is a point process on \mathbb{R}^3 .

Note that this definition requires the realizations of the projection of the marked point process to be locally finite counting measures in the sense of Definition 22.

Remark 10 (Simple point process). We have defined the counting measure to have values in $\{0, 1\}$. Such counting measures, as well as the point processes defined through them, are commonly called *simple*. We do not need this distinction here, therefore we do not use the term.

Poisson point process

The most important example of a point process is the Poisson point process which formalizes the notion of a complete spatial randomness. Before we define the Poisson point process, we first define a process closely related it.

Definition 24. Let ν be a measure on E , $B \in \mathcal{B}_0(E)$ such that $0 < \nu(B) < \infty$. For $n \in \mathbb{N}$ let X_1, \dots, X_n be independent and ν -uniformly distributed random variables on B , that is

$$P(X_i \in A) = \frac{\nu(A)}{\nu(B)}, \quad A \in \mathcal{B}(E), A \subset B.$$

Then we define the *binomial point process* of n points in B according to ν by

$$\Phi(n) = \sum_{i=1}^n \delta_{X_i}.$$

We use the convention $\sum_{i=1}^0 \delta_{X_i} = \emptyset$, where $\emptyset(E) = 0$ is the *empty point process*.

In the marked case, $X_i = (X'_i, M_i)$ where X'_i is the position and M_i the mark of X_i and we can write

$$\Phi(n) = \sum_{i=1}^n \delta_{(X'_i, M_i)}.$$

However, similarly to Chapter 1, we only specify the marks where needed, as this approach leads to a cleaner notation.

Proposition 7. Let $\Phi_n = \sum_{i=1}^n \delta_{X_i}$ be a binomial point process on $B \in \mathcal{B}_0(E)$ according to the measure ν . Then for a non-negative measurable function f and $k = 1, \dots, n$ we have

$$Ef(X_1, \dots, X_k) = \frac{1}{\nu(B)^k} \int_B \cdots \int_B f(x_1, \dots, x_k) \nu(dx_1) \cdots \nu(dx_k). \quad (2.1)$$

Proof. From the definition of Φ_n , we have for Borel $A_i \subset B, i = 1, \dots, k$ that

$$\begin{aligned} P(X_1 \in A_1, \dots, X_k \in A_k) &= P(X_1 \in A_1) \cdots P(X_k \in A_k) \\ &= \frac{1}{\nu(B)^k} \int_B \cdots \int_B 1_{A_1}(x_1) \cdots 1_{A_k}(x_k) \nu(dx_1) \cdots \nu(dx_k). \end{aligned}$$

That is (2.1) for $f(x_1, \dots, x_k) = 1_{A_1}(x_1) \cdots 1_{A_k}(x_k)$. By a standard argument, we first extend this to a general set $C \in \mathcal{B}^k(E), C \subset B^k$ using the Dynkin system

$$\{C \in \mathcal{B}^k(E) : E1_C(x_1, \dots, x_k) = \int \cdots \int 1_C(x_1, \dots, x_k) dx_1 \cdots dx_k\}$$

and then from indicators to any non-negative measurable function. \square

Using the binomial point process, we are ready to define the Poisson point process.

Definition 25. Let ν be a measure on E . A point process Φ satisfying

1. $\Phi(B)$ has a Poisson distribution with parameter $\nu(B)$ for each $B \in \mathcal{B}_0(E)$,
2. Conditionally on $\Phi_B = n, n \in \mathbb{N}$, $\Phi|_B$ is the binomial point process of n points in B , $B \in \mathcal{B}_0(E)$,

is a *Poisson process* on E with *intensity measure* ν . For $B \in \mathcal{B}_0(E)$, denote Π_B^ν the distribution of a Poisson point process with intensity measure ν restricted to B .

Definition 26. We define the *marked Poisson process* as a Poisson process on $\mathbb{R}^3 \times S$ with intensity measure $z\lambda \otimes \mu$. We call the parameter z the *intensity*. For $\Lambda \in \mathcal{B}_0$, denote Π_Λ^z the distribution of a marked Poisson point process with intensity $z\lambda \otimes \mu$ restricted to $\Lambda \times S$. For $z = 1$, we lose the z and denote the distribution simply Π_Λ .

Note that thanks to Proposition 7 we have for a marked Poisson process Φ with intensity z and $\Gamma \in \mathcal{N}_{lf}$

$$\begin{aligned} \Pi_\Lambda^z(\Gamma) &= P(\Phi \in \Gamma) = \sum_{k=0}^{\infty} P(\Phi \in \Gamma | \Phi(\Lambda) = k) P(\Phi(\Lambda) = k) \\ &= \sum_{k=0}^{\infty} \frac{(z|\Lambda|)^k}{k!} e^{-z|\Lambda|} P(\Phi^{(k)} \in \Gamma) \\ &= \sum_{k=0}^{\infty} \frac{z^k}{k!} e^{-z|\Lambda|} \int_{\Lambda \times S} \cdots \int_{\Lambda \times S} 1_\Gamma \left(\sum_{i=1}^k \delta_{X_i} \right) \tau(dx_1), \dots, \tau(dx_k) \end{aligned} \quad (2.2)$$

where $\Phi^{(k)} = \sum_{i=1}^k \delta_{(X_i, M_i)}$ denotes the binomial point process of k points in Λ .

Remark 11 (Points in general position). In Section 1.1 we introduced the sets \mathbf{N}_{gp} and \mathbf{N}_{rgp} . In Zessin [2008], it is proved¹ that these sets are measurable and that for $\Lambda \in \mathcal{B}_0$

$$\Pi_\Lambda^z(\mathbf{N}_{gp}) = \Pi_\Lambda^z(\mathbf{N}_{rgp}) = 0.$$

2.1.2 Finite point processes with density

A standard approach in probability theory is to define random variables with distributions absolutely continuous with respect to some reference measure. In Euclidean spaces, the reference measure is typically the Lebesgue or counting measure. In the space $(\mathbf{N}_{lf}, \mathcal{N}_{lf})$ the convenient properties of the Poisson point process make it the perfect candidate for the reference measure. In this chapter, we choose a fixed $\Lambda \in \mathcal{B}_0$ and restrict ourselves only to the space $(\mathbf{N}_\Lambda, \mathcal{N}_\Lambda)$ of finite counting measures. In this chapter, we limit ourselves entirely to the case $E = \mathbb{R}^3 \times S$. At the same time, we will stop using the term “marked” where we deem it redundant.

Definition 27. We say that a point process Ψ on $\mathbb{R}^3 \times S$ has the *density* p with respect to the Poisson process if its distribution is absolutely continuous w.r.t. Π_Λ with density function p . That is there exists a measurable function $p : \mathbf{N}_\Lambda \rightarrow \mathbb{R}^+$ such that $\int p(\gamma) \Pi_\Lambda(d\gamma) = 1$ and

$$P(\Psi \in \Gamma) = \int_\Gamma p(\gamma) \Pi_\Lambda(d\gamma), \quad \Gamma \in \mathcal{N}_\Lambda.$$

¹This fact seems to have been generally accepted as true in the literature for decades, yet — as far as we are aware — no formal proof was ever published until 2008.

Notice that using the calculations in Proposition 7 and (2.2) we have

$$P(\Psi \in \Gamma) = \sum_{k=0}^{\infty} \frac{1}{k!} e^{-|\Lambda|} \int_{\Lambda \times S} \cdots \int_{\Lambda \times S} 1_{\Gamma} \left(\sum_{i=1}^k \delta_{X_i} \right) p \left(\sum_{i=1}^k \delta_{X_i} \right) \tau(dx_1) \cdots \tau(dx_k).$$

The equation above is a special case of

$$Eh(\Psi) = Eh(\Phi)p(\Phi)$$

for Π_{Λ} -measurable function h , where $\Phi \sim \Pi_{\Lambda}$.

An example of a point process with a density, albeit uninteresting, is the Poisson process with intensity z , as the next proposition shows.

Denote the *counting function* for $\Delta \in \mathcal{B}_0$ and $\gamma \in \mathbf{N}_{lf}$:

$$N_{\Delta}(\gamma) = \gamma(\Delta \times S).$$

Proposition 8. $\Pi_{\Lambda}^z \ll \Pi_{\Lambda}$ with density $p(\gamma) = z^{N_{\Lambda}(\gamma)} \exp(|\Lambda|(1-z))$, $\gamma \in \mathbf{N}_{\Lambda}$.

Proof. Denote $\Phi \sim \Pi_{\Lambda}$, we have for $\Gamma \in \mathcal{N}_f$, using Proposition 7 and (2.2)

$$\Pi_{\Lambda}^z(\Gamma) = E(1_{\Gamma}(\Phi) z^{|\Phi|} e^{|\Lambda|} e^{-z|\Lambda|}).$$

□

2.2 Gibbs Point Processes

At the end of the last section we have found that $\Pi_{\Lambda}^z \ll \Pi_{\Lambda}$ with the density $p(\gamma) \propto z^{N_{\Lambda}(\gamma)}$. The introduction of the Gibbs point process is outwardly simple, since we merely add an additional term containing the energy function from Definition 20, so that the density is proportional to the expression

$$z^{N_{\Lambda}(\gamma)} e^{-H_{\Lambda}(\gamma)}. \tag{2.3}$$

By this seemingly small alteration we introduce a great complexity into the structure of the resulting process. Before we proceed with the formal definition of (finite volume) Gibbs point processes and their distribution, (finite volume) Gibbs measures, we must state some additional assumptions on the energy function.

2.2.1 The energy function

Thanks to the energy function, we can force the realizations of the finite volume GPP to obey a diverse set of geometrical properties. In our case those geometrical properties are expressed through the hypergraph structures \mathcal{D} and \mathcal{LD} , see Example 1.

In the following, we restrict ourselves to \mathbf{N}_f and for $\gamma \in \mathbf{N}_f$ we denote $H(\gamma) := H_{\mathbb{R}^3}(\gamma)$.

Traditionally, the energy function is required to satisfy some assumptions. Here we list those from Dereudre [2017].

- **Non-degeneracy:**

$$H(\emptyset) < +\infty.$$

- **Heredity:** For any $\gamma \in \mathbf{N}_f$ and $x \in \gamma$

$$H(\gamma) < +\infty \Rightarrow H(\gamma - \delta_x) < +\infty.$$

- **Stability:** there exists a constant $c_S \geq 0$ such that for any $\gamma \in \mathbf{N}_f$

$$H(\gamma) \geq c_S \cdot N_{\mathbb{R}^3}(\gamma).$$

Recall also that we assumed all potentials to be shift-invariant and thus any energy function inherits this property.

Stability bounds the density function $p(\gamma) \propto z^{N_\Lambda(\gamma)} e^{-H(\gamma)} \leq (ze^{-c_S})^{N_\Lambda(\gamma)}$ and thus ensures $Z_\Lambda^z < \infty$. Integrability of the density is obviously a necessary assumption and thus some form of stability cannot be avoided. Non-degeneracy, when paired with heredity, is a very natural assumption; without it, heredity would imply that the energy is always infinite.

The form (2.3) of the density function suggests that the resulting distribution will favor configurations with low energy. Configurations with high energy are unlikely to happen and an infinite energy means that the configuration is, with probability 1, not possible under the distribution. We call such a configuration *forbidden*. A configuration that is not forbidden is *permissible*.

Heredity ensures that removing a point will not result in a forbidden configuration. Equivalently it ensures that adding a point to a forbidden configuration will not result in an allowed configuration. This assumption is, however, not necessarily satisfied by our tessellation models. Take for example the hard-core exclusion potential from Example 1. Removing a point can lead to appearance of a tetrahedron with a larger circumdiameter, thus resulting in a forbidden configuration.

Unlike non-degeneracy or stability, it is not immediately clear what the role of heredity is. Luckily for us, it means that we can define Gibbs point processes without this assumption and only then explore its function.

2.2.2 Finite volume Gibbs point processes

We first define the finite counterpart of the Gibbs point process.

Definition 28. Let \mathcal{E} be a hypergraph structure and H an energy function on \mathcal{E} such that H is non-degenerate and stable. The *finite volume Gibbs measure* on $\Lambda \in \mathcal{B}_0$ with activity $z > 0$ is the distribution P_Λ^z such that $P_\Lambda^z \ll \Pi_\Lambda$ with density

$$p(\gamma) = \frac{1}{Z_\Lambda^z} z^{\gamma(\Lambda)} e^{-H(\gamma)}, \quad \gamma \in \mathbf{N}_f,$$

where $Z_\Lambda^z = \int z^{N_\Lambda} e^{-H} d\Pi_\Lambda$ is the normalizing constant, called *partition function*. The point process with the distribution P_Λ^z is called the *finite volume Gibbs point process* (finite volume GPP).

Before we proceed further, we must state one technical lemma.

Lemma 2. *Let $\Delta, \Lambda \in \mathcal{B}_0$ such that $\Delta \subset \Lambda$. There exists a measurable function $\psi_{\Delta, \Lambda} : \mathbf{N}_{lf} \rightarrow \mathbb{R} \cup \{+\infty\}$ such that*

$$\forall \gamma \in \mathbf{N}_{lf}, \quad H_{\Lambda}(\gamma) = H_{\Delta}(\gamma) + \psi_{\Delta, \Lambda}(\gamma_{\Delta^c}).$$

Proof. To find such function, we only need to realize that

$$H_{\Lambda}(\gamma) - H_{\Delta}(\gamma) = \sum_{\eta \in \mathcal{E}_{\Lambda}(\gamma) \setminus \mathcal{E}_{\Delta}(\gamma)} \varphi(\eta, \gamma)$$

depends only on γ_{Δ^c} . As noted below the Definition 19, both $\mathcal{E}_{\Delta}(\gamma)$ and $\mathcal{E}_{\Lambda}(\gamma)$ depend only on γ outside the window Λ and Δ respectively. By $\eta \notin \mathcal{E}_{\Delta}(\gamma)$ we have that $\forall \zeta \in \mathbf{N}_{\Delta} : \varphi(\eta, \gamma) = \varphi(\eta, \zeta \cup \gamma_{\Delta^c})$ and thus we can set

$$\psi_{\Delta, \Lambda}(\gamma_{\Delta^c}) = \sum_{\eta \in \mathcal{E}_{\Lambda}(\gamma_{\Delta^c}) \setminus \mathcal{E}_{\Delta}(\gamma_{\Delta^c})} \varphi(\eta, \gamma_{\Delta^c}).$$

□

An important characterization are the **Dobrushin-Lanford-Ruelle (DLR) equations**.

Proposition 9. *Let $\Delta, \Lambda \in \mathcal{B}_0$ with $\Delta \subset \Lambda$. Then for P_{Λ}^z -a.s. all γ_{Δ^c}*

$$P_{\Lambda}^z(d\gamma_{\Delta} | \gamma_{\Delta^c}) = \frac{1}{Z_{\Delta}^z(\gamma_{\Delta^c})} z^{N_{\Delta}(\gamma)} e^{-H_{\Delta}(\gamma)} \Pi_{\Delta}(d\gamma_{\Delta}),$$

where $Z_{\Delta}^z(\gamma_{\Delta^c}) = \int z^{N_{\Delta}(\gamma)} e^{-H_{\Delta}(\gamma)} \Pi_{\Delta}(d\gamma_{\Delta})$ is the normalizing constant.

Proof. Can be proved using the proof in Proposition 3 in Dereudre [2017] if we use our definition of $H_{\Delta}(\gamma)$ and the equality $H_{\Delta}(\gamma) = H_{\Lambda}(\gamma) + \psi_{\Delta, \Lambda}(\gamma_{\Delta^c})$, where $\psi_{\Delta, \Lambda}$ is the function from Lemma 2. □

The DLR equations express the conditional probability of configurations inside the window Δ , given the configuration outside it (boundary condition).

2.2.3 Infinite volume Gibbs point processes

As noted in section 1.2, without extra assumptions on γ , such as the range confinement, the energy H may not be well-defined. We will therefore restrict our definition of infinite volume Gibbs measures only to configurations γ such that $\gamma \in \mathbf{N}_{cr}^{\Lambda}$ for every $\Lambda \in \mathcal{B}_0$. We will learn in Proposition 13 that this restriction does not limit us in any way.

First, let $\Theta = (\vartheta_x)_{x \in \mathbb{R}^3}$ be the translation group defined by the translations ϑ_x from Definition 16. Let \mathcal{P}_{Θ} denote the set of all Θ -invariant probability measures on $(\mathbf{N}_{lf}, \mathcal{N}_{lf})$ with $\int N_{[0,1]^3} dP < \infty$.

Definition 29. Let \mathcal{E} be a hypergraph structure and H an energy function on \mathcal{E} such that H is non-degenerate and stable. A probability measure $P \in \mathcal{P}_{\Theta}$ on $(\mathbf{N}_{lf}, \mathcal{N}_{lf})$ is the (*infinite volume*) *Gibbs measure* with activity $z > 0$ if $P(\mathbf{N}_{cr}^{\Lambda}) = 1$ and

$$\int f dP = \int_{\mathbf{N}_{cr}^{\Lambda}} \frac{1}{Z_{\Lambda}^z(\gamma)} \int_{\mathbf{N}_{\Lambda}} f(\zeta \cup \gamma_{\Lambda^c}) e^{-H_{\Lambda}(\gamma \cup \zeta)} \Pi_{\Lambda}^z(d\zeta) P(d\gamma) \quad (2.4)$$

for every $\Lambda \in \mathcal{B}_0$ and every measurable $f : \mathbf{N}_{lf} \rightarrow [0, \infty)$. A point process whose distribution is a Gibbs measure is called a (*infinite volume*) *Gibbs point process*.

If we use the hypergraph structures \mathcal{D}_4 or \mathcal{LD}_4 , then we call the resulting GPP a *Gibbs-type tetrahedrization*.

The definition is a direct analogue of the DLR equations for finite volume GPP. In fact it is the same relationship, only expressed in integral form.

While defining the Gibbs measure is relative straight-forward, proving its existence is not. The existence and uniqueness of Gibbs measures is an active field of research and one where we still currently do not know much, particularly in case of uniqueness. We will not delve into the topic any further here and we refer the reader to an introductory text Dereudre [2017] and the paper on which we base the proof of existence (Chapter 3) for our models, Dereudre et al. [2012]. We also recommend reading the introduction to Georgii [2011] — although the book is about Gibbs random fields rather than point processes, the introduction gives an intuitive explanation for the form of the density and in particular the connection of the non-uniqueness with phase transitions.

2.2.4 Hereditary GPP

One of the disadvantages of the characterization through DLR equations is the presence of the normalization constant, as it is, in most cases, unknown. This is where the use of the heredity assumption comes in.

For $\gamma \in \mathbf{N}_f$ and $x \in \mathbb{R}^3 \times S$, for a hereditary energy function H , define the *local energy* of x in γ as

$$h(x, \gamma) = H(\gamma + \delta_x) - H(\gamma),$$

with the convention $+\infty - (+\infty) = 0$.

We then obtain the following result, known as the **Georgii-Nguyen-Zessin (GNZ) equation**.

Proposition 10. *Let P be a Gibbs measure and $\Lambda \in \mathcal{B}$ such that $|\Lambda| > 0$. For any non-negative measurable function f from $(\mathbb{R}^3 \times S) \times \mathbf{N}_{lf}$ to \mathbb{R} ,*

$$\int \sum_{x \in \gamma} f(x, \gamma - \delta_x) P(d\gamma) = z \int \int_{\Lambda \times S} f(x, \gamma) e^{-h(x, \gamma)} \tau(dx) P(d\gamma). \quad (2.5)$$

Furthermore, Gibbs measures are uniquely defined by (2.5) in the sense that if a probability measure P on \mathbf{N}_f satisfies (2.5), then P is a Gibbs measure.

Proof. The marked case is a direct adaptation of Nguyen and Zessin [1979], see e.g. Mase [2000]. \square

Heredity thus gives us a powerful characterization of the Gibbs measure which, as noted previously, is not always available in the Gibbs-type tetrahedrizations defined here.

Luckily, the approach in Dereudre and Lavancier [2009] allows us to directly use the GNZ equation even for the non-hereditary case.

2.2.5 Non-hereditary GPP

Having defined the Gibbs measure, we can now present the approach of Dereudre and Lavancier [2009] in extending the GNZ equation to Gibbs point processes with non-hereditary energy functions. First define

$$\mathbf{N}_\infty = \{\mathbf{x} \in \mathbf{N}_{lf} : \forall \Lambda \in \mathcal{B}_0 : H_\Lambda(\mathbf{x}) < \infty\},$$

the set of all permissible configurations.

Definition 30. Let $\gamma \in \mathbf{N}_\infty$. We say $x \in \gamma$ is *removable* if

$$\text{there exist } \Lambda \in \mathcal{B} \text{ such that } x \in \Lambda \text{ and } H_\Lambda(\gamma - \delta_x) < \infty.$$

Proposition 11. Let $\gamma \in \mathbf{N}_\infty$, then $x \in \gamma$ is removable if and only if $\gamma - \delta_x \in \mathbf{N}_\infty$.

Proof. Follows from Lemma 2 above and Proposition 1 in Dereudre and Lavancier [2009]. \square

Definition 31. Let x be a removable point in a configuration $\gamma \in \mathbf{N}_\infty$. The local energy of x in $\gamma - \delta_x$ is defined as

$$h(x, \gamma - \delta_x) = H_\Lambda(\gamma) - H_\Lambda(\gamma - \delta_x)$$

where $\Lambda \in \mathcal{B}_0$ such that $x \in \Lambda$. For convenience, we set $h(x, \gamma) = 0$ if $x \in \gamma$.

Let us remark that the set Λ always exists by Definition 30 and that the value of $h(x, \gamma - \delta_x)$ does not depend on the choice of Λ as a consequence of Lemma 2.

Proposition 12. Let P be a stationary Gibbs measure. For every bounded non-negative measurable $f : (\mathbb{R}^3 \times S) \times \mathbf{N}_{lf} \rightarrow \mathbb{R}$ we have

$$\int 1_{\mathbf{N}_\infty}(\gamma - \delta_x) \sum_{x \in \gamma} f(x, \gamma - \delta_x) P(d\gamma) = z \int \int f(x, \gamma) e^{-h(x, \gamma)} \tau(dx) P(d\gamma).$$

Proof. See Proposition 2 in Dereudre and Lavancier [2009]. \square

Note that we lose the converse implication. That is the GNZ equation no longer characterizes Gibbs point process with non-hereditary energy function. Imagine a measure P under which γ a.s. does not contain any removable points. The equation then becomes the trivial equation $0 = 0$.

Remark 12 (Measurability). Many of the quantities introduced thus far are only measurable with respect to the universal completion of the σ -algebras introduced. We will not deal with this further here and refer the reader to Remark 2.1. and Remark 3.7. in Dereudre et al. [2012] for more details.

3. Existence of Gibbs-type models

In this chapter, the theorem from Dereudre et al. [2012] will be presented and then we will proceed to verify its assumptions for our models. In this chapter, as well as in the remainder of this text, we will assume the mark distribution μ for \mathcal{LD} models to be equal to the Lebesgue measure on S .

3.1 Existence theorem

In this section we first state the two existence theorems from Dereudre et al. [2012]. The assumptions **(S)**, **(R)**, **(U)** and **(\hat{U})** are introduced in the following sections.

Theorem 1. *For every hypergraph structure \mathcal{E} , hyperedge potential φ and activity $z > 0$ satisfying **(S)**, **(R)** and **(U)** there exists at least one Gibbs measure.*

Theorem 2. *For every hypergraph structure \mathcal{E} , hyperedge potential φ and activity $z > 0$ satisfying **(S)**, **(R)** and **(\hat{U})** there exists at least one Gibbs measure.*

Proofs of both theorems can be found in Dereudre et al. [2012], see also Remark 3.7. in the same paper about the marked case.

3.1.1 Stability

A standard assumption without which it is impossible to define the Gibbs measure is the stability assumption.

(S) Stability. The energy function H is called *stable* if there exists a constant $c_S \geq 0$ such that

$$H_{\Lambda, \mathbf{x}}(\zeta) \geq -c_S \cdot \text{card}(\zeta \cup \partial_{\Lambda} \mathbf{x})$$

for all $\Lambda \in \mathcal{B}_0, \zeta \in \mathbf{N}_{\Lambda}, \mathbf{x} \in \mathbf{N}_{\text{cr}}^{\Lambda}$.

Note that when φ is non-negative, then we can simply choose $c_S = 0$. We will only deal with models whose potentials will be non-negative, leading to the following assumption.

Assumption 1: All hyperedge potentials in the remainder of this text are assumed to be non-negative.

3.1.2 Range condition

As stated previously, the fact that the hypergraph structures posses a type of locality property is crucial for the existence of Gibbs measures. The simplest such assumption is the *finite range* assumption, see Definition 7 in Dereudre [2017]. Finite range roughly means that there exists $R > 0$ such that the energy

of \mathbf{x} in Λ only depends on points in $\Lambda + b(0, R)$. This is a strong assumption and one that is not fulfilled by our models.

This is reflected in part in the range condition introduced here and later in the uniform confinement condition (3.1).

(R) Range condition. There exist constants $\ell_R, n_R \in \mathbb{N}$ and $\chi_R < \infty$ such that for all $(\eta, \mathbf{x}) \in \mathcal{E}$ there exists a finite horizon Δ satisfying: For every $x, y \in \Delta$ there exist ℓ open balls B_1, \dots, B_ℓ (with $\ell \leq \ell_R$) such that

- the set $\cup_{i=1}^\ell \bar{B}_i$ is connected and contains x and y , and
- for each i , either $\text{diam} B_i \leq \chi_R$ or $N_{B_i}(\mathbf{x}) \leq n_R$.

Apart from being one of the assumptions necessary for the existence, the range condition also gives us the following result we used in the definition of GPP.

Proposition 13. *Let $\Lambda \in \mathcal{B}_0$. Under the range assumption (R), there exists a set $\hat{\mathbf{N}}_{cr}^\Lambda \in \tilde{\mathcal{N}}_{\Lambda^c}$ such that $\hat{\mathbf{N}}_{cr}^\Lambda \subset \mathbf{N}_{cr}^\Lambda$ and $P(\hat{\mathbf{N}}_{cr}^\Lambda) = 1$ for all $P \in \mathcal{P}_\Theta$ with $P(\emptyset) = 0$.*

Proof. Can be found in Theorem 5.4. in Dereudre et al. [2012]. See also Remark 3.7. in connection to the marked case. \square

The proposition shows that any Θ -invariant probability measure on $(\mathbf{N}_{lf}, \mathcal{N}_{lf})$ is concentrated on the set \mathbf{N}_{cr}^Λ for any $\Lambda \in \mathcal{B}_0$, justifying the restriction in our definition of the Gibbs measure (Definition 29).

3.1.3 Upper regularity

In order to present the upper regularity conditions, we introduce the notion of *pseudo-periodic* configurations.

Let $M \in \mathbb{R}^{3 \times 3}$ be an invertible 3×3 matrix with column vectors (M_1, M_2, M_3) . For each $k \in \mathbb{Z}^3$ define the cell

$$C(k) = \{Mx \in \mathbb{R}^3 : x - k \in [-1/2, 1/2]^3\}.$$

These cells partition \mathbb{R}^3 into parallelepipeds, i.e. solids whose six faces are all parallelograms. We write $C = C(0)$. Let $\Gamma \in \mathcal{N}_C$ be non-empty. Then we define the *pseudo-periodic* configurations $\bar{\Gamma}$ as

$$\bar{\Gamma} = \{\mathbf{x} \in \mathbf{N}_{lf} : \vartheta_{Mk}(\mathbf{x}_{C(k)}) \in \Gamma \text{ for all } k \in \mathbb{Z}^3\},$$

the set of all configurations whose restriction to $C(k)$, when shifted back to C , belongs to Γ . The prefix pseudo- refers to the fact that the configuration itself does not need to be identical in all $C(k)$, it merely needs to belong to the same class of configurations.

(U) Upper regularity. M and Γ can be chosen so that the following holds.

(U1) *Uniform confinement:* $\bar{\Gamma} \subset \mathbf{N}_{cr}^\Lambda$ for all $\Lambda \in \mathcal{B}_0$ and

$$r_\Gamma := \sup_{\Lambda \in \mathcal{B}_0} \sup_{\mathbf{x} \in \bar{\Gamma}} r_{\Lambda, \mathbf{x}} < \infty. \quad (3.1)$$

(U2) *Uniform summability*:

$$c_\Gamma := \sup_{\mathbf{x} \in \bar{\Gamma}} \sum_{\eta \in \mathcal{E}(\mathbf{x}) : \eta' \cap C \neq \emptyset} \frac{\varphi(\eta, \mathbf{x})}{\#(\hat{\eta})} < \infty,$$

where $\hat{\eta} := \{k \in \mathbb{Z}^3 : \eta \cap C(k) \neq \emptyset\}$.

(U3) *Strong non-rigidity*: $e^{z|C|}\Pi_C^z(\Gamma) > e^{c_\Gamma}$.

Notice that (U1) is very close to the classic finite range property mentioned at the beginning of Section 3.1.2. The major difference is that here the property is only required of a chosen pseudo-periodic configuration.

As long as $\Pi_C^z(\Gamma) > 0$, (U3) will always hold for all z exceeding some threshold $z_0 \geq 0$. This is because the left hand side is an increasing function of z , as can be seen from the equality

$$e^{z|C|}\Pi_C^z(\Gamma) = \sum_{k=1}^{\infty} \frac{z^k}{k!} \int_C \cdots \int_C 1_\Gamma \left(\sum_{i=1}^k \delta_{x_i} \right) dx_1, \dots, dx_k,$$

which can be derived using (2.2).

For some models it is possible to replace the upper regularity assumptions by their alternative and prove the existence for all $z > 0$.

($\hat{\mathbf{U}}$) *Alternative upper regularity*. M and Γ can be chosen so that the following holds.

($\hat{\mathbf{U}}$ 1) *Lower density bound*: There exist constants $c, d > 0$ such that

$$\text{card}(\zeta) \geq c|\Lambda| - d$$

whenever $\zeta \in \mathbf{N}_f \cap \mathbf{N}_\Lambda$ is such that $H_{\Lambda, \mathbf{x}}(\zeta) < \infty$ for some $\Lambda \in \mathcal{B}_0$ and some $\mathbf{x} \in \bar{\Gamma}$.

($\hat{\mathbf{U}}$ 2) = (U2) *Uniform summability*.

($\hat{\mathbf{U}}$ 3) *Weak non-rigidity*: $\Pi_C^z(\Gamma) > 0$.

3.2 Verifying the assumptions

In this section, we will verify the assumptions for the existence of Gibbs measures with the energy function defined on the hypergraphs \mathcal{D}_4 and \mathcal{LD}_4 . We use the general letter \mathcal{E} when we mean either \mathcal{D} or \mathcal{LD} . Two potentials will be considered
Smooth interaction: For $\eta \in \mathcal{E}_4(\mathbf{x})$ define the potential φ_S as a unary potential such that

$$\varphi_S(\eta, \mathbf{x}) \leq K_0 + K_1 \chi(\eta)^\beta$$

for some $K_0, K_1 \geq 0, \beta > 0$

Hard-core interaction: For $\eta \in \mathcal{E}_4(\mathbf{x})$ define the potential φ_{HC} as a unary potential such that

$$\sup_{\eta: d_0 \leq \chi(\eta) \leq d_1} \varphi_{HC}(\eta, \mathbf{x}) < \infty \text{ and } \varphi_{HC}(\eta, \mathbf{x}) = \infty \text{ if } \chi(\eta) > \alpha$$

for some $0 \leq d_0 < d_1 \leq \alpha$.

We assume by Assumption 1 that $\varphi_S, \varphi_{HC} \geq 0$. Denote the four models as $(\mathcal{D}_4, \varphi_S), (\mathcal{D}_4, \varphi_{HC}), (\mathcal{LD}_4, \varphi_S)$ and $(\mathcal{LD}_4, \varphi_{HC})$.

The first step is to find a suitable form of the pseudo-periodic configurations defined by Γ and the matrix M .

3.2.1 The choice of Γ and M for Laguerre-Delaunay models

Before we choose a specific pseudo-periodic configuration, we first look at some of the properties the resulting configurations should have. To satisfy **(U1)**, we will ideally want bounded finite horizons — bounded circumradii for \mathcal{D} models and bounded radii of the characteristic points for \mathcal{LD} models. We further need boundedness of the potentials for **(U2)** and we need to find a specific bound for **(U3)**. Finally, for **(U2)** we also need the number of incident tetrahedra to each point to be bounded.

With this in mind, we present our choice and then proceed to show its properties.

Fix some $A \subset C \times S$ and define

$$\Gamma^A = \{\zeta \in \mathbf{N}_C : \zeta = \{p\}, p \in A\},$$

the set of configurations consisting of exactly one point in the set A . The set of pseudo-periodic configurations $\bar{\Gamma}$ thus contains only one point in each $C(k), k \in \mathbb{Z}^3$.

Let M be such that $|M_i| = a > 0$ for $i = 1, 2, 3$ and $\angle(M_i, M_j) = \pi/3$ for $i \neq j$.

Choice of the set A

In Dereudre et al. [2012], A is chosen to be $B(0, b)$ for $b \leq \rho a$ for some sufficiently small $\rho > 0$.

We will use this form for the positions of the points as well — the question, however, is how to choose the mark set. For Delaunay models, we choose $A = B(0, b) \times \{0\}$. It would be convenient to do this in the Laguerre case as well and only deal with the Delaunay tetrahedrization. However, for Laguerre-Delaunay models, this would mean that $\Pi_{\mathcal{C}}^z(\Gamma) = 0$, conflicting with both **(U3)** and **(U3)**. The choice $A = B(0, b) \times S$ could, for a small enough a , result in some balls being fully contained in their neighboring balls, possibly resulting in redundant points, thus changing the desired properties of Γ . It is thus necessary to choose the mark set dependent on a . For given a, ρ , the minimum distance between individual points, is $a - 2\rho a = a(1 - 2\rho)$. For \mathcal{LD} models we therefore choose

$$A = B(0, b) \times \left[0, \sqrt{\frac{a}{2}(1 - 2\rho)}\right] \quad (3.2)$$

in order for balls to never overlap. We further assume $\rho < 1/4$, see Appendix A.2.

Remark 13 (Simplification of (U2) and (U3)). Using the set Γ^A , we can simplify the assumptions (U2) and (U3).

(U2) We now have $\#(\hat{\eta}) = \text{card}(\eta)$, since now each point of η is necessarily in a different set $C(k)$.

(U3) $\Pi_C^z(\Gamma)$ can now be directly calculated.

$$\begin{aligned}\Pi_C^z(\Gamma) &= \Pi_C^z(\{\zeta \in N_C : \zeta = \{p\}, p \in A\}) \\ &= e^{-z|A|} z|A| e^{-z|C \setminus A|} \\ &= e^{-z|C|} z|A|,\end{aligned}$$

and thus (U3) becomes

$$z|A| > e^{c_A},$$

where $c_A := c_{\Gamma^A}$.

In the case $A = B(0, \rho a) \times [0, \sqrt{\frac{a}{2}(1-2\rho)}]$ for \mathcal{LD} , we have

$$|A| = \frac{4}{3}\pi(\rho a)^3 \cdot \sqrt{\frac{a}{2}(1-2\rho)} = \frac{4\pi}{3\sqrt{2}} \cdot \rho^3 \sqrt{1-2\rho} \cdot a^{7/2}.$$

3.2.2 Geometric properties of the tetrahedrizations defined by Γ^A and M

In this section we inspect the geometric structure of the tetrahedrizations generated by the configurations in $\bar{\Gamma}^A$.

To understand the advantage of the particular choice of M and Γ^A we first turn to the two-dimensional case. For \mathbb{R}^2 , the two column vectors with angle $\pi/3$ define a triangulation made of equilateral triangles. Depending on the bound for ρ , the points never become collinear ($\rho = \sqrt{3}/4$), have a bound for the circumradius that is linear in ρ ($\rho = \sqrt{3}/6$) or even always generate the same triangulation ($\rho = (\sqrt{3} - 1)/4$) up to the movement of points within their respective set A . Thus the resulting triangulation has many desirable properties.

Using an analogous definition of M in \mathbb{R}^2 forms a triangulation containing (perturbed) equilateral triangles. Sadly, the three-dimensional case is not as simple¹.

The structure of the tetrahedrization formed by $\bar{\Gamma}^A$

To better understand the structure of the resulting tetrahedrizations, we choose a particular example of a configuration from $\bar{\Gamma}^A$.

$$\mathbf{x}_0 = \{(M_a k, 0) \in \mathbb{R}^3 \times S : k \in \mathbb{Z}^3\} \in \bar{\Gamma},$$

the set of zero-weight points lying in the center of their respective cells $C(k)$, where

¹And it could not be, because the analogue of the two-dimensional equilateral triangle, the regular tetrahedron, does not tessellate, as Aristotle famously wrongly claimed, see e.g. Lagarias and Zong [2012]

$$M_a := a \begin{pmatrix} 1 & \frac{1}{2} & \frac{1}{2} \\ 0 & \frac{\sqrt{3}}{2} & \frac{1}{2\sqrt{3}} \\ 0 & 0 & \sqrt{\frac{2}{3}} \end{pmatrix}$$

is a particular example of the matrix M . By the definition of $\bar{\Gamma}^A$, any other configuration in the class can be seen as a “perturbed” \mathbf{x}_0 .

From Remark 5 we know that $\mathcal{LD}_4(\mathbf{x}_0) = \mathcal{D}_4(\mathbf{x}_0)$, therefore we can work with its Delaunay tetrahedrization. For the remainder of this section we will drop the marks from the points and consider them elements of \mathbb{R}^3 .

To further simplify the line of reasoning, we will look at only a subset $\mathbf{x}_1 \subset \mathbf{x}_0$ of the points whose preimage under M_a are the boundary points of the unit cube $[0, 1]^3$. The points of \mathbf{x}_1 , denoted p_1, \dots, p_8 then are:

$$\begin{aligned} p_1 &: (0, 0, 0) \mapsto a(0, 0, 0) \\ p_2 &: (1, 0, 0) \mapsto a(1, 0, 0) \\ p_3 &: (0, 1, 0) \mapsto a(1/2, \sqrt{3}/2, 0) \\ p_4 &: (1, 1, 0) \mapsto a(3/2, \sqrt{3}/2, 0) \\ p_5 &: (0, 0, 1) \mapsto a(1/2, 1/(2\sqrt{3}), \sqrt{2/3}) \\ p_6 &: (1, 0, 1) \mapsto a(3/2, 1/(2\sqrt{3}), \sqrt{2/3}) \\ p_7 &: (0, 1, 1) \mapsto a(1, 2/\sqrt{3}, \sqrt{2/3}) \\ p_8 &: (1, 1, 1) \mapsto a(2, 2/\sqrt{3}, \sqrt{2/3}) \end{aligned}$$

where the points p_1, \dots, p_8 are listed on the right.

To obtain the tetrahedrization of the parallelepiped formed by \mathbf{x}_1 , we could mechanically perform the INCIRCLE test on all quintuples of points in \mathbf{x}_1 (see Remark 3). Such approach is lengthy and ultimately not very illuminative. We will therefore derive its structure through a few geometric observations.

Note that in the following, we use the word regular in the geometric sense — referring to all edges being equal in length — and not in the sense of Definition 10.

Lemma 3. *NNG(\mathbf{x}_1) is formed by two regular tetrahedra, $\{p_1, p_2, p_3, p_5\}$ and $\{p_4, p_6, p_7, p_8\}$, and a regular octahedron $\{p_2, \dots, p_7\}$.*

Proof. Any invertible linear transformation maps a parallelepiped onto a parallelepiped. Since $\|p_2 - p_1\| = \|p_3 - p_1\| = \|p_5 - p_1\| = a$ by definition of M , we obtain that all the edges of the parallelepiped $\{p_1, \dots, p_8\}$ have length a . Furthermore, each face of the parallelepiped can be split into two equilateral triangles, e.g. $\|p_3 - p_2\| = a$. Consequently $\{p_1, p_2, p_3, p_5\}$ and $\{p_4, p_6, p_7, p_8\}$ are regular tetrahedra, the regularity coming from the fact that all edges have length a . Similarly, the sextuple $\{p_2, \dots, p_7\}$ is a regular octahedron, as all its edges have length a . \square

This polyhedral configuration is well known to tessellate² and is depicted in

² The tessellation is of great importance to many fields and thus is known under many names. In mathematics, it is most commonly called the *tetrahedral-octahedral honeycomb*, or

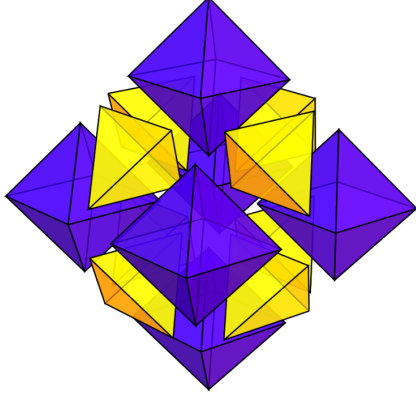


Figure 3.1: The tetrahedral-octahedral tessellation in an exploded view. (Source: Froppuff [2006])

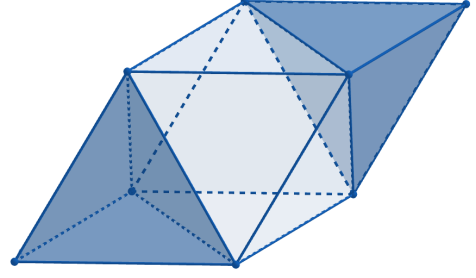


Figure 3.2: The nearest neighbour graph $\text{NNG}(\mathbf{x}_1)$, forming a tessellation of two tetrahedra and an octahedron.

Figures 3.1 and 3.2. The knowledge of $\text{NNG}(\mathbf{x}_1)$ allows us to fully categorize the tetrahedra in $\mathcal{D}_4(\mathbf{x}_0)$.

Proposition 14. $\mathcal{D}_4(\mathbf{x}_0)$ contains two types of tetrahedra, T_1 and T_2 , with edge lengths

$$T_1 : (a, a, a, a, a, a) \quad T_2 : (a, a, a, a, a, \sqrt{2}a).$$

Proof. From Proposition 1 we know that $\text{NNG}(\mathbf{x}_1) \subset \mathcal{D}_2(\mathbf{x}_1)$ which, by (1.1), already gives us a part of the structure of $\mathcal{D}_4(\mathbf{x}_1)$.

We know that $\text{NNG}(\mathbf{x}_1)$ is composed of two regular tetrahedra and one regular octahedron O with all edge lengths equal to a . Therefore all that remains to be done is to tetrahedronize the octahedron. By the symmetry of the regular octahedron, all the tetrahedra inside O are the same up to rotation. Each tetrahedron has five out of six edge lengths equal to a , therefore we only need to determine the length of the remaining edge. We can take e.g. any four points forming a square with side lengths a to immediately see that the remaining edge length is $\sqrt{2}a$.

Since $\mathcal{D}_4(\mathbf{x}_0)$ is tessellated by copies of $\mathcal{D}_4(\mathbf{x}_1)$ translated by vectors $k \in \mathbb{Z}^3$, we have fully characterized the tetrahedra of $\mathcal{D}_4(\mathbf{x}_0)$. \square

We note that the circumradii of the tetrahedra can be calculated using the Cayley-Menger determinant (see Appendix A.1) and are $\sqrt{6}/4 \cdot a$ for T_1 and $1/\sqrt{2} \cdot a$ for T_2 .

the *alternated cubic honeycomb*. In structural engineering, it is known as the *octet truss*, as named by Buckminster Fuller, or the *isotropic vector matrix*. It is stored as *fcu* in the Reticular Chemistry Structure Resource (O’Keeffe et al. [2008]). It is also the nearest-neighbor-graph of the face-centered cubic (fcc) crystal in crystallography (Gabbrielli et al. [2012]).

Combinatorial structure of $\mathcal{D}_4(\mathbf{x}_0)$

Now we turn to the combinatorial structure of $\mathcal{D}_4(\mathbf{x}_0)$, in particular, we are interested in the number

$$n_T = \text{card}\{\eta \in \mathcal{D}_4(\mathbf{x}_0) : \eta' \cap C \neq \emptyset\}.$$

In the tetrahedronized regular octahedron, each vertex is incident to $\binom{5}{3} - 2 = 8$ tetrahedra. In the tetrahedron-octahedron tessellation, each vertex is incident to eight regular tetrahedra and six regular octahedra. This gives us $n_T = 8 + 6 \cdot 8 = 56$. While still large, this is less than a quarter of $8 \cdot \binom{7}{3} - 6 = 274$ for the case of regular cube tessellation induced by the choice $M = aE$. Note that n_T is much smaller for the non-degenerate case, when O contains only 4 tetrahedra and its vertices are incident either to 2 or 4 tetrahedra. In this case, $n_T \leq 8 + 6 \cdot 4 = 32$. We define the quantity

$$n_S = \sup_{\mathbf{x} \in \bar{\Gamma}^A} \text{card}\{\eta \in \mathcal{LD}_4(\mathbf{x}) : \eta' \cap C \neq \emptyset\},$$

and we have $n_S \leq 56$.

Circumdiameter and characteristic point weight

The bound on circumdiameters of the circumballs and characteristic point weights is crucial for the assumption **(U1)** as well as **(U2)** and **(U3)** for potentials that include them. Without such a bound, we have no uniform confinement and the hyperedge potential can grow to infinity.

For the circumdiameter, we derive the following bound.

Proposition 15. *Let $\eta \in \mathbf{x}$, $\mathbf{x} \in \bar{\Gamma}^A$. Then*

$$\chi(\eta) \leq 2a \frac{2\rho + \sqrt{2 - 32\rho^2 + 64\rho^4}}{2 - 32\rho^2},$$

where $\chi(\eta) = \text{diam}B(\eta)$.

Proof. Theorem 7 in Appendix A.2. □

For the weights of the characteristic points, we do not need a specific bound and thus only prove their boundedness.

Proposition 16. *Let $\mathbf{x} \in \bar{\Gamma}^A$. Then the weight of the characteristic point is uniformly bounded. That is, there exists $c > 0$ such that $p''_\eta \leq c$ for all $\eta \in \mathcal{LD}_4(\mathbf{x})$.*

Proof. Denote $\eta = \{p_1, p_2, p_3, p_4\}$, with positions η' and weights η'' . From Theorem 3 and the remark below it we know that $p'_\eta = H(p_1, p_2) \cap H(p_1, p_3) \cap H(p_1, p_4)$.

Fix the positions η' . Changing any of the points' weights amounts to translation of the radical hyperplanes defined by that point (see note after Theorem 3). Given the fact that weights are bounded, $S = [0, W]$, we find

that for given positions η' there exists $W_{\eta'} > 0$ such that $p''_{\eta} \leq W_{\eta'}$ regardless of the weights.

It remains to prove that $\sup_{\eta \in \mathcal{LD}_4(\mathbf{x}), \mathbf{x} \in \bar{\Gamma}^A} W_{\eta'} < \infty$, i.e. changing the points' positions can produce only bounded p''_{η} . This amounts to proving that the points of η are not allowed to come arbitrarily close to (or even attain) a non-general position. This is equivalent with boundedness of the circumradius of η' which is given by Proposition 15. \square

3.2.3 Existence theorems

With the knowledge from the previous sections, we can now proceed to prove the existence of the four models.

We first present a general lemma. Recall the definition of r_{Γ} from (U1).

Lemma 4. *Let $\Gamma \subset \mathbf{N}_{lf}$ be a class of configurations. If there exists $d_{max} > 0$ such that $\text{diam} \Delta < d_{max}$ for the horizon Δ of any $(\eta, \mathbf{x}), \eta \in \mathcal{E}(\mathbf{x}), \mathbf{x} \in \Gamma$, then*

$$r_{\Gamma} < d_{max}.$$

Proof. Choose $\Lambda \in \mathcal{B}_0$ and $\mathbf{x} \in \Gamma$. Let $\zeta \in \mathbf{N}_{\Lambda}$, $\eta \in \mathcal{E}_{\Lambda}(\zeta \cup \mathbf{x}_{\Lambda^c})$ and denote Δ the finite horizon of (η, \mathbf{x}) . From Lemma 1 we obtain $\Delta \cap \Lambda \neq \emptyset$. Then $\Delta \subset \Lambda + B(0, d_{max})$. If we take $\tilde{\mathbf{x}} \in \Gamma$ such that $\tilde{\mathbf{x}} = \mathbf{x}$ on $\partial\Lambda(\mathbf{x})$ then $\varphi(\eta, \zeta \cup \mathbf{x}_{\Lambda^c}) = \varphi(\eta, \zeta \cup \tilde{\mathbf{x}}_{\Lambda^c})$ since $\zeta \cup \mathbf{x}_{\Lambda^c}$ and $\zeta \cup \tilde{\mathbf{x}}_{\Lambda^c}$ differ only on Δ^c . \square

We define the following quantities for $\rho < 1/4$

$$\chi_1(\rho) := 2(\sqrt{6}/4 + \rho), \quad \chi_2(\rho) := 2 \frac{2\rho + \sqrt{2 - 32\rho^2 + 64\rho^4}}{2 - 32\rho^2},$$

the bounds for the tetrahedra derived in Theorem 7 in Appendix A.2. For simplicity, we sometimes refer to them as simply χ_1, χ_2 . Since any $\mathbf{x} \in \bar{\Gamma}^A$ can be seen as a perturbed version of \mathbf{x}_0 , we will refer to T_1 and T_2 tetrahedra in \mathbf{x} which correspond to the tetrahedra T_1, T_2 from Proposition 14.

Theorem 3. *There exists at least one Gibbs measure for the model $(\mathcal{D}_4, \varphi_S)$ and every activity*

$$z > \frac{3}{4\pi} e^{14K_0} (2K_1 \beta e^3 / 3)^{1/\beta} \frac{(\chi_1(\rho)^\beta + 6\chi_2(\rho)^\beta)^{1/\beta}}{\rho^3}.$$

Proof. **(R)** The finite-horizon $\Lambda = \bar{B}(\eta)$ with $\ell_R = 1, n_R = 0$ and χ_R arbitrary can be used. This is because it itself contains no points of \mathbf{x} by definition of \mathcal{D} and acts as the open ball from the definition of the range condition.

(S) Stability is satisfied because of φ is non-negative.

(U) We choose M and Γ as in Section 3.2.1.

(U1) We know from 7 that there exists $d_{max} > 0$ such that $\text{diam} B(\eta) \leq d_{max}$. By Lemma 4 $r_{\Gamma} \leq d_{max}$.

(U2) is trivially satisfied since $n_S < 58$ and φ_S is bounded by Proposition 15.

(U3) By Remark 13 we want to find z as small as possible such that $z|A| > e^{c_A}$. We know from Section 3.2.2 that there are at most 8 T_1 and 48 T_2 tetrahedra intersecting C , therefore from Theorem 7 in Appendix A.2

$$c_A \leq \frac{a}{4}(8(K_0 + K_1(a\chi_1)^\beta) + 48(K_0 + K_1(a\chi_2)^\beta)).$$

This yields the bound

$$\begin{aligned} z &> \frac{3}{4\pi\rho^3} e^{2(K_0+K_1(a\chi_1)^\beta)+12(K_0+K_1(a\chi_2)^\beta)} / a^3 \\ &= C_0 e^{C_1 a^\beta} / a^3, \end{aligned}$$

where $C_0 = 3e^{14K_0}/(4\pi\rho^3)$ and $C_1 = 2K_1(\chi_1^\beta + 6\chi_2^\beta)$.

We now choose a to minimize the expression above. By optimizing over a we obtain $a = (3/(C_1\beta))^{1/\beta}$ which yields the bound

$$z > C_0(C_1\beta e^3/3)^{1/\beta}.$$

□

Theorem 4. *There exists at least one Gibbs measure for the model $(\mathcal{D}_4, \varphi_{HC})$ and every activity $z > 0$.*

Proof. **(R)** Again, $\Lambda = \bar{B}(\eta)$ with $\ell_R = 1, n_R = 0$. Because of the hard-core condition, we can also take $\chi_R = 2\beta$.

(S) Stability is satisfied because of φ is non-negative.

(\hat{U}) We choose M and Γ as in Section 3.2.1.

($\hat{U}1$) For all $\eta \in \mathcal{D}_4(\mathbf{x})$ for $\mathbf{x} \in \Gamma^A$ such that $H_\Lambda(\mathbf{x}) < \infty$ we have $\chi(\eta) < \beta$. This imposes a minimum density of points, since e.g. no ball with diameter β can be empty.

($\hat{U}2$) We have $n_S < 56$ and thus the only quantity in question is φ_{HC} . By Theorem 7, we have $\chi(\eta) \leq a\chi_2(\rho)$, thus we only need to choose a and ρ such that $\chi_2(\rho) \leq \beta/a$.

($\hat{U}3$) $\Pi_\Lambda^z(\Gamma) > 0$ by Remark 13.

□

Theorem 5. *There exists at least one Gibbs measure for the model $(\mathcal{LD}_4, \varphi_S)$ and every activity*

$$z > \frac{3\sqrt{2}}{4\pi} e^{14K_0} (4K_1\beta e^{7/2}/7)^{1/\beta} \frac{(\chi_1(\rho)^\beta + 6\chi_2(\rho)^\beta)^{1/\beta}}{\rho^3 \sqrt{1-2\rho}}.$$

Proof. **(R)** Take the horizon set $\Delta = B(p'_\eta, \sqrt{p''_\eta + W})$. Δ can be decomposed into the sphere p_η and $\Delta \setminus p_\eta$, a 3-dimensional annulus with width

$$\sqrt{p''_\eta + W} - \sqrt{p''_\eta} = W/(\sqrt{p''_\eta + W} + \sqrt{p''_\eta}).$$

By definition of \mathcal{LD} and Remark 6, p_η cannot contain any points of \mathbf{x} . Although the annulus $\Delta \setminus p_\eta$ does not have any bound on the number of points, its width is bounded by $\sqrt{W} \geq W/(\sqrt{p''_\eta + W} + \sqrt{p''_\eta})$. This means that any $x, y \in \Delta$ can be connected by the spheres $B(x, \sqrt{W}), p_\eta, B(y, \sqrt{W})$, yielding the parameters $\ell_R = 3, n_R = 0, \chi_R = 2\sqrt{W}$.

(S) Stability is satisfied because of φ is non-negative.

(U) We choose M and Γ as in Section 3.2.1.

(U1) By Proposition 16 there is $C > 0$ such that $p''_\eta \leq C$ for all $\eta \in \mathcal{LD}_4(\mathbf{x}), \mathbf{x} \in \bar{\Gamma}^A$. By Lemma 4 we have $r_\Gamma \leq \sqrt{C + W}$.

(U2) is trivial since $n_S < 56$ and φ_S is bounded by Proposition 15.

(U3) We proceed similarly as in Theorem 3 and obtain

$$z > C_0 e^{C_1 a^\beta} / a^{7/2}$$

where $C_0 = 3\sqrt{2}e^{14K_0}/(4\pi\rho^3\sqrt{1-2\rho})$, $C_1 = 2K_1(\chi_1^\beta + 6\chi_2^\beta)$. Optimizing over a we obtain $a = (7/(2C_1\beta))^{1/\beta}$ arriving at the bound

$$z > C_0(C_1\beta e^{7/2}/(7/2))^{1/\beta}.$$

□

Theorem 6. *There exists at least one Gibbs measure for the model $(\mathcal{LD}_4, \varphi_{HC})$ and every activity*

$$z > 0.$$

Proof. (R) The horizon set is $\Delta = B(p'_\eta, \sqrt{p''_\eta + W})$. Parameters can be chosen as in Theorem 5.

(S) Stability is satisfied because of φ is non-negative.

(\hat{U}) We choose M and Γ as in Section 3.2.1.

(U1) The same as in Theorem 4. Although the underlying structure is different, the potential still depends on $\chi(\eta)$ and ($\hat{U}1$) requires the configuration to have a non-infinite energy.

(U2) The same as in Theorem 4, $n_S < 56$ and we choose an appropriate a and ρ .

(U3) $\Pi_\Lambda^z(\Gamma) > 0$ by Remark 13.

□

Using the same approach and the same pseudo-periodic configurations $\bar{\Gamma}$, it is easy enough to prove the existence of many different forms of unary hyperedge potentials. In the following, we suggest some alternate hyperedge potentials.

Remark 14 (Other smooth interaction potentials). Alternate smooth interaction models could be considered using characteristics of k -faces of η instead of the circumdiameter. An example is the volume potential φ_V defined as a unary potential such that for $\eta \in \mathcal{E}_4(\mathbf{x})$, $\mathbf{x} \in \bar{\Gamma}$ we have

$$\varphi_V(\eta, \mathbf{x}) \leq K_0 + K_1 V(\eta)^\beta$$

for some $K_0, K_1 \geq 0, \beta > 0$, where $V(\eta) = |\text{conv}(\eta)|$ is the volume of the tetrahedron $\text{conv}(\eta)$. Volume of a 3-simplex with positions $\eta' = \{x_0, x_1, x_2, x_3\} \subset \mathbb{R}^3$ can be calculated using the Cayley-Menger determinant (Appendix A.1), but the following expression (Stein [1966]) lends itself better to finding a bound:

$$V(\eta) = \left| \frac{1}{n!} \det(x_1 - x_0, x_2 - x_0, x_3 - x_0) \right|,$$

where the determinant is of a 3×3 matrix with column vectors $x_1 - x_0, x_2 - x_0, x_3 - x_0$. This quantity can be bounded using Hadamard's inequality (Hadamard [1893]),

$$\det(x_1 - x_0, x_2 - x_0, x_3 - x_0) \leq \prod_{i=1}^3 \|x_i - x_0\|.$$

Notice that we only need the length of three edges of the tetrahedron. Thanks to this, tetrahedra of type T1 and T2 both can be bounded by

$$\varphi_V(\eta, \mathbf{x}) \leq K_0 + K_1 \left(\frac{1}{6} a(1 + 2\rho)^3 \right)^\beta, \quad \eta \in \mathcal{E}_4(\mathbf{x}), \mathbf{x} \in \bar{\Gamma}.$$

The bound for the intensity z in the model $(\mathcal{LD}_4, \varphi_V)$ then becomes

$$z > \frac{3\sqrt{2}}{4\pi} e^{14K_0} (4K_1 \beta e^{7/2})^{1/\beta} \frac{\frac{1}{6}(1 + 2\rho)^3}{\rho^3 \sqrt{1 - 2\rho}}. \quad (3.3)$$

Note that the same approach could be used for e.g. surface area of the tetrahedron, where we would simply replace $\frac{1}{6}(1 + 2\rho)^3$ for $\frac{4}{2}(1 + 2\rho)^2$ in (3.3).

Remark 15 (Other hardcore interaction potentials). Other forms of the hard-core potential can be obtained relatively easily. For example, additional constraints can be added, e.g. minimum edge length $\ell > 0$. Finite horizons remain the same for all unary potentials, and therefore **(R)** holds. Stability **(S)** is satisfied, as the potential is still non-negative. The alternate upper regularity conditions **($\hat{\mathbf{U}}1$)** and **($\hat{\mathbf{U}}3$)** are satisfied for the same reasons. Care has to be taken for **($\hat{\mathbf{U}}2$)** to hold, since the pseudo-periodic configurations $\mathbf{x} \in \bar{\Gamma}$ now must satisfy the new criterion. This can be done by choosing a and ρ such that $a(1 - 2\rho) < \ell$.

Note also that while we have used the sets \mathcal{D}_4 and \mathcal{LD}_4 for the definition of our models, it would be just as possible to consider the sets $\mathcal{D}_2, \mathcal{D}_3$, or $\mathcal{LD}_2, \mathcal{LD}_3$, or even combinations of them.

Remark 16 (Concrete values of z). For the smooth-interaction models, we have only proved the existence for any z exceeding some bound. The actual values of the bound depend strongly on the choice of the parameters K_0, K_1, β . The following table gives a few examples of the bounds, where ρ is always chosen in order to minimize the bound.

Model	K_0	K_1	β	Bound for z
$(\mathcal{D}_4, \varphi_S)$	0	0.5	1	4669
$(\mathcal{LD}_4, \varphi_S)$	0	0.5	1	12062
$(\mathcal{LD}_4, \varphi_V)$	0	0.5	1	1138
$(\mathcal{LD}_4, \varphi_S)$	0	1	5	701
$(\mathcal{LD}_4, \varphi_V)$	0	1	2	280
$(\mathcal{D}_4, \varphi_V)$	0	1	2	118

In general, the bound is extremely sensitive to values of K_0 which in practice means that it has to be set to 0. For $\beta \leq 1$, the bound is also very sensitive to values of K_1 , but increasing β then quickly weakens this dependence. The values for φ_S are overall quite high, choosing e.g. surface area, or even better the volume yields much lower bounds.

A Mathematica script used for exploring the bounds for different settings of the parameters K_0, K_1, β and ρ can be found in the file `zBounds.nb` (see Appendix B).

Given the high requirements on z in most models, we have decided to only work with hard-core models in the next chapters. This is in line with Dereudre and Lavancier [2011], who also only considered hard-core models. Note that while this might seem as a limitation, in practice we can always introduce a hard-core parameter that will not limit our model, but ensure that it exists for all $z > 0$. These bounds therefore have a theoretical, rather than practical value.

Remark 17 (Improving the bounds). There is a number of steps one could possibly take to improve the bounds for z . Any of the presented bounds for c_A are not minimal. For example, not all tetrahedra in any given tetrahedrization will attain the bounds χ_1 and χ_2 . Furthermore, (3.2) is perhaps unnecessarily conservative — no problems may arise if we allow the balls to overlap to a certain degree. Finally, it may be possible to prove that **(U3)** requires only Π -almost all configurations in the supremum in the term c_A , which would result in a decrease in number terms in the sum, see end of Section 3.2.2.

Of course, one may also be able to use an entirely different approach than the one from Dereudre et al. [2012] to obtain lower bounds.

4. Simulation

The Gibbs point process allows us a great flexibility in specifying the energy function. One of the disadvantages is that both simulating the GPP and estimating its parameters is computationally demanding. This chapter outlines the approach taken in simulating the GPP.

This (and the following) chapter is a direct extension of Dereudre and Lavancier [2011]. Dereudre and Lavancier investigate random Voronoi tessellations and Delaunay triangulations on the plane \mathbb{R}^2 based on the Gibbs point process. This text attempts to generalize their results for the Delaunay triangulations to Laguerre tetrahedrizations, that is from \mathbb{R}^2 to \mathbb{R}^3 and from Delaunay to the Laguerre-Delaunay case.

The principal issue in simulating GPP is that we do not know the value of the partition function Z_Λ^z . To that end, we employ Monte chain Markov Carlo (MCMC) techniques.

4.1 Monte Chain Markov Carlo

Before formulating the algorithm used to simulate our models, we first present some basic theory of Markov chains and their use in Monte Carlo techniques. For an introduction to these techniques with point processes with density in mind, see Chapter 7 in Møller and Waagepetersen [2003]. For a more general and comprehensive text, we refer to Robert and Casella [2004] or Meyn and Tweedie [1993].

4.1.1 Basic notions

We first define the basic terms to do with general state-space Markov chains.

Definition 32. A measurable mapping $P : \Omega \times \mathcal{A} \rightarrow [0, 1]$ such that

1. for each $B \in \mathcal{A}$, $P(\cdot, B)$ is a non-negative measurable function on Ω ,
2. for each $x \in \Omega$, $P(x, \cdot)$ is a probability measure on Ω

is called a *probability kernel* on (Ω, \mathcal{A}) .

Definition 33. A stochastic process $Y = \{Y_n, n \in \mathbb{N}_0\}$ defined on (Ω, \mathcal{A}) is called a *time-homogeneous Markov chain* with *initial distribution* μ and *transition probability kernel* $P(x, A)$, $x \in \Omega$, $A \in \mathcal{A}$, if for any $n \in \mathbb{N}_0$ and any sets A_0, \dots, A_n we have

$$\begin{aligned} P_\mu(Y_0 \in A_0, \dots, Y_n \in A_n) \\ = \int_{A_0} \dots \int_{A_{n-1}} P(y_{n-1}, A_n) P(y_{n-2}, dy_{n-1}) \dots P(y_0, dy_1) \mu(dy_0) \end{aligned}$$

where $P_\mu(B)$, $B \in \bigotimes_{n=0}^\infty \mathcal{A}$ is the probability of the event $[Y \in B]$.

Such process exists by Theorem 3.4.1 in Meyn and Tweedie [1993] if \mathcal{A} is generated by a countable collection of sets. This is true for \mathcal{N}_{lf} , see Proposition B.1 in Møller and Waagepetersen [2003].

The definition suggests that the probability kernel $P(x, A)$ can be interpreted as the probability that $Y_{m+1} \in A$ given that $Y_m = x$. Note that the probability is independent of m , which motivates the name *time-homogeneous*.

Next we iteratively define the *m-step transition probability*. Set $P^0(x, A) = \delta_x(A)$ and for $n \geq 1$ define

$$P^m(x, A) = \int_{\Omega} P(y, A) P^{m-1}(x, dy).$$

In the following, let $Y = \{Y_n, n \in \mathbb{N}_0\}$ always be a Markov chain and π a probability distribution on (Ω, \mathcal{A}) .

Definition 34. A Markov chain $\{Y_n, n \in \mathbb{N}_0\}$

1. has an *invariant distribution* π if $Y_m \sim \pi$ implies $Y_{m+1} \sim \pi$. In the integral form

$$\int_{\Omega} P(x, A) \pi(dx) = \int_A \pi(dx), \quad A \in \mathcal{A}.$$

2. is *reversible* with respect to the distribution π if $Y_m \sim \pi$ then (Y_m, Y_{m+1}) and (Y_{m+1}, Y_m) are identically distributed. In the integral form

$$\int_B P(x, A) \pi(dx) = \int_A P(x, B) \pi(dx), \quad A, B \in \mathcal{A}.$$

3. is *irreducible*, or ψ -*irreducible* if there exists a nonzero measure ψ such that for any $x \in \Omega, A \in \mathcal{A}$ with $\psi(A) > 0$ we have $P^m(x, A) > 0$ for some $m \in \mathbb{N}_0$.

From the definition it is immediately observable that if Y is reversible with respect to π , then π is also its invariant distribution.

Definition 35. Let Y be ψ -irreducible. Then we call Y *periodic* if there exists a partitioning D_0, \dots, D_{d-1}, A of Ω such that $\psi(A) = 0$ and

$$P(x, D_j) = 1, \quad x \in D_i, \quad j = (i + 1) \bmod d,$$

with $d > 1$. In the opposite case Y is *aperiodic*.

The partitioning always exists for an irreducible Markov chain Y by Theorem 5.4.4 in Meyn and Tweedie [1993]. For the Markov chain to be aperiodic it is sufficient to have $P(x, \{x\}) > 0$ for some $x \in \Omega$.

To measure the distance between two probability distributions, we recall the definition of the total variation norm.

Definition 36. Let μ, ν be two probability distributions on Ω . Then we define the *total variation norm* by

$$\|\mu - \nu\|_{TV} = \sup_{F \subset \Omega} |\mu(F) - \nu(F)|.$$

Note that convergence in the total variation norm is quite a strong property and in particular implies weak convergence.

Definition 37. We say that π is a *limiting distribution* of Y if there exists $A \in \mathcal{A}$, $\pi(A) = 0$ such that

$$\lim_{m \rightarrow \infty} \|P^m(x, \cdot) - \pi\|_{TV} = 0$$

for all $x \in \Omega \setminus A$.

Proposition 17. *Let Y be irreducible and π its invariant distribution. Then π is the unique invariant distribution (up to null sets).*

Proof. Proposition 7.2 in Møller and Waagepetersen [2003] □

Proposition 18. *Let Y be irreducible and aperiodic and π its invariant distribution. Then π is also the limiting distribution of Y .*

Proof. Proposition 7.7 in Møller and Waagepetersen [2003]. □

Consider a probability distribution π on some measurable space (Ω, \mathcal{A}) . We wish to construct a Markov chain Y on Ω with its stationary distribution equal to π . By the theory introduced in this section, we must construct an irreducible and aperiodic Markov chain reversible with respect to π . Then π is also the unique invariant distribution and thus the limiting distribution. Since convergence in total variation implies weak convergence, our task is complete.

The question, however, is how to build such a Markov chain. The next section answers that question.

4.1.2 Birth-Death-Move Metropolis-Hastings algorithm

In the last section we outlined how Markov chains may be used to sample from a distribution in general. Imagine now that we wish to sample from a finite point process with the unnormalized density f with respect to Π_Λ . In this section we introduce a variation of the Metropolis-Hastings algorithm for points processes with a density, the algorithm used to construct a Markov chain with the required properties. We first describe the algorithm in general, adapted from Section 7.1. in Møller and Waagepetersen [2003].

Let $\Omega \subset \mathbf{N}_f$ be the state space. A natural choice is

$$\Omega = \{\gamma \in \mathbf{N}_f : f(\gamma) > 0\} = \mathbf{N}_f \cap \mathbf{N}_\infty.$$

We first introduce the quantities to be used in the algorithm.

Let $\gamma = \{x_1, \dots, x_n\} \in \Omega$ be the current state and denote $\bar{\gamma} = (x_1, \dots, x_n)$ the current state represented as a vector. We further denote

- $p(\gamma)$ Probability of a birth proposal if the current state is γ .
- $q_i(\bar{\gamma}, \cdot)$ Density for the location of the point replacing the point x_i .
- $q_b(\gamma, \cdot)$ Density for the location of the point at birth proposal.
- $q_d(\gamma, \cdot)$ Density for the selection of the point at death proposal.

Finally we introduce the so called *Hasting ratios*

$$\begin{aligned} r_i(\bar{\gamma}, y) &= \frac{f(\gamma \setminus \{x_i\} \cup \{y\})q_i((x_1, \dots, x_{i-1}, y, x_{i+1}, \dots, x_n), x_i)}{f(\gamma)q_i(\bar{\gamma}, y)}, \\ r_b(\gamma, x) &= \frac{f(\gamma \cup \{x\})(1 - p(\gamma \cup \{x\}))q_d(\gamma \cup \{x\}, \{x\})}{f(\gamma)p(\gamma)q_b(\gamma, x)}, \\ r_d(\gamma, x) &= \frac{f(\gamma \setminus \{x\})p(\gamma \setminus \{x\})q_b(\gamma \setminus \{x\}, x)}{f(\gamma)(1 - p(\gamma))q_d(\gamma, x)}, \end{aligned}$$

with the convention $a/0 = 1$ for $a \geq 0$.

Algorithm A

Let $\gamma_0 \in \Omega$ be an initial configuration. For $m = 0, 1, \dots$, given $\gamma_m \in N_f$, generate γ_{m+1} as follows

1. Generate b and r_m independently and uniformly on $[0, 1]$.
2. If $r_m \leq q$, then set $\bar{\gamma}_m = (x_1, \dots, x_n)$, generate i uniformly on $\{1, \dots, n\}$, generate $y \sim q_i(\bar{\gamma}_m, \cdot)$ and set

$$\gamma_{m+1} = \begin{cases} \gamma_m \setminus \{x_i\} \cup \{y\} & \text{if } b < r_i(\bar{\gamma}_m, y) \\ \gamma_m & \text{otherwise.} \end{cases} \quad (4.1)$$

3. If $r_m > q$, perform the birth/death step.

- (a) Generate r_b uniformly on $[0, 1]$.
- (b) If $r_b \leq p(\gamma_m)$, then generate $x \sim q_b(\gamma_m, \cdot)$ and set

$$\gamma_{m+1} = \begin{cases} \gamma_m \cup \{x\} & \text{if } b < r_b(\gamma_m, x) \\ \gamma_m & \text{otherwise.} \end{cases} \quad (4.2)$$

- (c) If $r_b > p(\gamma_m)$ and $\gamma_m = \emptyset$ then set $\gamma_{m+1} = \emptyset$. Else if $\gamma_m \neq \emptyset$ generate $x \sim q_d(\gamma_m, \cdot)$ and set

$$\gamma_{m+1} = \begin{cases} \gamma_m \setminus \{x\} & \text{if } b < r_d(\gamma_m, x) \\ \gamma_m & \text{otherwise.} \end{cases} \quad (4.3)$$

The correctness of this approach is guaranteed by the following proposition.

Proposition 19. *The Markov chain generated by Algorithm A is*

1. *reversible with respect to f ,*
2. *Ψ -irreducible and aperiodic if the following conditions are satisfied*

- (i) $p(\emptyset) < 1$,
- (ii) *for all $\gamma \in E, \gamma \neq \emptyset$, there exists $x \in \gamma$ such that*

$$(1 - p(\gamma))q_d(\gamma, x) > 0 \text{ and } f(\gamma \setminus \{x\})p(\gamma \setminus \{x\})q_b(\gamma \setminus \{x\}, x) > 0. \quad (4.4)$$

Proof. Proposition 7.15 in Møller and Waagepetersen [2003]. \square

Condition (i) ensures that the chain can remain in \emptyset . Condition (ii) ensures that a point can always be deleted and thus the chain can move from γ to \emptyset in $N_\Lambda(\gamma)$ steps.

4.2 Simulating Gibbs-Laguerre-Delaunay tetrahedrizations

In this section, we present the details of the MCMC simulation in our setting.

4.2.1 Definition of the model

Our goal is to simulate a hardcore-interaction potentials defined in Section 3.2.3 on \mathcal{D} and \mathcal{LD} models. To that end, we choose a particular parametric form of potentials depending on the parameters θ and α .

$$\varphi_{HC}^{\theta, \alpha}(\eta, \mathbf{x}) = \begin{cases} \infty & \text{if } \chi(\eta) > \alpha, \\ \theta \text{Sur}(\eta) & \text{otherwise,} \end{cases} \quad (4.5)$$

$$\varphi_S^\theta(\eta, \mathbf{x}) = \theta \text{Sur}(\eta), \quad (4.6)$$

where $\text{Sur}(\eta)$ is the surface area of $\text{conv}(\eta)$, $\alpha > 0$, $\theta \in \mathbb{R}$. We then consider the models $(\mathcal{D}_4, \varphi_{HC}^{\theta, \alpha})$, $(\mathcal{D}_4, \varphi_S^\theta)$, $(\mathcal{LD}_4, \varphi_{HC}^{\theta, \alpha})$ and $(\mathcal{LD}_4, \varphi_S^\theta)$. We note that here φ_S^θ has the form suggested on Remark 14, that is we are using Sur instead of the circumdiameter.

4.2.2 Simulation algorithm

We now present the variations of Algorithm A for our setting. The simulation window will be taken to be $[0, 1]^3$ and we let $\Lambda \in \mathcal{B}_0$ be such that $[0, 1]^3 \subset \Lambda$. All simulation takes place on $[0, 1]^3$ and $\Lambda \setminus [0, 1]^3$ contains the outside configuration, the boundary condition.

The first algorithm simulates the Delaunay tetrahedrization. In the description, all unmarked points formally represent marked points with marks set to 0. The state space thus is

$$\Omega = \{\gamma \in \mathbf{N}_f : f(\gamma) > 0, \gamma \subset \Lambda \times \{0\}\},$$

the set of permissible configurations with zero marks. **Algorithm A- \mathcal{D}**

First, start from a permissible initial configuration γ_0 .

1. Let $n = N_{[0,1]^3}(\gamma)$.
2. Draw independently r and b uniformly on $[0, 1]$.
3. If $r < 1/3$, then generate x uniformly on $[0, 1]^3$ and set

$$\gamma_1 = \begin{cases} \gamma_0 \cup \{x\} & \text{if } b < \frac{zf(\gamma_0 \cup \{x\})}{(n+1)f(\gamma_0)}, \\ \gamma_0 & \text{otherwise.} \end{cases} \quad (4.7)$$

4. If $r > 2/3$, then generate x uniformly on γ_0 and set

$$\gamma_1 = \begin{cases} \gamma_0 \setminus \{x\} & \text{if } b < \frac{nf(\gamma_0 \setminus \{x\})}{zf(\gamma_0)}, \\ \gamma_0 & \text{otherwise.} \end{cases} \quad (4.8)$$

5. If $1/3 < r < 2/3$, then generate x uniformly on γ_0 , generate $y \sim \mathcal{N}(x, \sigma^2 I)$ such that $y \in [0, 1]^3$ and set

$$\gamma_1 = \begin{cases} \gamma_0 \setminus \{x\} \cup \{y\} & \text{if } b < \frac{f(\gamma_0 \setminus \{x\} \cup \{y\})}{f(\gamma_0)}, \\ \gamma_0 & \text{otherwise.} \end{cases} \quad (4.9)$$

6. Set $\gamma_0 \leftarrow \gamma_1$ and go to 1.

The second algorithm is for the simulation of the Laguerre tetrahedrization. The algorithm functions in the same way with one significant difference. In Section 1.1.2 we introduced the notion of redundant points. It would be inconvenient to have a newly added point render other points redundant and vice versa. To prevent that, we define the set of point configurations producing Laguerre-Delaunay hypergraph structures with no redundant points,

$$\mathbf{N}_{nr} = \{\gamma \in \mathbf{N}_{lf} : \mathcal{LD}(\gamma) \text{ does not contain redundant points}\}.$$

Using this set, we set the state space of the chain to

$$\Omega = \mathbf{N}_f \cap \mathbf{N}_\infty \cap \mathbf{N}_{nr}.$$

We further denote the set

$$A_\gamma = \{x \in \Lambda \times S : \gamma \cup \{x\} \in \mathbf{N}_{nr}\},$$

the set of points which we can propose if the chain is in the state γ . Generation of points in A_γ is done through rejection sampling, that is repeatedly sampling a point $x \in \Lambda \times S$ until the point satisfies $x \in A_\gamma$.

Algorithm A- \mathcal{LD}

First, start from a permissible initial configuration γ_0 .

1. Let $n = N_{[0,1]^3}(\gamma_0)$.
2. Draw independently r and b uniformly on $[0, 1]$.
3. If $r < 1/3$, then generate x uniformly on A_{γ_0} and set

$$\gamma_1 = \begin{cases} \gamma_0 \cup \{x\} & \text{if } b < \frac{zf(\gamma_0 \cup \{x\})}{(n+1)f(\gamma_0)}, \\ \gamma_0 & \text{otherwise.} \end{cases} \quad (4.10)$$

4. If $r > 2/3$, then generate x uniformly on γ_0 and set

$$\gamma_1 = \begin{cases} \gamma_0 \setminus \{x\} & \text{if } b < \frac{nf(\gamma_0 \setminus \{x\})}{zf(\gamma_0)}, \\ \gamma_0 & \text{otherwise.} \end{cases} \quad (4.11)$$

5. If $1/3 < r < 2/3$, then generate x uniformly on γ_0 , generate $y' \sim \mathcal{N}(x, \sigma^2 I)$ and y'' uniformly on S such that $y = (y', y'') \in A_{\gamma_0 \setminus \{x\}}$ and set

$$\gamma_1 = \begin{cases} \gamma_0 \setminus \{x\} \cup \{y\} & \text{if } b < \frac{f(\gamma_0 \setminus \{x\} \cup \{y\})}{f(\gamma_0)}, \\ \gamma_0 & \text{otherwise.} \end{cases} \quad (4.12)$$

6. Set $\gamma_0 \leftarrow \gamma_1$ and go to 1.

During the move step, the moved point might fall outside of $[0, 1]^3$. In Dereudre and Lavancier [2011], the point would be replaced by the periodic property. We do not use the periodic configuration (Section 4.2.4) and this approach would not be in line with the idea that a small perturbation to the point's position should not result in a radically different position. In our case the point is reflected back inside $[0, 1]^3$, as if it was 'bounced back' from the boundary of $[0, 1]^3$.

Remark 18. Recall that the mark space $S = [0, W]$ limits the maximum weight. It is worth noting to what extent this is a limitation. From a practical perspective, the maximum weight W limits the resulting tetrahedrization in the sense that the difference of weights can never be greater than W . Marks greater than W are not necessarily a problem, as we can always find an identical tetrahedrization with marks bounded by W , as long as there are no two points p, q with $|p'' - q''| > W$ (see Remark 4).

4.2.3 Simplified form of proposal densities

The Hastings ratios require us to calculate a ratio of densities f both containing the energy function. Such calculation would be lengthy and would render the whole approach unfeasible. However, here again the locality of the tetrahedrization allows us to express the Hastings ratios with only those tetrahedra which are affected by the added, removed, or moved point. If we recall Remark 8, we obtain the following simplifications for the ratios in Algorithm A- \mathcal{LD} . In the following, let $\varphi(\eta, \mathbf{x})$ denote either of the potentials φ_S^θ and $\varphi_{HC}^\theta(\theta, \alpha)$.

The ratio of densities in birth step (4.10) then becomes:

$$\begin{aligned} \frac{f(\gamma_0 \cup \{x\})}{f(\gamma_0)} &= \exp \left(\sum_{\eta \in \mathcal{E}_\Lambda(\gamma_0 \cup \{x\})} \varphi(\eta, \gamma_0 \cup \{x\}) - \sum_{\eta \in \mathcal{E}_\Lambda(\gamma_0)} \varphi(\eta, \gamma_0) \right) \\ &= \exp \left(\sum_{T \in \mathcal{LD}^\otimes(x, \gamma_0)} \varphi(\eta, \gamma_0) - \sum_{T \in \mathcal{LD}^\ell(x, \gamma_0 \cup \{x\})} \varphi(\eta, \gamma_0 \cup \{x\}) \right). \end{aligned}$$

Ratio for death step (4.11) becomes:

$$\begin{aligned} \frac{f(\gamma_0 \setminus \{x\})}{f(\gamma_0)} &= \exp \left(\sum_{\eta \in \mathcal{E}_\Lambda(\gamma_0 \setminus \{x\})} \varphi(\eta, \gamma_0 \setminus \{x\}) - \sum_{\eta \in \mathcal{E}_\Lambda(\gamma_0)} \varphi(\eta, \gamma_0) \right) \\ &= \exp \left(\sum_{T \in \mathcal{LD}^\ell(x, \gamma_0)} \varphi(\eta, \gamma_0) - \sum_{T \in \mathcal{LD}^\otimes(x, \gamma_0 \setminus \{x\})} \varphi(\eta, \gamma_0 \setminus \{x\}) \right). \end{aligned}$$

Ratio for move step (4.12) becomes:

$$\begin{aligned}
\frac{f(\gamma_0 \setminus \{x\} \cup \{y\})}{f(\gamma_0)} &= \frac{f(\gamma_0 \setminus \{x\} \cup \{y\})}{f(\gamma_0 \setminus \{x\})} \frac{f(\gamma_0 \setminus \{x\})}{f(\gamma_0)} \\
&= \exp \left(\sum_{T \in \mathcal{LD}^\otimes(y, \gamma_0 \setminus \{x\})} \varphi(\eta, \gamma_0 \setminus \{x\}) - \sum_{T \in \mathcal{LD}^\ell(y, \gamma_0 \setminus \{x\} \cup \{y\})} \varphi(\eta, \gamma_0 \setminus \{x\} \cup \{y\}) \right. \\
&\quad \left. + \sum_{T \in \mathcal{LD}^\ell(x, \gamma_0)} \varphi(\eta, \gamma_0) - \sum_{T \in \mathcal{LD}^\otimes(x, \gamma_0 \setminus \{x\})} \varphi(\eta, \gamma_0 \setminus \{x\}) \right).
\end{aligned}$$

These expressions simplify the energy calculation immensely. Whereas calculating the energy for the whole tetrahedrization requires all the tetrahedra, and thus depends on the complexity of the sets \mathcal{E}_Λ , the final expressions only contain the tetrahedra local to x through the sets of type \mathcal{LD}^\otimes and \mathcal{LD}^ℓ , and thus the energy can be calculated in constant time.

We have presented the simplified ratios for Algorithm A- \mathcal{LD} . The case for Algorithm A- \mathcal{D} is analogous, see Remark 8.

4.2.4 Practical implementation

All simulations were written in C++. More details on the implementation can be found in Appendix B.

Initial configuration

In Dereudre and Lavancier [2011], three options for the initial configuration are suggested: the empty configuration, a specific fixed outside configuration, and periodic configuration. We decided against using the periodic configuration since the CGAL implementation of 3D periodic triangulations Caroli et al. [2018] has a much longer running time than in the non-periodic case. Dereudre and Lavancier [2011] rejects the empty configuration on the basis that it "produces non bounded Delaunay-Voronoi cells". While this is true for a Voronoi diagram, it does not hold for the Delaunay or Laguerre case and so such configuration would in fact be possible in our case. However, the method chosen was to fix a regular grid of points in and out of Λ such that the resulting tessellation fulfills the hardcore conditions. This does mean that the initial configuration is dependent on the values of the hardcore parameter α .

4.2.5 Convergence of the algorithm

By Propositions 17 and 18, the convergence of Algorithms A- \mathcal{D} and A- \mathcal{LD} requires the generated Markov chain to be irreducible, aperiodic, and to have an invariant distribution given by f . Reversibility (and thus the invariant distribution property) is given by point 1 in Proposition 19. Aperiodicity is satisfied since the chain can stay in any state with non-zero probability. It only remains to verify the irreducibility.

For irreducibility, all that remains is to prove (4.4). This assumption is trivially satisfied in the models $(\mathcal{D}_4, \varphi_S^\theta)$ and $(\mathcal{LD}_4, \varphi_S^\theta)$. However, for the hard-core interaction models, this assumption is in general not satisfied, as the empty configuration does not even have to be in the state space, as it might not be permissible. In order to prove the irreducibility, Dereudre and Lavancier [2011] utilized an algorithmic procedure which connected any two configurations $\gamma, \bar{\gamma} \in \mathbf{N}_\infty$ by a finite series of specific steps of point addition and removal, all of which produce permissible configurations.

Although it seems very plausible that a similar approach could be taken in our case, we have not succeeded in extending this result to our case. In \mathbb{R}^2 , the geometric arguments rely on simple relationships between the lengths of sides of the triangles and their circumradii which no longer work in \mathbb{R}^3 . Furthermore, the extension to the Laguerre-Delaunay case adds an additional constraint as the configurations now must not contain any redundant points.

If the chain is indeed not irreducible, then the algorithms converge to a restriction of the limiting distribution to some connected component of the state space. The limiting distribution thus depends on the initial condition and never equals to the desired distribution.

5. Estimation

Assume now that we obtain the point configuration γ from model $(\varphi_{HC}^{\theta,\alpha}, \mathcal{LD}_4)$ on the observation window $\Lambda_n = [-n, n]^3$ and wish to estimate the model parameters (z, θ, α) . To simplify the notation, we introduce the set $\Lambda_n^S = \Lambda_n \times S$.

The estimation procedure closely follows that from Dereudre and Lavancier [2011]. That is a two-step approach, first estimating the hardcore parameter α and then using the estimates to obtain the estimates of θ and z through maximum pseudolikelihood (MPLE). The numerical results are presented in Chapter 6.

To underscore the dependence on the maximum circumdiameter α and smooth interaction parameter θ , we now denote the energy $H^{\theta,\alpha}$.

5.1 Estimation of the hardcore parameter

In the first step we estimate the hardcore parameter α . Thanks to the fact that the hardcore parameter α satisfies

$$\text{if } \alpha < \alpha' \text{ then } \forall \Lambda \in \mathcal{B}_0, H_{\Lambda}^{\theta,\alpha}(\gamma) < \infty \Rightarrow H_{\Lambda}^{\theta,\alpha'}(\gamma) < \infty,$$

we can estimate it as

$$\hat{\alpha} = \inf\{\alpha > 0, H_{\Lambda_n}^{\theta,\alpha}(\gamma) < \infty\} = \max\{\chi(\eta), \eta \in \mathcal{LD}_{4\Lambda_n}(\gamma)\},$$

where $\mathcal{LD}_{4\Lambda_n}$ denotes the set \mathcal{E}_{Λ_n} for the hypergraph structure $\mathcal{E} = \mathcal{LD}_4$.

The estimate $\hat{\alpha}$ is then used in the pseudo-likelihood function in the second estimation step.

5.2 Estimation of the smooth interaction parameters

In the second step we estimate the smooth interaction parameters through maximum pseudolikelihood. The classical version of MPLE requires heredity of the energy function. Recall that heredity means every point of the configuration is removable, see Section 2.2.1 for a definition and discussion. The hardcore interaction in the model $(\mathcal{LD}_4, \varphi_{HC}^{\theta,\alpha})$ does not satisfy this condition. For that purpose, Section 2.2.5 presented the extension to the non-hereditary case from Dereudre and Lavancier [2009].

We denote the set of removable points of γ by $\mathcal{R}^\alpha(\gamma)$. Similarly, the notion of an addable point will be useful. A point $x \in \gamma$ is *addable* in γ if $\gamma \cup \{x\}$ is permissible and we denote $\tilde{\Lambda}_n^S$ the set of addable points in Λ_n^S .

In the non-hereditary case, the pseudo-likelihood function then becomes (Dereudre and Lavancier [2011]):

$$PLL_{\Lambda_n}(\gamma, z, \theta, \alpha) = \int_{\Lambda_n^S} z \exp(-h^{\theta,\alpha}(x, \gamma)) dx + \sum_{x \in \mathcal{R}^\alpha(\gamma) \cap \Lambda_n^S} (h^{\theta,\alpha}(x, \gamma \setminus \{x\}) - \ln(z)), \quad (5.1)$$

where $h^{\theta,\alpha}(x, \gamma \setminus \{x\})$ is local energy of x in γ defined in Definition 31. The estimates $\hat{\theta}$ and \hat{z} are obtained through minimizing the PLL_{Λ_n} function:

$$(\hat{z}, \hat{\theta}) = \operatorname{argmin}_{z, \theta} PLL_{\Lambda_n}(\gamma, z, \hat{\alpha}, \theta).$$

By differentiating the PLL function (5.1) with respect to z , respectively θ , and setting them equal to zero, we obtain the estimate for \hat{z} ,

$$\hat{z} = \frac{\operatorname{card}(\mathcal{R}^{\hat{\alpha}}(\gamma) \cap \Lambda_n^S)}{\int_{\Lambda_n^S} \exp(-h^{\hat{\alpha}, \theta}(x, \gamma)) dx}, \quad (5.2)$$

and the estimate $\hat{\theta}$ as the solution of

$$z \int_{\tilde{\Lambda}_n^S} h^{\hat{\alpha}, 1}(x, \gamma) \exp(-h^{\hat{\alpha}, \theta}(x, \gamma)) dx = \sum_{x \in \mathcal{R}^{\hat{\alpha}}(\gamma) \cap \Lambda_n^S} h^{\hat{\alpha}, 1}(x, \gamma \setminus \{x\}), \quad (5.3)$$

where we have used the fact that the local energy depends on θ linearly, yielding

$$\frac{\partial h^{\hat{\alpha}, \theta}}{\partial \theta}(x, \gamma) = h^{\hat{\alpha}, 1}(x, \gamma).$$

5.2.1 Practical implementation

We obtain the estimate of θ by substituting the expression for \hat{z} (5.2) into (5.3). This leads to the equation

$$\frac{\int_{\tilde{\Lambda}_n^S} h^{\hat{\alpha}, 1}(x, \gamma) \exp(-h^{\hat{\alpha}, \theta}(x, \gamma)) dx}{\int_{\Lambda_n^S} \exp(-h^{\hat{\alpha}, \theta}(x, \gamma)) dx} = \frac{\sum_{x \in \mathcal{R}^{\hat{\alpha}}(\gamma) \cap \Lambda_n^S} h^{\hat{\alpha}, 1}(x, \gamma \setminus \{x\})}{\operatorname{card}(\mathcal{R}^{\hat{\alpha}}(\gamma) \cap \Lambda_n^S)}. \quad (5.4)$$

In order to simplify the estimation of θ , we can simplify this equation further. First, we denote the right-hand side of (5.4) as c as it is constant with respect to θ . Second, we note that $x \notin \tilde{\Lambda}_n^S \Rightarrow \exp(-h^{\hat{\alpha}, \theta}(x, \gamma)) = 0$ which enables us to integrate over $\tilde{\Lambda}_n^S$ instead of the whole window Λ_n^S . Lastly we denote the local energy $h^{\hat{\alpha}, 1}(x, \gamma) =: h(x)$, yielding the equation

$$\int_{\tilde{\Lambda}_n^S} h(x) \exp(-\theta h(x)) dx = c \int_{\tilde{\Lambda}_n^S} \exp(-\theta h(x)) dx,$$

leading into the final equation

$$\int_{\tilde{\Lambda}_n^S} \exp(-\theta h(x))(h(x) - c) dx = 0. \quad (5.5)$$

The integral in (5.5) is estimated using Monte-Carlo integration, i.e. is approximately equal to

$$\frac{|\tilde{\Lambda}_n^S|}{N} \sum_{i=0}^N 1_{\tilde{\Lambda}_n^S}(x_i) \exp(-\theta h_i)(h_i - c) dx,$$

where $h_i = h^{\hat{\alpha}, 1}(x_i, \gamma)$ and x_1, \dots, x_N is a random sample from the uniform distribution on Λ_n^S . Note that although $|\tilde{\Lambda}_n^S|$ would be very difficult to obtain, the solution of the equation does not depend on it.

After $\hat{\theta}$ is estimated, we then obtain the estimate \hat{z} by substituting θ by $\hat{\theta}$ in (5.2) and with the integral replaced by a Monte-Carlo integration approximation.

5.2.2 Consistency

For the \mathbb{R}^2 case, consistency of this estimation approach is proven in Dereudre and Lavancier [2009]. However, similarly to the irregularity of the Markov chains in Chapter 4, the verification of the required assumptions relies on arguments that are not easy to extend to \mathbb{R}^3 and the Laguerre-Delaunay case. We have sadly not succeeded at proving the consistency of this approach for our models. This shortcoming is especially unfortunate as the numerical results given in Chapter 6 seem to point to a bias of the estimates.

6. Numerical Results

This chapter summarizes the numerical results for two models, both using the hyperedge potential,

$$\varphi_{HC}^{\theta,\alpha}(\eta, \mathbf{x}) = \begin{cases} \infty & \text{if } \chi(\eta) > \alpha, \\ \theta \text{Sur}(\eta) & \text{otherwise,} \end{cases} \quad (6.1)$$

where $\text{Sur}(\eta)$ is the surface of the tetrahedron $\text{conv}(\eta)$. We introduce a shortened notation for the models, $\text{L}+$ for $(\mathcal{LD}_4, \varphi_{HC}^{\theta,\alpha})$ and $\text{D}+$ for $(\mathcal{D}_4, \varphi_{HC}^{\theta,\alpha})$, where the $+$ indicates the presence of hard-core parameters.

6.1 Simulation

In this section we present the results of the MCMC simulation as presented in Chapter 4. Let $\mathbf{x} \in \mathbf{N}_{lf}$. We define the *vertex degree* of a vertex $p \in \mathbf{x}$ as the number of vertices adjacent to p , where two vertices $p, q \in \mathbf{x}$ are adjacent if there exists a tetrahedron $\eta \in \mathcal{D}_4(\mathbf{x})$ (or $\eta \in \mathcal{LD}_4(\mathbf{x})$) such that $\{p, q\} \subset \eta$.

6.1.1 Convergence

The first important question is to check whether the Markov chain is actually converging to its limit distribution (see Chapter 4 for details). As noted in Section 4.2.5, we did not obtain a proof of the irreducibility of the Markov chain generated by Algorithm A and thus we cannot know whether the chain converges to the desired measure or its restriction. We have employed some basic metrics to check whether the chain appears to be converging, see Figure 6.1 for a representative example for one simulation.

6.1.2 Role of the parameter θ

In this section, we investigate the role of the parameter θ in our model. As noted before, the GPP favours configurations with lower energy. In case of the potential $\varphi_{HC}^{\theta,\alpha}$, the configurations are forced to contain fewer larger tetrahedra (called *cells* in the figures) in order to minimize the overall surface area. The parameter θ then controls the strength of this effect. A higher θ should therefore result in a smaller number of larger tetrahedra. This effect can be seen in Figure 6.2 for one realization of the model $\text{L}+$.

Negative θ

Although we have restricted ourselves to the case of non-negative potentials, it is still interesting to attempt to simulate models with a $\theta < 0$, even if we do not know whether they exist. Choosing θ negative reverses the relationship mentioned above. The GPP now favours configurations with greater overall surface area, which should result into a larger number of smaller tetrahedra. This is in fact what happens in the simulation, see Figure 6.3.

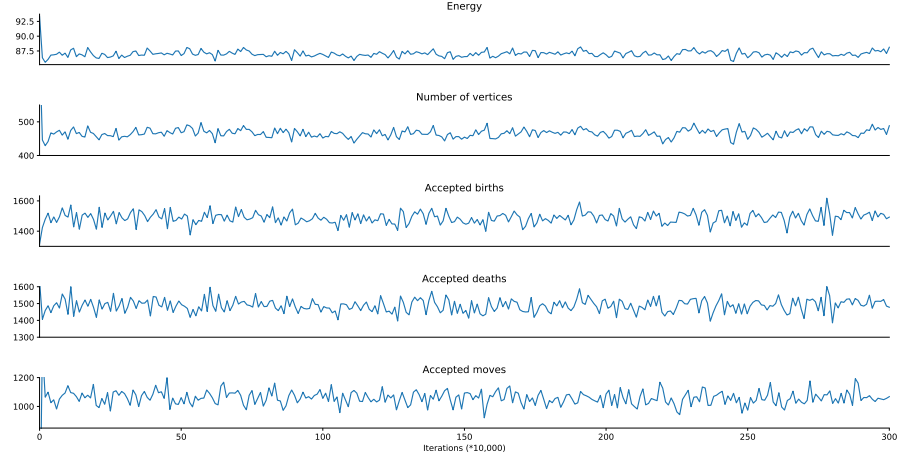


Figure 6.1: Convergence metrics for one simulation of L+. Total number of iterations: 3×10^6 . $\theta = 1, \alpha = 0.15, z = 500, W = 0.01$.

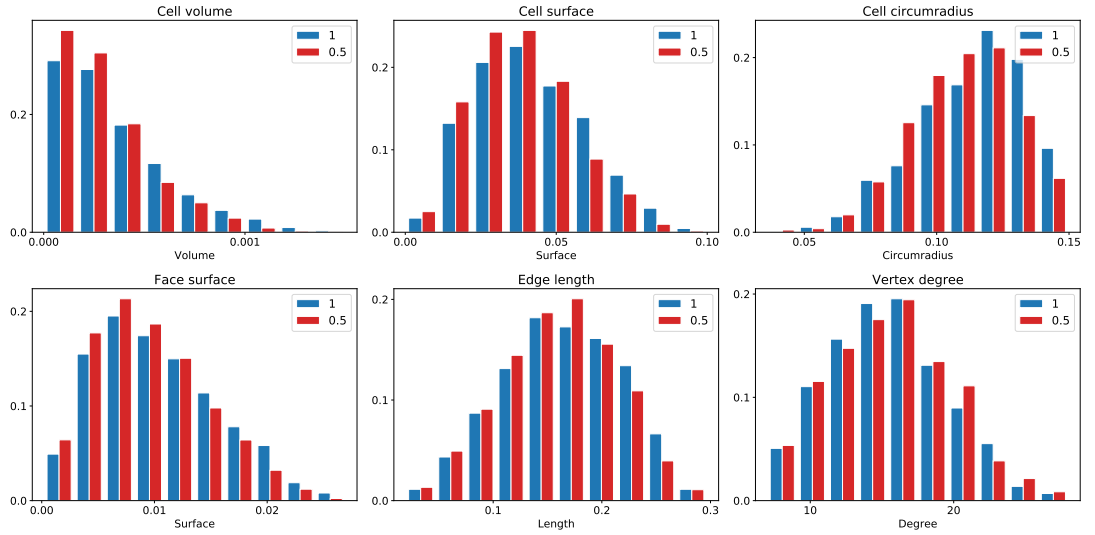


Figure 6.2: Comparison of the distribution of facet statistics for one realization of L+ model with $\alpha = 0.15, z = 500, W = 0.01$ and $\theta = 0.5, 1$.

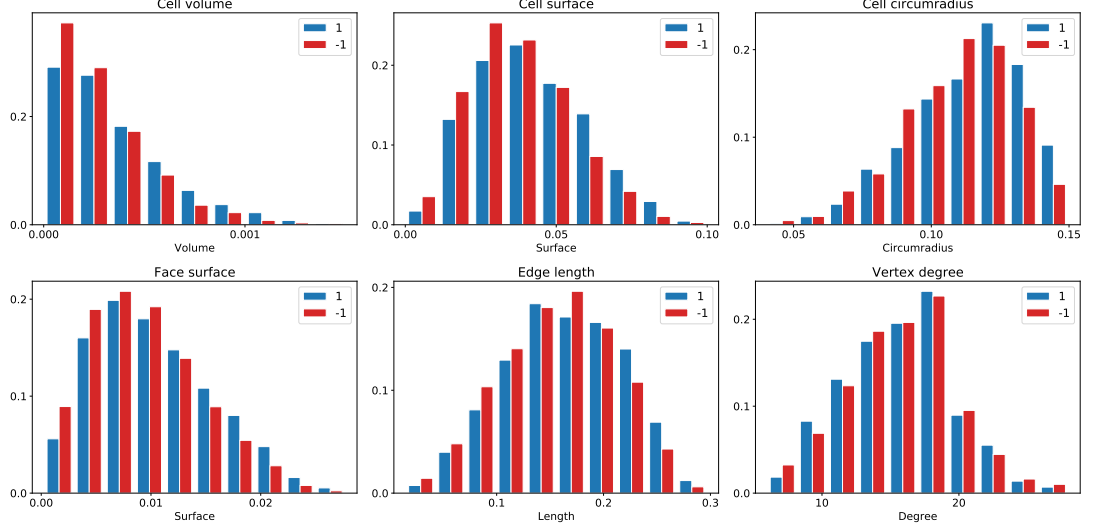


Figure 6.3: Comparison of the distribution of facet statistics for one realization of L+ model with $\alpha = 0.15$, $z = 500$, $W = 0.01$ and $\theta = -1, 1$.

Obtaining the Poisson tetrahedrization

From Proposition 8, we know that for $\Lambda \in \mathcal{B}_0$ the Poisson point process with intensity z has the density $f(\gamma) \propto z^{N_\Lambda(\gamma)}$, $\gamma \in \mathbf{N}_\Lambda$. From Definition 29 of the Gibbs point process we can deduce that if the energy function is zero for all configurations, then the Gibbs point process with activity z reduces to the Poisson point process with intensity z . Figure 6.4 illustrates this point, where the facet distributions of a realization of the model L+ with $\theta = 0.01$ are compared to the expected values of their counterparts for the Poisson process (found on page 393 in Okabe et al. [1992]).

6.1.3 Difference between Laguerre and Delaunay

Perhaps the most interesting comparison to make is between the two models D+ and L+ with identical parameters. A summary of facet distributions for a realization of both models is shown in Figure 6.5. There we can see that the Delaunay model produces a greater number of smaller tetrahedra than the Laguerre model.

All of the results for both D+ and L+ with four θ levels are summarized in Table 6.1, which shows the averages and standard deviations for a 100 simulations of each model.

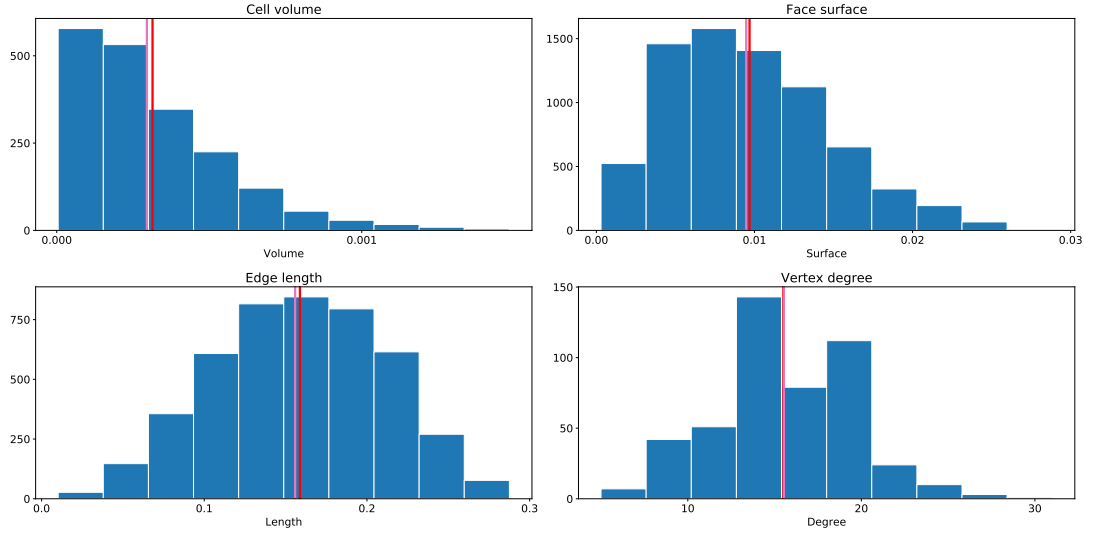


Figure 6.4: Facet distributions of a realization of the L+ model with $\alpha = 0.15$, $z = 500$, $W = 0.01$ and $\theta = 0.01$. Purple line is the expected value for a Poisson-tetrahedrization, red line is the empirical mean of the realization.

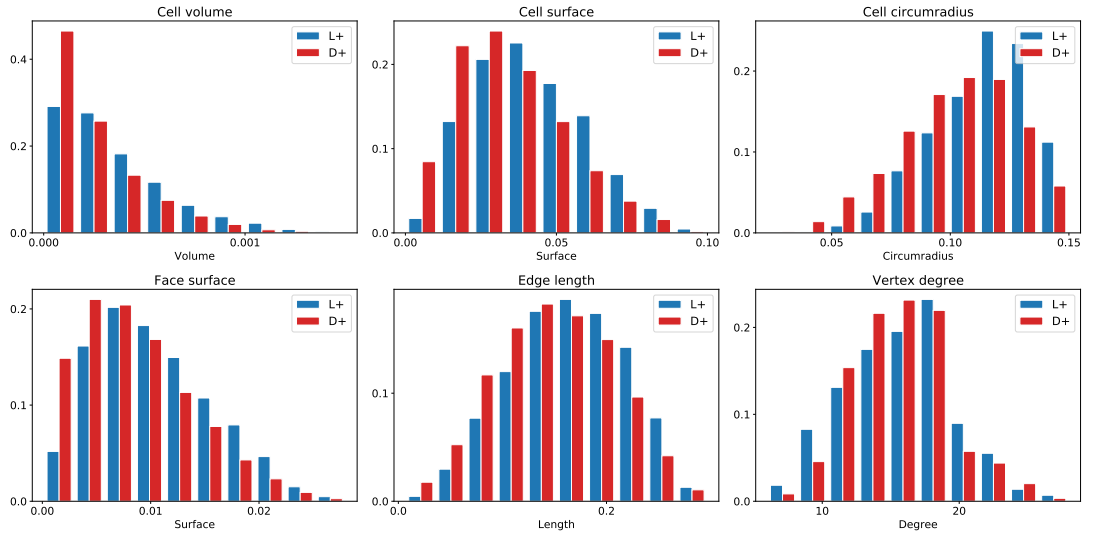


Figure 6.5: Facet distribution for a realization of the models D+ and L+. Parameters $\theta = 1$, $\alpha = 0.15$, $z = 500$, $W = 0.01$ for both models.

	Theta	Cell				Face	Edge		Vertex	
		Count	Volume	Circumradius	Surface		Surface	Length	Count	Degree
D+	-1.0	2761.3 (108.1)	0.00023 (0.00001)	0.1011 (0.0012)	0.0322 (0.0008)	0.0081 (0.0002)	0.1453 (0.0017)	639.6 (20.0)	15.4 (0.1)	
	-0.5	2685.7 (119.9)	0.00024 (0.00001)	0.1015 (0.0016)	0.0326 (0.0010)	0.0082 (0.0003)	0.1461 (0.0024)	626.2 (22.5)	15.4 (0.1)	
	0.5	2509.0 (103.3)	0.00025 (0.00001)	0.1028 (0.0014)	0.0337 (0.0009)	0.0085 (0.0002)	0.1481 (0.0020)	595.2 (19.0)	15.4 (0.1)	
	1.0	2416.4 (100.9)	0.00026 (0.00001)	0.1036 (0.0013)	0.0344 (0.0009)	0.0086 (0.0002)	0.1495 (0.0018)	577.3 (19.3)	15.4 (0.1)	
L+	-1.0	2082.9 (81.4)	0.00030 (0.00001)	0.1090 (0.0013)	0.0373 (0.0010)	0.0094 (0.0003)	0.1565 (0.0020)	496.7 (16.5)	15.5 (0.1)	
	-0.5	2022.4 (92.7)	0.00030 (0.00001)	0.1096 (0.0012)	0.0378 (0.0009)	0.0095 (0.0002)	0.1574 (0.0019)	484.4 (18.0)	15.5 (0.1)	
	0.5	1909.3 (84.8)	0.00032 (0.00002)	0.1105 (0.0015)	0.0388 (0.0012)	0.0097 (0.0003)	0.1593 (0.0024)	460.8 (16.1)	15.6 (0.1)	
	1.0	1855.3 (86.7)	0.00033 (0.00001)	0.1110 (0.0013)	0.0394 (0.0011)	0.0099 (0.0003)	0.1603 (0.0020)	451.9 (16.3)	15.6 (0.1)	

Table 6.1: Mean facet statistics and standard deviations (in parentheses) computed from 100 realizations of each of the models D+ and L+ and each θ setting. Other parameters were set to $\alpha = 0.15$, $z = 500$, $W = 0.01$.

	θ	$\hat{\alpha}$	$\hat{\theta}$	\hat{z}	Vertices	Removable
D+						
	0.5	0.14933	1.16643	595.83387	595.24	538.37
		(0.00069)	(0.94777)	(52.15171)	(18.98)	(23.18)
	1.0	0.14946	1.84958	605.18565	577.32	515.81
		(0.00050)	(1.03663)	(58.29123)	(19.28)	(24.94)
L+						
	0.5	0.15455	1.20596	306.40235	460.83	269.36
		(0.02235)	(1.44752)	(41.40474)	(16.13)	(15.71)
	1.0	0.15580	1.71939	312.60278	451.88	261.60
		(0.04506)	(1.41497)	(46.78521)	(16.31)	(17.60)

Table 6.2: Estimation results with mean values of the estimates (standard deviations in parentheses), total number of vertices in the observation window, and the number of removable vertices. Each θ was simulated 100 times. Other parameters set to $\alpha = 0.15, z = 500, W = 0.01$.

6.2 Estimation

This section presents the results of the estimation procedure presented in Chapter 5. Figures 6.6, and 6.7 each show the results for the models D+ and L+ with θ equal to 1.

Table 6.2 summarizes all estimation results. For 100 realizations for each of the models D+ and L+ with $\theta = 0.5$, the estimates $\hat{\theta}$ were equal to 1.167 with standard deviation 0.95 for D+ and 1.21 with standard deviation 1.45 for L+.

The activity z can be seen as the intensity of the Poisson point process with respect to which the Gibbs measure is absolutely continuous. It therefore controls the number of points, which in turn influences the number of tetrahedra, a number that is connected to the parameter θ . This fact is manifested in the bottom-right plot in each figure, which suggests a linear relationship between the estimates $\hat{\theta}$ and \hat{z} , a relationship that can be seen in the results of Dereudre and Lavancier [2011] as well.

Note that in particular the estimate \hat{z} seems biased, especially for the model L+. The low quality of the estimator \hat{z} is seen in Dereudre and Lavancier [2011] (see page 510 there) as well. Its comparably worse quality in here could be caused by the increase in the complexity of the model, particularly by the introduction of point weights in Laguerre models.

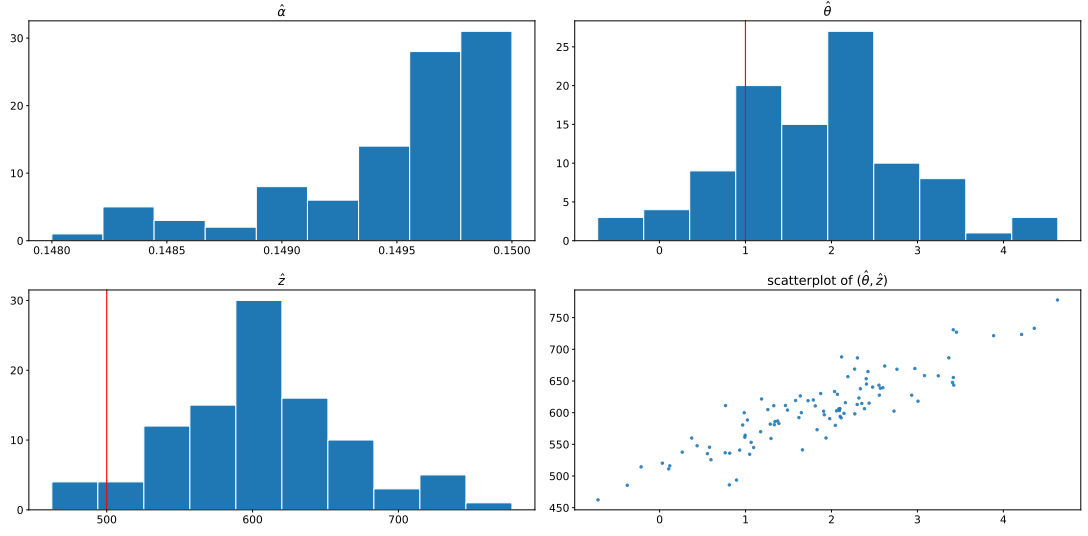


Figure 6.6: Estimation results for the model D+ with parameters $\theta = 1, \alpha = 0.15, z = 500, W = 0.01$ for 100 realizations. Average number of removable points: 516.

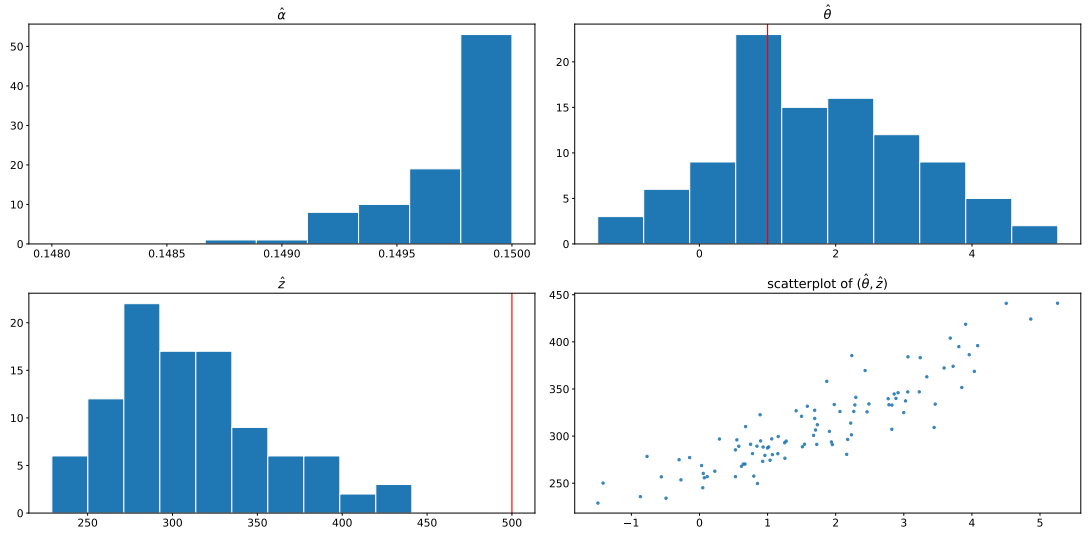


Figure 6.7: Estimation results for the model L+ with parameters $\theta = 1, \alpha = 0.15, z = 500, W = 0.01$ for 100 realizations. Average number of removable points: 262.

Conclusion

This text has dealt with stochastic Laguerre-Delaunay tetrahedrizations based on the Gibbs point process. We have presented parametric hard-core models which allow us to control various properties of the resulting tetrahedrizations, such as the surface area of the tetrahedra. Existence of these models has been proven using the approach in Dereudre et al. [2012]. Then we focused on extending the results of Dereudre and Lavancier [2011] in simulation and estimation of model parameters for these models. Simulation was done through a Markov chain Monte Carlo procedure and implemented in `C++`. Estimation was done through the maximum pseudolikelihood method, extended to the non-hereditary case in Dereudre and Lavancier [2009].

A considerable number of results is outside the scope of this text.

The first extension would be to complete the results in this text — that is extend the existing results of Dereudre and Lavancier [2009] in irreducibility of the Markov chain and Dereudre and Lavancier [2011] in consistency of the MPLE estimates to the three-dimensional Laguerre-Delaunay case. As with existence, it is likely the case that the extension to Laguerre would be easier than the extension to three dimensions.

Second extension is to study the stability of the potentials without the assumptions of non-negativity. The answer depends on the complexity of the tetrahedrization. It seems likely to us that there are relatively easily obtainable results on the complexity of the tetrahedrization of the Poisson process and then perhaps even for the Gibbs point process. Obtaining some results for the tetrahedrization generated by the Poisson process would be interesting in and of itself, as the study of such structures is popular in the field of computational geometry (see e.g. Amenta et al. [2007], Erickson [2005]).

A number of other extensions were considered. There are many possibilities in specifying potentials of a different form, in particular studying non-unary potentials by including explicit tetrahedral interactions. This would require new proofs of existence, convergence of MCMC and consistency of the estimation techniques. In the practical sense, it should be relatively easy to extend our `C++` implementation to include tetrahedral interactions.

Different estimation techniques could be tried. Although we are limited in their choice by the absence of heredity, options do exist. One of them is the variational estimator which is applicable even in the non-hereditary case (Baddeley and Dereudre [2013]).

In the practical implementation, an interesting comparison would be to try to use the periodic outside configuration as Dereudre and Lavancier [2011] does.

Finally, instead of using the power distance to define the tetrahedrization, we could use a weighted Euclidean metric (Gavrilova [1998]), resulting in the dual of the so-called Apollonius diagram, or Johnson-Mehl tessellation.

Bibliography

- N. Amenta, D. Attali, and O. Devillers. Complexity of delaunay triangulation for points on lower-dimensional polyhedra. In *Proceedings of the Eighteenth Annual ACM-SIAM Symposium on Discrete Algorithms*, SODA '07, pages 1106–1113, Philadelphia, PA, USA, 2007. Society for Industrial and Applied Mathematics.
- F. Aurenhammer. Power diagrams: Properties, algorithms and applications. *SIAM Journal on Computing*, 16(1):78–96, 1987.
- F. Aurenhammer, R. Klein, and D.T. Lee. *Voronoi Diagrams and Delaunay Triangulations*. World scientific, 2013.
- A. Baddeley and D. Dereudre. Variational estimators for the parameters of gibbs point process models. *Bernoulli*, 19(3):905–930, 2013.
- M. Caroli, A. Pellé, M. Rouxel-Labbé, and M. Teillaud. 3D periodic triangulations. In *CGAL User and Reference Manual*. CGAL Editorial Board, 4.12 edition, 2018. URL <https://doc.cgal.org/4.12/Manual/packages.html#PkgPeriodic3Triangulation3Summary>.
- A. Cayley. On a theorem in the geometry of positions. *Cambridge Math*, 2: 267–271, 1841.
- J.A. De Loera, J. Rambau, and F. Santos. *Triangulations: Structures for Algorithms and Applications*. Springer Publishing Company, Incorporated, 1st edition, 2010.
- D. Dereudre. Introduction to the theory of Gibbs point processes. *ArXiv 1701.08105 [math.PR]*, 2017.
- D. Dereudre and F. Lavancier. Campbell equilibrium equation and pseudo-likelihood estimation for non-hereditary Gibbs point processes. *Bernoulli*, 15(4):1368–1396, 2009.
- D. Dereudre and F. Lavancier. Practical simulation and estimation for Gibbs Delaunay-Voronoi tessellations with geometric hardcore interaction. *Computational Statistics and Data Analysis*, 55(1):498–519, 2011.
- D. Dereudre, R. Drouilhet, and H.O. Georgii. Existence of gibbsian point processes with geometry-dependent interactions. *Probability Theory and Related Fields*, 153(3):643–670, 2012.
- H. Edelsbrunner and N. R. Shah. Incremental topological flipping works for regular triangulations. *Algorithmica*, 15(3):223–241, 1996.
- J. Erickson. Dense point sets have sparse delaunay triangulations or "... but not too nasty". *Discrete Comput. Geom.*, 33(1):83–115, 2005.
- Fropuff. The vertex configuration of a tetrahedral-octahedral honeycomb., 2006. URL <https://en.wikipedia.org/wiki/File:TetraOctaHoneycomb-VertexConfig.svg>.

- R. Gabbrielli, Y. Jiao, and S. Torquato. Families of tessellations of space by elementary polyhedra via retessellations of face-centered-cubic and related tilings. *Phys. Rev. E*, 86:041141, 2012.
- M Gavrilova. *Proximity and Applications in General Metrics*. PhD thesis, The University of Calgary, 1998.
- H.O. Georgii. *Gibbs Measures and Phase Transitions*. De Gruyter Studies in Mathematics 9. Walter de Gruyter Inc, 2nd edition, 2011.
- D. Gisch and J.M. Ribando. Apollonius’ problem: A study of solutions and their connections, 2004.
- J. Hadamard. Résolution d’une question relative aux déterminants. *Bull. Sci. Math.*, 17(3):240–246, 1893.
- M. Hummel. *Delaunay-Laguerre Geometry For Macromolecular Modeling and Implicit Solvation*. PhD thesis, University of New Mexico, 2015.
- C. Jamin, S. Pion, and M. Teillaud. 3D triangulations. In *CGAL User and Reference Manual*. CGAL Editorial Board, 4.12 edition, 2018. URL <https://doc.cgal.org/4.12/Manual/packages.html#PkgTriangulation3Summary>.
- B. Joe. Three-dimensional triangulations from local transformations. *SIAM Journal on Scientific and Statistical Computing*, 10(4):718–741, 1989.
- B. Joe. Construction of three-dimensional delaunay triangulations using local transformations. *Comput. Aided Geom. Des.*, 8(2):123–142, 1991.
- J. Kocik. A theorem on circle configurations. *ArXiv*, 0706.0372 [math.PR], 2007.
- J.C. Lagarias and C. Zong. Mysteries in packing regular tetrahedra. *Notices of the American Mathematical Society*, 59(11):1392, 2012.
- C.L. Lawson. Transforming triangulations. *Discrete Math.*, 3(4):365–372, 1972.
- S. Mase. Marked gibbs processes and asymptotic normality of maximum pseudo-likelihood estimators. *Mathematische Nachrichten*, 209(1):151–169, 2000.
- K. Menger. Untersuchungen uber allgemeine metrik. *Mathematische Annalen*, 100:120,133, 1928.
- S.P. Meyn and R.L. Tweedie. *Markov Chains and Stochastic Stability*. Springer London, 1993.
- J. Møller and R.P. Waagepetersen. *Statistical Inference and Simulation for Spatial Point Processes*. Chapman & Hall/CRC Monographs on Statistics & Applied Probability. CRC Press, 2003.
- X.X. Nguyen and H. Zessin. Integral and differential characterizations of the gibbs process. *Mathematische Nachrichten*, 88(1):105–115, 1979.
- A. Okabe, B. Boots, and K. Sugihara. *Spatial Tessellations: Concepts and Applications of Voronoi Diagrams*. John Wiley & Sons, Inc., New York, NY, USA, 1992.

- M. O’Keeffe, M.A. Peskov, S.J. Ramsden, and O.M. Yaghi. The reticular chemistry structure resource (rcsr) database of, and symbols for, crystal nets. *Accounts of Chemical Research*, 41(12):1782–1789, 2008.
- R. Quey, P.R. Dawson, and F. Barbe. Large-scale 3D random polycrystals for the finite element method: Generation, meshing and remeshing. *Computer Methods in Applied Mechanics and Engineering*, 200(17-20):1729–1745, 2011. URL <https://hal.archives-ouvertes.fr/hal-00858028>.
- C.P. Robert and G. Casella. *Monte Carlo Statistical Methods*. Springer New York, 2004.
- R. Schneider and W. Weil. *Stochastic and Integral Geometry*. Probability and Its Applications. Springer-Verlag Berlin Heidelberg, 2008.
- D.M.Y. Sommerville. *An introduction to the geometry of n-dimensions*. Methuen and Co, 1929.
- P. Stein. A note on the volume of a simplex. *The American Mathematical Monthly*, 73(3):299, 1966.
- The CGAL Project. *CGAL User and Reference Manual*. CGAL Editorial Board, 4.12 edition, 2018. URL <https://doc.cgal.org/4.12/Manual/packages.html>.
- J. V. Uspensky. *Theory of equations*. McGraw-Hill, 1948.
- Wolfram Research Inc. Mathematica, Version 11.3. Champaign, IL, 2018.
- H. Zessin. Point processes in general position. *Journal of Contemporary Mathematical Analysis*, 43(1):59–65, 2008.

List of Figures

1.1	Geometrical interpretation of the power distance.	8
1.2	Geometrical interpretation of the power product. Horizontal scale depicts values of $\rho(p, q)$, diagrams show an illustration of the arrangement of the balls B_p and B_q	8
1.3	Laguerre-cospherical points in \mathbb{R}^2 . The characteristic point is in red.	10
1.4	Illustration of the circumsphere (blue) and characteristic point (red). Note also that there is no simple relationship between the two objects.	10
3.1	The tetrahedral-octahedral tessellation in an exploded view. (Source: Fropuff [2006])	35
3.2	The nearest neighbour graph $\text{NNG}(\mathbf{x}_1)$, forming a tessellation of two tetrahedra and an octahedron.	35
6.1	Convergence metrics for one simulation of L+. Total number of iterations: 3×10^6 . $\theta = 1, \alpha = 0.15, z = 500, W = 0.01$	55
6.2	Comparison of the distribution of facet statistics for one realization of L+ model with $\alpha = 0.15, z = 500, W = 0.01$ and $\theta = 0.5, 1$	55
6.3	Comparison of the distribution of facet statistics for one realization of L+ model with $\alpha = 0.15, z = 500, W = 0.01$ and $\theta = -1, 1$	56
6.4	Facet distributions of a realization of the L+ model with $\alpha = 0.15, z = 500, W = 0.01$ and $\theta = 0.01$. Purple line is the expected value for a Poisson-tetrahedrization, red line is the empirical mean of the realization.	57
6.5	Facet distribution for a realization of the models D+ and L+. Parameters $\theta = 1, \alpha = 0.15, z = 500, W = 0.01$ for both models.	57
6.6	Estimation results for the model D+ with parameters $\theta = 1, \alpha = 0.15, z = 500, W = 0.01$ for 100 realizations. Average number of removable points: 516.	60
6.7	Estimation results for the model L+ with parameters $\theta = 1, \alpha = 0.15, z = 500, W = 0.01$ for 100 realizations. Average number of removable points: 262.	60
A.1	All solutions to Apollonius problem with $T_1, a = 1$	73
A.2	All solutions to Apollonius problem with $T_2, a = 1$	73

List of Tables

6.1	Mean facet statistics and standard deviations (in parentheses) computed from 100 realizations of each of the models D+ and L+ and each θ setting. Other parameters were set to $\alpha = 0.15, z = 500, W = 0.01$.	58
6.2	Estimation results with mean values of the estimates (standard deviations in parentheses), total number of vertices in the observation window, and the number of removable vertices. Each θ was simulated 100 times. Other parameters set to $\alpha = 0.15, z = 500, W = 0.01$.	59

A. Appendix: Geometry

This appendix investigates some facts and propositions pertaining to geometry in \mathbb{R}^3 . Since marked points are not present here, the dashed notation introduced in Chapter 1 will be dropped.

A.1 Calculating the circumdiameter

Here we describe how to calculate the circumradius (or circumdiameter) of a 3-simplex through the Cayley-Menger determinant (Cayley [1841], Menger [1928], Uspensky [1948]).

First, consider the points $p_1, \dots, p_5 \in \mathbb{R}^4$ which form a 4-simplex. Denote $d_{ij} = \|p_i - p_j\|, i, j = 1, \dots, 5$. Then the area A of the 4-simplex is given by the **Cayley-Menger determinant** (Sommerville [1929]). We have .

$$-9216A^2 = \begin{vmatrix} 0 & 1 & 1 & 1 & 1 & 1 \\ 1 & 0 & d_{12}^2 & d_{13}^2 & d_{14}^2 & d_{15}^2 \\ 1 & d_{21}^2 & 0 & d_{23}^2 & d_{24}^2 & d_{25}^2 \\ 1 & d_{31}^2 & d_{32}^2 & 0 & d_{34}^2 & d_{35}^2 \\ 1 & d_{41}^2 & d_{42}^2 & d_{43}^2 & 0 & d_{45}^2 \\ 1 & d_{51}^2 & d_{52}^2 & d_{53}^2 & d_{54}^2 & 0 \end{vmatrix}.$$

Now consider non-coplanar points $p_1, \dots, p_4 \in \mathbb{R}^3$ forming a 3-simplex, i.e. a tetrahedron. To obtain the circumradius of this tetrahedron we imagine p_1, \dots, p_4 to lie on a 3-dimensional hyperplane H in \mathbb{R}^4 and we consider the point $c \in H$ such that $\|c - p_i\| = r$ for all $i = 1, \dots, 4, r \in \mathbb{R}$. The point c is, by definition, the center of the circumsphere of p_1, \dots, p_4 and r is the circumradius. The circumradius r can be obtained using the Cayley-Menger determinant, since p_1, \dots, p_4, c now form a 4-dimensional simplex of volume 0. We therefore have

$$0 = \begin{vmatrix} 0 & 1 & 1 & 1 & 1 & 1 \\ 1 & 0 & d_{12}^2 & d_{13}^2 & d_{14}^2 & r^2 \\ 1 & d_{21}^2 & 0 & d_{23}^2 & d_{24}^2 & r^2 \\ 1 & d_{31}^2 & d_{32}^2 & 0 & d_{34}^2 & r^2 \\ 1 & d_{41}^2 & d_{42}^2 & d_{43}^2 & 0 & r^2 \\ 1 & r^2 & r^2 & r^2 & r^2 & 0 \end{vmatrix}, \quad (\text{A.1})$$

where we again have $d_{ij} = \|p_i - p_j\|, i, j = 1, \dots, 4$.

It would be possible to solve A.1 as an equation of r . A better approach is to subtract r^2 times the first row from the last row and subtract r^2 times the first column from the last column to obtain the determinant

$$\begin{vmatrix} 0 & 1 & 1 & 1 & 1 & 1 \\ 1 & 0 & d_{12}^2 & d_{13}^2 & d_{14}^2 & 0 \\ 1 & d_{21}^2 & 0 & d_{23}^2 & d_{24}^2 & 0 \\ 1 & d_{31}^2 & d_{32}^2 & 0 & d_{34}^2 & 0 \\ 1 & d_{41}^2 & d_{42}^2 & d_{43}^2 & 0 & 0 \\ 1 & 0 & 0 & 0 & 0 & -2r^2 \end{vmatrix}.$$

By expanding by the last row, we obtain the equation

$$2r^2 \begin{vmatrix} 0 & 1 & 1 & 1 & 1 \\ 1 & 0 & d_{12}^2 & d_{13}^2 & d_{14}^2 \\ 1 & d_{21}^2 & 0 & d_{23}^2 & d_{24}^2 \\ 1 & d_{31}^2 & d_{32}^2 & 0 & d_{34}^2 \\ 1 & d_{41}^2 & d_{42}^2 & d_{43}^2 & 0 \end{vmatrix} - \begin{vmatrix} 1 & 1 & 1 & 1 & 1 \\ 0 & d_{12}^2 & d_{13}^2 & d_{14}^2 & 0 \\ d_{21}^2 & 0 & d_{23}^2 & d_{24}^2 & 0 \\ d_{31}^2 & d_{32}^2 & 0 & d_{34}^2 & 0 \\ d_{41}^2 & d_{42}^2 & d_{43}^2 & 0 & 0 \end{vmatrix} = 0,$$

from which r^2 is directly expressible as

$$r^2 = \frac{\begin{vmatrix} 1 & 1 & 1 & 1 & 1 \\ 0 & d_{12}^2 & d_{13}^2 & d_{14}^2 & 0 \\ d_{21}^2 & 0 & d_{23}^2 & d_{24}^2 & 0 \\ d_{31}^2 & d_{32}^2 & 0 & d_{34}^2 & 0 \\ d_{41}^2 & d_{42}^2 & d_{43}^2 & 0 & 0 \end{vmatrix}}{2 \begin{vmatrix} 0 & 1 & 1 & 1 & 1 \\ 1 & 0 & d_{12}^2 & d_{13}^2 & d_{14}^2 \\ 1 & d_{21}^2 & 0 & d_{23}^2 & d_{24}^2 \\ 1 & d_{31}^2 & d_{32}^2 & 0 & d_{34}^2 \\ 1 & d_{41}^2 & d_{42}^2 & d_{43}^2 & 0 \end{vmatrix}}. \quad (\text{A.2})$$

It is worth noting that the determinant in the quotient cannot equal zero, since it is again a Cayley-Menger determinant and we assumed p_1, \dots, p_4 to be non-coplanar.

A.2 Bounding the circumdiameter

This section derives the bounds used in Theorems 3, 4, 5, 6, and Propositions 15 and 16. There, we considered the problem of bounding the circumdiameter of tetrahedra present in the tetrahedrization of a pseudo-periodic configuration $\mathbf{x} \in \bar{\Gamma}$. This problem can be seen finding the bound for the tetrahedra defined in Proposition 14 with “perturbed” points. We first state the problem in clear terms and then proceed to find the bound.

A.2.1 Statement of the problem

The problem of founding the bounds can be stated as the following two optimization problems. Recall the definition of ρ and a from Section 3.2.1.

For the tetrahedron T_1 , the problem is

$$\begin{aligned} & \underset{p_1, p_2, p_3, p_4 \in \mathbb{R}^3}{\text{maximize}} && \chi(\{p_1, p_2, p_3, p_4\}) \\ & \text{subject to} && \|p_i - t_i\| \leq \rho a, \quad t_i \in \mathbb{R}^3, i = 1, 2, 3, 4, \\ & && \|t_i - t_j\| = a, \quad i = 1, 2, 3, 4. \end{aligned} \quad (\text{A.3})$$

To state the problem for the tetrahedron T_2 , first denote

$$D = \begin{pmatrix} 0 & \sqrt{2}a & a & a \\ \sqrt{2}a & 0 & a & a \\ a & a & 0 & a \\ a & a & a & 0 \end{pmatrix},$$

and denote the entries of matrix D as d_{ij} , $i, j = 1, 2, 3, 4$. Then the statement is:

$$\begin{aligned} & \underset{p_1, p_2, p_3, p_4 \in \mathbb{R}^3}{\text{maximize}} && \chi(\{p_1, p_2, p_3, p_4\}) \\ & \text{subject to} && \|p_i - t_i\| \leq \rho a, \quad t_i \in \mathbb{R}^3, i = 1, 2, 3, 4, \\ & && \|t_i - t_j\| = d_{ij}, \quad i, j = 1, 2, 3, 4. \end{aligned} \quad (\text{A.4})$$

This is a non-linear optimization problem. We can arrive at its solution through some careful geometric arguments.

A.2.2 Solution to the problem

First, define the *circumdiameter function* of point $p \in \mathbb{R}^3$ with respect to non-collinear points $p_1, p_2, p_3 \in \mathbb{R}^3$:

$$c(p) = \chi(\{p, p_1, p_2, p_3\}).$$

Denote (x_i, y_i, z_i) the coordinates of p_i , $i = 1, \dots, 3$. Denote $\chi(\{p_1, p_2, p_3\})$ the circumdiameter of the triangle formed by p_1, p_2, p_3 . Lastly, we remind the reader that a closed halfspace is a set of the form $\{y \in \mathbb{R}^3 : \langle y, x \rangle \geq a\}$, $x \in \mathbb{R}^3$, $a \in \mathbb{R}$, and a open halfspace has the same form with a strict inequality.

The following lemma describes the properties of $c(p)$.

Lemma 5. *$c(p)$ is continuous, has a global minimum $c_{\min} := \chi(\{p_1, p_2, p_3\})$ and level sets*

$$L_a := \{p \in \mathbb{R}^3 : c(p) = a\} = S_{a1} \cup S_{a2}, \quad a \geq c_{\min},$$

where S_{a1} and S_{a2} are two spheres with diameter a such that $p_1, p_2, p_3 \in S_{a1} \cap S_{a2}$. Furthermore, the centers c_1, c_2 of S_{a1}, S_{a2} respectively, lie in the closed halfspaces

$$H_+ = \{x \in \mathbb{R}^3 : Ax \geq 0\}, \quad H_- = \{x \in \mathbb{R}^3 : Ax \leq 0\},$$

respectively, where A defines the hyperplane $H = \{x \in \mathbb{R}^3 : Ax = 0\}$ such that $p_1, p_2, p_3 \in H$.

Proof. Continuity: From A.2 we see that $c(p)$ can be seen as a composition of a norm, determinants and division. Determinant is continuous as a function of elements of the matrix since it is a polynomial function. Thus $c(p)$ is continuous.

We can rewrite L_a as

$$\{p \in \mathbb{R}^3 : \exists \text{ sphere } S \text{ s.t. } p_1, p_2, p_3, p \in S \text{ and } \text{diam} S = a\}.$$

We must therefore find the number of spheres through the points p_1, p_2, p_3 with the diameter a . Denote S a sphere such that $\{p_1, p_2, p_3\} \subset S$ with $\text{diam}(S) = a$. Define the hyperplanes

$$H_{12} = \{x \in \mathbb{R}^3 : \|x - p_1\| = \|x - p_2\|\}, \quad H_{23} = \{x \in \mathbb{R}^3 : \|x - p_2\| = \|x - p_3\|\}.$$

The intersection $H_{12} \cap H_{23}$ is a line L , as p_1, p_2, p_3 are non-collinear. The center of S is at distance $a/2$ from all three points and thus lies on L . For any point, there are at most two points on the line L at a given distance from the point. This proves that there are at most two spheres satisfying the definition of S .

The point on L at a minimum distance to p_1, p_2, p_3 is the point $p_{min} := L \cap H$. We know that p_{min} is equidistant from p_1, p_2, p_3 and that it lies on the hyperplane H , therefore it is the circumcenter of the triangle defined by p_1, p_2, p_3 and we have $c(p_{min}) = \chi(\{p_1, p_2, p_3\})$.

To see that c_1 and c_2 must be (non-strictly) separated by the hyperplane H , assume, without loss of generality, that $\{c_1, c_2\} \subset H_+, c_1 \neq c_2$. Let $p \in S_{a1} \setminus H$ and let $p_H \in \mathbb{R}^3$ be the reflection of p through the hyperplane H . The tetrahedron p_1, p_2, p_3, p_H then is a reflection of the tetrahedron p_1, p_2, p_3, p and therefore its circumsphere has diameter a . However, its centre lies in H_- , which is a contradiction. \square

Note that S_{a1} and S_{a2} are not necessarily distinct. In fact, we can see from the proof that $S_{a1} = S_{a2}$ precisely when $a = c_{min}$.

We are now ready to characterize the set of solutions to A.3 and A.4. For the next proposition, we say a point lies “inside” or “outside” of the sphere S if the point lies in B or in B^c respectively, where B is the closed ball such that $\partial B = S$. Further define $S(q_1, q_2, q_3, q_4)$ to be the sphere on which $q_1, q_2, q_3, q_4 \in \mathbb{R}^3$ lie. We further define *tangent spheres* as two spheres intersecting at a point. If one sphere lies inside the other, they are *internally tangent*, otherwise they are *externally tangent*.

Proposition 20. *Any solution (p_1, p_2, p_3, p_4) of the problem A.3 will lie on a sphere S that is (internally or externally) tangent to the spheres $\partial B(t_i, \rho_a), i = 1, 2, 3, 4$.*

Proof. Let (p_1, p_2, p_3, p_4) be a solution of A.3. Denote $c(p) = \chi(\{p, p_2, p_3, p_4\})$, $p \in \mathbb{R}^3$ and S the circumsphere of $\{p_1, \dots, p_4\}$. First assume that $p_1 \in B(t_1, \rho_a)$. Because p_1 maximizes the function $c(p)$, we have $c(p_1) \geq c(p), p \in U$, where U is some small neighborhood of p_1 . Choose two points, $p_O, p_I \in U \setminus S$ such that

1. $c(p_O) = c(p_I) = b$,
2. p_I is on the inside of S and p_O on the outside of S ,
3. $S(p_I, p_2, p_3, p_4)$ and $S(p_O, p_2, p_3, p_4)$ do not equal and their centers lie on the same open halfspace (with respect to the hyperplane defined by p_2, p_3, p_4) as S .

Such choice is possible due to continuity of $c(p)$. Yet we arrive at a contradiction, as the level set L_b now contains two distinct spheres with centres in the same open halfspace.

Assume now that $p_1 \in \partial B(t_1, \rho_a)$ and denote $S_1 = \partial B(t_1, \rho_a)$. We now choose p_I and p_O with the additional requirement that they must both lie on $\partial B(t_1, \rho_a)$. Such choice is not possible precisely when S_1 and S are tangent, since then S_1 lies either completely inside or outside S and it is no longer possible to choose points both outside and inside. \square

Note that Proposition 20 is formulated for problem A.3. However, we could repeat the same exact argument for A.4 and thus the same holds for both problems.

We have found that the solutions to A.3 and A.4 must lie on a sphere that is tangent to the spheres within which points can move. This is a dramatic improvement — we have narrowed the previously infinite space of possible solutions down to just $2^4 = 16$ possible quadruples of points (and even fewer because of symmetries). We also note that the set of solutions to our problem is precisely the set of solutions of a three-dimensional equivalent of the more than two thousand years old **Apollonius problem** (Gisch and Ribando [2004]).

A.2.3 Apollonius problem in \mathbb{R}^3

We want to find all the spheres that are externally or internally tangent to the spheres $\partial B(t_i, \rho a)$, $i = 1, 2, 3, 4$ as defined in problems A.3 and A.4.

First note that two externally tangent spheres $S_1 = ((x_1, y_1, z_1), r_1)$, $S_2 = ((x_2, y_2, z_2), r_2)$ satisfy

$$\|(x_1, y_1, z_1) - (x_2, y_2, z_2)\| = r_1 + r_2.$$

Similarly, two internally tangent spheres satisfy

$$\|(x_1, y_1, z_1) - (x_2, y_2, z_2)\| = |r_1 - r_2|.$$

By squaring both equations, we obtain the equality

$$(x_1 - x_2)^2 + (y_1 - y_2)^2 + (z_1 - z_2)^2 = (r_1 \pm r_2)^2$$

Where we use $+$ for externally and $-$ for internally tangent spheres.

The Apollonius problem for spheres S_1, S_2, S_3, S_4 is therefore solved by any $S = ((x, y, z), r)$ such that

$$\begin{aligned} (x_1 - x)^2 + (y_1 - y)^2 + (z_1 - z)^2 &= (r_1 \pm r)^2 \\ (x_2 - x)^2 + (y_2 - y)^2 + (z_2 - z)^2 &= (r_2 \pm r)^2 \\ (x_3 - x)^2 + (y_3 - y)^2 + (z_3 - z)^2 &= (r_3 \pm r)^2 \\ (x_4 - x)^2 + (y_4 - y)^2 + (z_4 - z)^2 &= (r_4 \pm r)^2, \end{aligned} \tag{A.5}$$

where we can take any combination of $+$ or $-$, yielding altogether 16 possible solutions. We do not consider degenerate cases as they cannot happen in our setting.

As noted previously, the number of solutions for both T_1 and T_2 will reduce significantly. For T_1 , the spheres are completely interchangeable and thus only solutions with different number of $+$ will differ. This yields 5 possible solutions. Geometrically the number of $+$ can be seen as the number of spheres the solution is externally tangent to. For T_2 the situation is more complex, as the problem is not entirely symmetric with respect to the four points. Still, symmetries do exist and the number of solution will be reduced.

Sadly, for most choices of $+$ and $-$, these equations still seem to be too complex for Mathematica to solve. Luckily, we can simplify them further.

Solving the equations (A.5) by linearizing

We formulate the solution as a theorem.

Theorem 7. *For $\rho < 1/(2\sqrt{6})$, the maximum in A.3 is $a\chi_1$, where*

$$\chi_1 := 2(\sqrt{6}/4 + \rho).$$

For $\rho < 1/4$, the maximum in A.4 is $a\chi_2$, where

$$\chi_2 := 2 \frac{2\rho + \sqrt{2 - 32\rho^2 + 64\rho^4}}{2 - 32\rho^2}.$$

Proof. Recall that the solution must lie on a sphere solving the equations (A.5). We must therefore solve them and find the solution with the largest circumdiameter.

First, for clarity, we define the variables $s_i \in \{+1, -1\}, i = 1, \dots, 4$ instead of relying on the notation \pm . We begin by expanding the parentheses to obtain the equations

$$x^2 + y^2 + z^2 + x_i^2 + y_i^2 + z_i^2 - 2xx_i - 2yy_i - 2zz_i = r^2 + r_i^2 + 2s_i r_i r, \quad i = 1, 2, 3, 4$$

By subtracting the second, third, and fourth equation from the first, we get rid of the quadratic terms and obtain a system of linear equations with four variables and three equations:

$$\begin{aligned} & -2(x_1 - x_i)x - 2(y_1 - y_i)y - 2(z_1 - z_i)z - 2(s_1 r_1 - s_i r_i)r \\ & + x_1^2 - x_i^2 + y_1^2 - y_i^2 + z_1^2 - z_i^2 - r_1^2 + r_i^2 = 0, \quad i = 2, 3, 4 \end{aligned}$$

This system can be solved to obtain expression of x, y, z in terms of r . We then substitute those expression into (A.5) to obtain r^1 .

We have used Wolfram Mathematica (Wolfram Research Inc.) to find the solutions. The full implementation can be found in the file `ApolloniusProblem.nb`. By comparing the circumdiameters of the solutions, we obtain the proposition. □

All the solutions for the choice $a = 1$ can be seen in Figures A.1 and A.2. We can see that for $T_1, \rho < 1/\sqrt{6}$, we have the two solutions

$$a(\sqrt{6}/4 + \rho), a \frac{\rho - \sqrt{6}(4\rho^2 - 1)}{4 - 24\rho^2}$$

which intersect at $\rho = 1/(2\sqrt{6})$.

Notice the simple linear form of the first solution — it is precisely the sphere which is internally tangent to all four spheres. This sphere has the same center as the circumsphere of tetrahedron $\{t_1, t_2, t_3, t_4\}$. Thus the solution is a sum of circumradius of the tetrahedron, $a\sqrt{6}/4$, and the radius of the four spheres, ρ . We can see similar behaviour in the solution that is externally tangent to all four spheres.

For T_2 , the linear solution will no longer be the largest, as now we obtain a larger circumradius by using a sphere that is externally tangent to some of the spheres.

¹Note that exact solutions of x, y, z , which we are not interested in, could then be obtained through substituting r back into the linear system.

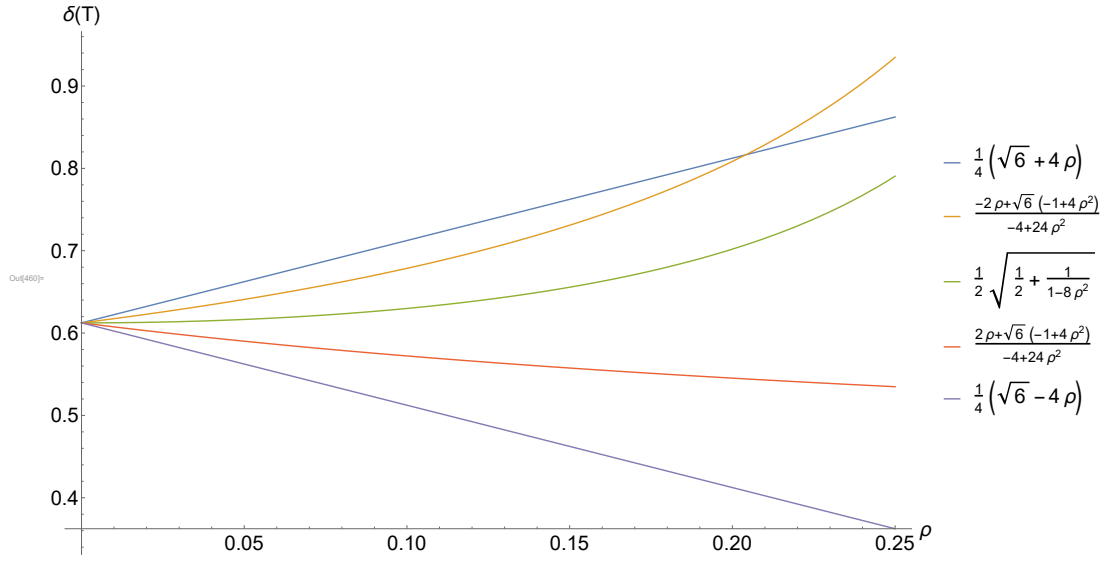


Figure A.1: All solutions to Apollonius problem with T_1 , $a = 1$.

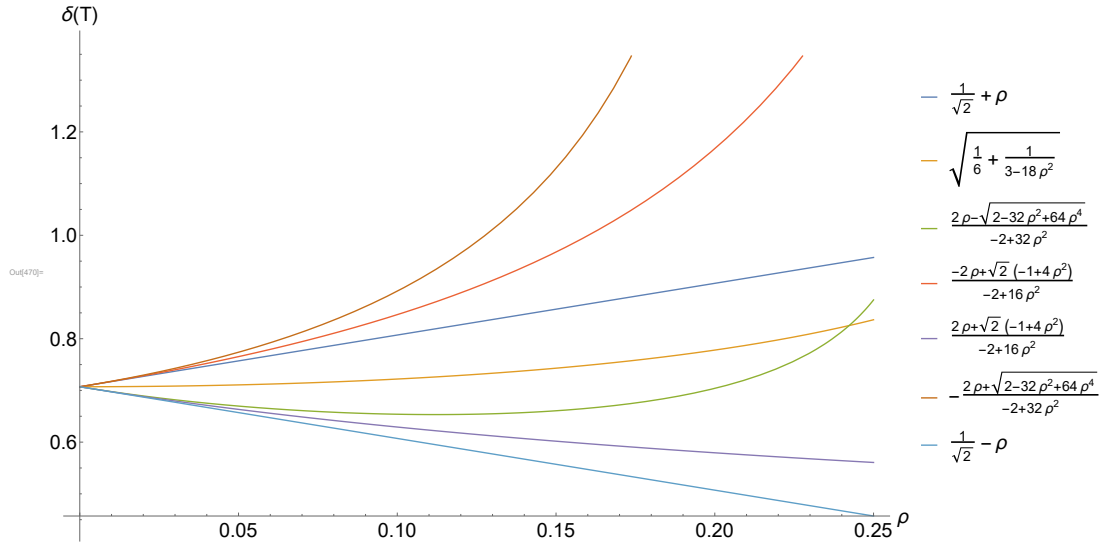


Figure A.2: All solutions to Apollonius problem with T_2 , $a = 1$

Remark 19 (General position). From the form of the solutions one can also obtain the necessary bounds for ρ for the points to remain in general position. The points cease to be in general position precisely when any one of the solutions becomes infinite. This gives us $\rho < 1/(2\sqrt{6})$ for T_1 and $\rho < 1/4$ for T_2 . Since we must control the circumdiameter for all tetrahedra, we must assume $\rho < 1/4$.

B. Appendix: Implementation details

C++ and CGAL

The MCMC procedure introduced in Chapter 4, as well as the maximum pseudolikelihood estimation procedure introduced in Chapter 5, was implemented in C++ using the Computational Geometry Algorithms Library (The CGAL Project [2018]). In particular, the package for 3D-triangulations (Jamin et al. [2018]) was used. CGAL provides an implementation of both Delaunay and Laguerre¹ tetrahedrizations which allows both adding and removing points.

The current implementation allows control of the model parameters as well as number of iterations through command line arguments. For anything else, alterations of the code are required, although many changes (such as specifications of the form of the potential) can be done quickly, as functions for various characteristics such as volume, surface area, minimum edge length, etc., are already implemented.

Three files are outputted for each simulation: cell data and estimation results, the tetrahedrization itself, and a log of the MCMC procedure.

In the near future, a simple documentation will be provided.

The latest version of the code is available at <https://github.com/DahnJ/Gibbs-Laguerre-Delaunay>.

Python analysis

The C++ program outputs cell data in a standard `csv` format. These were subsequently analyzed in Python using the Jupyter notebook environment. The notebook can be found in the same repository as the C++ code in the folder `python`.

Wolfram Mathematica

In Remark 16 and in Theorem 7, Wolfram Mathematica (Wolfram Research Inc.) was used. The Mathematica notebooks are contained in the repository of this thesis, available at <https://github.com/DahnJ/Thesis> in the folder `mathematica`.

¹Laguerre tetrahedrization is called the *3D regular triangulation* in CGAL.